University of Nevada, Reno

# Interplay of Brain Derived Neurotrophic Factor and Protein Kinase A in Modulating Mitochondrial Structure and Function in Brain Homeostasis and Disease

A dissertation submitted in partial fulfillment of the requirements for the degree of Doctor of Philosophy in Neuroscience

By

Maryann Swain

Dr, Ruben K. Dagda / Dissertation Advisor

May 2023

THE GRADUATE SCHOOL

We recommend that the dissertation
prepared under our supervision by

**Maryann Swain**

entitled

**Role of Mitochondrially-Localized Protein Kinase A and Brain-Derived Neurotrophic Factor in Modulating Mitochondrial Structure/Function and Dendrites in Neurons and in Brain Disease**

be accepted in partial fulfillment of the
requirements for the degree of

**Doctor of Philosophy**

Ruben K. Dagda
*Advisor*

Thomas Kidd
*Committee Member*

Dennis Mathew
*Committee Member*

Thomas Gould
*Committee Member*

Subhash Verma
*Graduate School Representative*

Markus Kemmelmeier, Ph.D., Dean
*Graduate School*

May 2023

**Abstract**:

Neurons are postmitotic cells that contain elongated specialized structures that emanate from their cell bodies termed neurites (axons and dendrites). In order to form neuronal networks, neurons rely on continuous neurotrophic support mediated by Brain-Derived Neurotrophic Factor (BDNF). My dissertation work characterized new physiological roles that BDNF play in maintaining neuronal homeostasis, specifically by regulating mitochondrial structure and function and neuronal metabolism. Specifically, I found that exposure of neurons to the mature form of BDNF which binds and activates the Tropomyosin Kinase $\beta$ (Trk$\beta$) receptor to promote rapid endocytosis and translocation of the signaling endosome to the mitochondria leading to elevated activation of Protein Kinase A (PKA). BDNF-mediated activation of mitochondrial PKA led to an increase in phosphorylation of fission modulator Drp1, and of mitochondrial adaptor protein Miro-2 to promote mitochondrial elongation and increase the trafficking and content of mitochondria in dendrite trees. Secondly, exposure of neurons to BDNF enhanced neuronal metabolism (oxidative phosphorylation and glycolysis) and increased the transmembrane potential of mitochondria; processes that required activation of trk$\beta$. Furthermore, BDNF-mediated enhancement of mitochondrially-localized PKA was associated with increased resistance of primary cortical neurons against neurodegeneration and oxidative stress induced by rotenone or exposure to amyloid β, *in vitro* models of Parkinson's and Alzheimer's disease respectively. Finally, I provide new methodology that I co-developed that allows neuroscientists to analyze neuronal metabolism and connectivity in the same population of neurons in a rigorous manner by multiplexing the Seahorse XFe24 analyzer with ImageXpress® Nano high content imaging microscopes. By using this novel

methodology, I was able to characterize the temporal effects of BDNF on brain energy production and connectivity with high resolution. Overall, my dissertation work provides new mechanisms by which BDNF exerts neuroprotection that goes beyond the classical model of inhibition of apoptosis signaling. Specifically, by BDNF activating mitochondrially localized PKA to govern mitochondrial structure/function which increases neuronal survival and connectivity.

I would like to dedicate my dissertation, to my children,
to Ares and Athena, whom I love the most in the world!

**Acknowledgements:**

**Authors**

**Contributions**

Maryann Swain, Smijin K. Soman, Kylea Tapia, Raul Y. Dagda,

Tania Das Banerjee, Kelly Reihl, Mariana Torres and Ruben K. Dagda

**Chapter 1**

MS wrote the intro RKD helped edit.

**Chapter 2**

RKD and MS designed the study. RKD supervised the study. MS, SKS, RYD, and KT collected the data. MS, SKS, RKD and KT analyzed the data and interpreted the results. MS and SKS first drafted the manuscript. MS, SKS, and RKD critically revised for important intellectual content. All authors revised and approved the submitted version of the manuscript.

**Chapter 3**

TDB, KR, MS, and MT performed the experiments. RKD and TDB, designed the study. TDB, MS, KR and RKD analyzed the data and wrote the paper. All authors read and approved the final manuscript.

**Chapter 4**

MS and SKS performed the experiments. MS and SKS designed the study. MS and SKS analyzed the data and wrote the paper RKD helped in editing. All authors read and approved the final manuscript.

**Chapter 5**

MS wrote the conclusion RKD helped edit.

**Funding**

This project was supported by the NIH grant 5R01NS105783 and the administrative supplement to support diversity 3R01NS105783-05S1. These studies were supported by a Women's Health Initiative grant (2015-2017, to RKD) and partly by NIH grants R01 (to RKD), GM103554 (to RKD) and P20GM103440, and a Sanford Center for Aging Faculty Fellowship (to RKD).

**Conflict of Interest**

The authors declare that the research was conducted in the absence of any commercial or financial relationships that could be construed as a potential conflict of interest.

Table of Contents Page Number


| | | |
|---|---|---|
| Chapter 1 | Introduction | 1 |
| Chapter 2 | BDNF Regulates Mitochondrial Physiology and function in Neurons through PKA-Dependent Mechanisms | 23 |
| Chapter 3 | Mitochondrial PKA is neuroprotective in a cell culture model of Alzheimer's disease | 86 |
| Chapter 4 | Multiplexing Seahorse XF$^{e}$24 and ImageXpress® Nano platforms for comprehensive evaluation of mitochondrial bioenergetic profile and neuronal morphology | 118 |
| Chapter 5 | Discussion and future directions | 140 |
| References | | 151 |

| Chapter | List of Figures | Page Number |
|---|---|---|
| Chapter 1 Figure 1 | Graphical abstract | 22 |
| Chapter 2 Figure 1 | Trkβ receptor translocates to dendritic mitochondria of primary cortical neurons in response to BDNF treatment. | 58 |
| Chapter 2 Figure 2 | BDNF promotes mitochondrial fusion in a PKA-dependent manner | 60 |
| Chapter 2 Figure 3 | BDNF promotes mitochondrial length through phosphorylation of Drp1 | 62 |
| Chapter 2 Figure 4 | Exogenous recombinant BDNF treatment increases anterograde and retrograde mitochondrial trafficking to dendrites | 64 |
| Chapter 2 Figure 5 | BDNF treatment increases anterograde and retrograde mitochondrial trafficking in dendrites in a PKA-dependent manner | 65 |
| Chapter 2 Figure 6 | Exposure of primary cortical neurons with BDNF enhances mitochondrial content in dendrites through PKA | 67 |
| Chapter 2 Figure 7 | BDNF increases oxidative phosphorylation in live primary neurons and in isolated mitochondria | 70 |
| Chapter 2 Figure 8 | BDNF promotes mitochondria and protects dendrites from oxidative stress. | 72 |
| Chapter 2 Figure 9 | Mechanistic conceptual model on the role of BDNF in regulating mitochondrial structure/function in neurons. | 74 |
| Chapter 2 Figure S.1 | BDNF does not increase the mean number of Trkβ - GFP puncta in the dendrites or soma of neurons | 76 |

| | | |
|---|---|---|
| Chapter 2 Figure S.2 | BDNF increases PKA activity | 78 |
| Chapter 2 Figure S.3 | BDNF increases the endogenous level of D-AKAP1 | 79 |
| Chapter 2 Figure S.4 | Co-transfection of Mito-RFP with PKI and MITO-PKI | 80 |
| Chapter 2 Figure S.5 | Co-transfection of Mito-RFP with Drp1-WT and Drp1-S656A | 82 |
| Chapter 2 Figure S.6 | BDNF increases the phosphorylation of Drp1 but not in the presence of ANA12 | 84 |
| Chapter 2 Figure S.7 | Trkβ is required for BDNF to modulate mitochondrial respiration | 85 |
| Chapter 3 Figure 1 | The level of endogenous D-AKAP121 is significantly decreased in mitochondria of neurons in *in vitro* and *in vivo* models of Alzheimer's disease | 110 |
| Chapter 3 Figure 3 | D-AKAP1/PKA protects dendrites and mitochondrial structure from $A\beta_{42}$-mediated toxicity via PKA-mediated phosphorylation of Drp1 | 113 |
| Chapter 3 Figure 4 | D-AKAP1/PKA decreases neuronal apoptosis induced by Aβ42 via PKA-mediated phosphorylation of Drp1 | 115 |
| Chapter 3 Figure 5 | D-AKAP1/PKA exerts neuroprotection in primary cortical neurons against $A\beta_{42}$ in a similar manner as estrogen treatment | 116 |
| Chapter 3 Figure S.1 | The level of endogenous D-AKAP121 is significantly reduced in the hippocampus and cortex of asymptomatic 5X-FAD mice | 118 |

| | | |
|---|---|---|
| Chapter 3 Figure S.2 | The level of endogenous D-AKAP121 is significantly reduced in the cortex of asymptomatic 5X-FAD mice | 119 |
| Chapter 4 Figure 1 | Basal respiration: OCR | 138 |
| Chapter 4 Figure 2 | OCR and ECAR | 140 |
| Chapter 4 Figure 3 | Morphology | 141 |

**TITLE:**

**Interplay of Brain Derived Neurotrophic Factor and Protein Kinase A in Modulating Mitochondrial Structure and Function in Brain Homeostasis and Disease.**

## Chapter I Introduction

Neurons are postmitotic cells that contain specialized structures termed axons and dendrites that emanate from their cell bodies that allow them to receive and conduct electrochemical signals termed action potentials. However, in order to propagate electrical signals, neurons need to be able to form neuronal circuits and networks by maintaining well-formed dendritic trees and axons. The physiological processes that allow the neurons to thrive include a high level of neurotrophic signaling, a sufficient amount of neuronal activity and synthesis and turnover of macromolecules to generate energy through glycolysis or oxidative phosphorylation (OXPHOS). In order to meet the energy demands that neurons require to maintain neuronal connections, they rely on the proper functioning, structure and distribution of mitochondria, specialized organelles that synthesize energy in the form of ATP which allows neurons to release neurotransmitter vesicles and generate antioxidants to quench detrimental levels of reactive oxygen species (ROS). A high level of ROS in neurons can induce progressive degeneration of neurons starting with the loss of dendrites and axons.

What are the neuronal survival responses that neurons activate to avert cellular toxicity and ensuing apoptosis? Neuronal survival responses require a certain level of stress to be activated by an accumulation of ROS, which can cause injury and dysfunction of organelles

including mitochondria, in the case that the response needed it can initiate transcription programs to stimulate neuronal survival by synthesizing proteins such as neurotrophic factors (Lewin & Carter, 2014). Neurotrophins, such as Brain Derived Neurotropic Factor (BDNF), play a crucial role in activating pro-survival signaling pathways, including the activation of the peroxisome proliferator activated receptor gamma coactivator (PGC-1α) pathway that mediates transcription of antioxidant genes in response to mitochondrial dysfunction and ROS, which can then activate additional neuronal survival pathways that are activated in response to harmful stimuli including ER stress, hypoxia, oxidative stress, nutrient deprivation, and cellular trauma (Nikoletopoulou et al., 2013).Without a proper level of pro-survival signaling, degenerative cell processes like autophagy, necrosis, and apoptosis may occur (Klener et al., 2006). In neurons, an increase in pro-survival pathways involves activation of kinases, such as phosphatidylinositol 3′ kinase (PI3K)/ protein kinase B (AKT)/ mammalian target of rapamycin (mTOR), mitogen-activated protein kinase (MAPK)/ extracellular signal-regulated kinase (ERK), Phospholipase C gamma (PLCγ)/ Calmodulin-Dependent Protein Kinase (CaMK), and the transcription factor nuclear factor kappa B (NF-kB) pathway, which can counteract these apoptosis, necrosis, and autophagy degenerative processes (Saragovi et al., 2019). However, dysregulation of these pathways is often seen in degenerative brain disorders such as cerebral vascular disease, Alzheimer's disease (AD), multiple sclerosis (MS), Amyotrophic lateral sclerosis (ALS), Parkinson's disease (PD), ischemia, and traumatic brain injury. BDNF activates downstream signaling cascades, including the mitochondrial Dual-specificity protein kinase A anchoring protein 1 (D-AKAP1)/ protein kinase A (PKA) pathway (Swain et al., 2023), leading to various downstream effects that can promote neuroprotection and survival, including promoting

the trafficking of mitochondria in axons and mRNA in dendrites, making it a potential therapeutic target for treating neurodegenerative diseases and psychiatric disorders (Lai et al., 2019).

So how do neurons activate these pro-survival signaling pathways in response to heightened stress? Neurotrophins (NTs) play a crucial role in neuronal growth, differentiation, and survival through their function as signaling proteins. This family of signaling molecules include brain-derived neurotrophic factor (BDNF), nerve growth factor (NGF), neurotrophin-3 (NT-3), and neurotrophin-4/5 (NT-4/5), which have been well characterized in neurons by the book Neurotrophic factors (Lewin & Carter, 2014). These signaling molecules bind to specific receptors, via the coupling of TrkA with NGF, Trkβ binding to BDNF and NT-4, TrkC receptor being bound by NT-3 (which can also bind to TrkA and Trkβ), and P75NTR receptor can be bound by all the neurotrophins mentioned, but with a higher affinity to the pro-NTs. The neurotrophins are essential for the development, maintenance, and survival of neurons, and dysregulation in their signaling has been associated with various psychiatric and neurological disorders (Lewin & Carter, 2014). Transcription factors regulate the expression of neurotrophin genes in response to cellular communication and neuronal survival pathways. BDNF expression in primary cortical neurons is specifically regulated by cAMP response element-binding protein (CREB) family transcription factors (Esvald et al., 2020), which play a critical role in BDNF transcriptional autoregulation. In addition, retinoic acid upregulates the endogenous levels of Trkβ by activating canonical E-box sequences in their promoters (Liu et al., 2004), with basic Helix-Loop-Helix (bHLH) proteins coordinating cell cycle arrest and neuronal

differentiation. Trkβ expression is stimulated by Hypoxia-Inducible Factor (HIF-1) in hypoxic conditions, promoting differentiation of neuroblastoma cells (Martens et al., 2007).

There are several BDNF isoforms that are produced in cellular activation. BDNF gene transcription results in multiple transcripts that undergo enzymatic modifications in the endoplasmic reticulum and Golgi apparatus to synthesize the different isoforms (Rocío & Silvina, 2016). Pro-BDNF is cleaved to yield mature form of BDNF (mBDNF), which subsequently binds to Trkβ receptors. BDNF is post translationally regulated as it contains cysteine residues and myristoylation sites allowing binding to membranes (Notaras & van den Buuse, 2019). Once translated, pro-BDNF can undergo several posttranslational modifications through proteolytic cleavage: intracellular cleavage and release of mBDNF, secretion as pro-BDNF with extracellular cleavage, or secretion as pro-BDNF without any further modifications (Rocío & Silvina, 2016). In addition, sortilin and carboxypeptidase E interact with N and C terminal domains of BDNF to direct pro-BDNF inside the cell towards the regulated secretory pathway via dense core vesicles released at the axon terminals (Lewin & Carter, 2014). In addition, plasmin and MMPs cleave pro-BDNF extracellularly, while furin and convertases cleave it intracellularly (Notaras & van den Buuse, 2019). Therefore, the regulated balance between pro-BDNF and mBDNF is critical for proper physiological function in the brain, and an imbalance in the ratio (mBDNF/ pro-BDNF) can lead to pathological conditions in the brain.

Why are there so many isoforms of BDNF? Do they activated different signaling pathways? There exists multi-receptor complexes of various types of receptors that are crucial for selectively activating distinct signaling pathways (Reichardt, 2006). Recent studies suggest that BDNF activates multiple pathways in neurons by interacting with Trks and p75NTR receptors which trigger a myriad of intracellular signaling cascades (Yu et al., 2018). Trk receptors such as Trkβ participate in the activation of multiple kinase signaling pathways, including the MAP kinase pathways and induce the invagination of signaling endosomes, whereas p75NTR facilitates cell death pathways. Adenosine A2A receptors also modulate BDNF's action on synaptic transmission via the cAMP-PKA signaling pathway (Tebano et al., 2010). Overall, these research findings highlight the complex interactions between various receptors and signaling pathways in neurons, which could lead to future research on the roles of specific receptor complexes in neurological disorders including Alzheimer's and Huntington's disease. Future research needs to address the complexity of signaling pathways involved. Several features of the sorting and processing of BDNF receptors and the amyloid precursor protein (APP) strengthen a causal relationship of both pathways. APP is cleaved by the ß-secretase and $\gamma$-secretase to produce beta amyloid in AD pathology. APP Further studies should investigate the impact of BDNF and APP interplay as well as interactions with other signaling partners in AD diagnosis and therapy. It has been postulated that the quantification of protein ratios of BDNF and APP could be used as an indicator of early stages of the disease and potentially uncover new biomarkers of the disease. Pharmacological drugs that inhibit specific protein-protein interactions such as ligands and receptors or APP and BDNF receptor Trkβ could be a new therapeutic approach. (Eggert et al., 2022).

There are different Trkβ isoforms that are produced in cellular activity. The Trk receptors are large cell membrane bound receptors that typically contain five extracellular domains, an alpha-helical transmembrane domain, and an intracellular kinase domain. While there are subtle sequence differences between the various isoforms of Trk receptors in terms of amino acid homology and secondary structure/topology, their expression and location are factors that distinguish them. For instance, TrkA is primarily expressed in cholinergic basal forebrain neurons whereas Trkβ is predominately found in hippocampus and cortex. On the other hand, TrkC is located and expressed in cortical and hippocampal pyramidal neurons as well as cochlear neurons. (Conroy & Coulson, 2022). Adding a layer of complexity in their regulation and functional roles in the brain, the Trkβ receptor gene undergoes alternative splicing, resulting in different isoforms that modulate pro-survival signaling pathways. These include the active full-length Trkβ receptor (Trkβ-FL) receptor and truncated isoforms lacking the kinase domain, such as Trkβ-T1, Trkβ-T2, and Trkβ-Shc (Notaras & van den Buuse, 2019). Truncated isoforms can regulate Trkβ-FL activity, by competing for endogenous BDNF binding or forming inactive (non-functional) heterodimers, and Trkβ-T1 may activate independent signaling pathways (Vidaurre et al., 2012). Trkβ receptors are present throughout axons and dendrites and are sorted into full-length and truncated isoforms, with full-length Trkβ expressed in both neurons and glia, whereas truncated Trkβ is mainly expressed by glia. It is worth noting that all neurotrophins act via autocrine, paracrine, or anterograde trafficking mechanisms in the CNS (Kryl et al., 1999).

What is the purpose of having the different BDNF and Trkβ isoforms? BDNF and Trkβ isoforms are important for regulating neuronal function and survival via activating distinct signaling pathways. For instance, the expression levels of neurotrophins are regulated at multiple levels including transcriptional, post-transcriptional, and post-translational. Neurotrophins availability can also be influenced by proteolytic processing, degradation, and transport (Lewin & Carter, 2014). Trk receptors activate various intracellular signaling pathways, such as PI3K/Akt, MAPK/Erk, and PLCγ, while also regulating Rac (a subfamily of the Rho family of GTPases, which are regulators of endosome formation) activation and transcriptional regulation (Phuyal & Farhan, 2019). The pan-neurotrophin receptor p75NTR and caveolin isoforms can modulate Trkβ signaling via SH2-containing protein tyrosine phosphatase-2 Shp2 (Gupta et al., 2013). Additionally, other receptor pairs such as p75NTR and sortilin can impact BDNF signaling. The adenosine A2A receptor (A2AR) and G-protein-coupled receptors (GPCRs) can also cross activate Trk receptors and enhance BDNF's influence on synaptic plasticity and transmission in the hippocampus (Vaz et al., 2015).

A proper level of signaling by neurotrophins is required to maintain neuronal survival and avert the onset of neurodegenerative disorders like AD. Indeed, a reduction in the expression of Trkβ in the brain contributes to AD and PD pathology as evident by a substantial reduction in expression in the hippocampus of postmortem AD tissue and in midbrain of Parkinson’s disease patients and also in clinical depression (Singh et al., 2023). These molecular mechanisms are significant in the pathophysiology of various disorders, including neurodegenerative, psychiatric, and proliferative disorders (Tebano et al., 2010)

How does the cell know where to send the BDNF signaling endosomes?

BDNF activates the Trkβ receptor, initiating the PLC $Ca^{+2}$ PKA pathway. However, there is evidence that endocytosis of the Trkβ receptor is required for activating these intracellular pathways. The resulting BDNF/ Trkβ signaling endosome ("signalosome") is then transported via dynein/kinesin motors. However, the molecular mechanism by which signaling endosomes containing BDNF/Trkβ are formed and how they traffic to other organelles like mitochondria merits further investigation (Swain et al., 2023). While the majority of signaling transduction pathways activated by Trk receptors occurs in the neuronal membrane of the body and dendrites, some of these receptors bound to neurotrophins can propagate intracellular signaling through endocytosis to traffic to other organelles. For instance, Trkβ receptors have been reported to be trafficked to organelles including the mitochondria via endosomes that are regulated by endosomal Ras-associated binding (Rab) proteins Rab5, Rab7, and Rab10, (Lazo & Schiavo, 2023). Mechanistically, trafficking Rab proteins located on the cell membrane initiate endosomal pathways by activation of signaling endosomes containing Trk receptors. Rab proteins control the location of Trkβ/BDNF signaling endosomes. Rab5-positive early endosomes facilitate signaling, while recycling of Trkβ from Rab11 endosomes is necessary for sustained BDNF signaling (Moya-Alvarado et al., 2022). Rab11 recycling endosomes integrate signaling receptors for neuronal function, and the BDNF-Rab5/Rab11-Erk1/2-CREB pathway triggers genes that regulate neurotrophic responses for homeostasis (González-Gutiérrez et al., 2020). Dysfunctions in endosomal trafficking and receptor defects play a pathological role in neurodegenerative diseases including the degeneration of dendrites and loss of synaptic plasticity (Moya-Alvarado et al., 2022). While BDNF and Trkβ can traffic to

organelles such as mitochondria, the significance of increased trafficking of activated Trkβ to mitochondria remains to be elucidated. This poses the following question. Does increased trafficking of Trkβ lead to alterations in mitochondrial physiology? Emerging evidence suggests that BDNF can regulate some aspects of mitochondrial structure and function including mitochondrial trafficking to areas of high energy demand such as neurites, where they can carry out ATP production and calcium signaling (Faria-Pereira & Morais, 2022; Giménez-Palomo et al., 2021). In the brain, BDNF also protects mitochondria from dysfunction by promoting mitochondrial turnover through the degradation pathway of the lysosomes (mitophagy) through HIF-1α/ Bcl-2 interacting protein 3 (BNIP3) signaling (Jin et al., 2019).

How does the mitochondria behave in neurons? Mitochondria are multi-functional organelles that regulate various physiological roles, including energy production by synthesizing ATP, mediate the anabolism and catabolism of lipids, synthesize some essential amino acids, enable the synthesis pyrimidines through the urea cycle, govern calcium signaling, and they regulate cell fate by modulating apoptosis. Mitochondria also act as independent signaling entities that can undergo dynamic processes including fragmentation (fission), increased interconnectivity between mitochondria (fusion), transport, degradation, and biogenesis to maintain homeostasis (Trigo et al., 2022). Mitochondria fission and fusion is regulated via the mitochondrial fission/fusion or mitochondrial fission factor (MFF) machinery. In addition, mitochondria also have the ability to move by gliding through cytoskeletal networks by engaging with mitochondrial transport machinery. Both physiological processes (fission/fusion) and motility is termed

mitochondrial dynamics. In neurons, mitochondria dynamics is an essential process for regulating mitochondrial morphology and content by fission, fusion, transport, and their disruption in degradation and biogenesis is linked to neurodegenerative diseases. (Markham et al., 2004). Mitochondria also play a critical role in buffering calcium levels during synaptic transmission and sense the energetic needs of the neuron. (Faria-Pereira & Morais, 2022). Mitochondrial biogenesis, the process by which new mitochondria are synthesized from macromolecules, first involves mitochondrial DNA (mtDNA) replication, gene expression, protein synthesis, and membrane formation (Trigo et al., 2022). PGC-1α increases the expression of genes responsible for mtDNA replication and transcription, including the essential regulator Transcription Factor A, Mitochondrial (TFAM), which stimulates mitochondria biogenesis. This results in an increased expression of mitochondrial-encoded polypeptides, OXPHOS respiration, and ATP concentrations. PGC-1α also promotes the expression of nuclear-encoded subunits of mitochondrial respiratory complexes via the nuclear respiratory factors (NRF-1/NRF-2) pathway, leading to increased mitochondrial bioenergetic output. PGC-1α governs mitochondrial biogenesis by increasing mitochondrial mass, leading to oxidative phosphorylation as well as increased import of nuclear-encoded mitochondrial proteins, a physiological process that requires an intact mitochondrial membrane potential (Uittenbogaard & Chiaramello, 2014). Metabolic changes affect mitochondrial fission and fusion, and stress-induced mitochondrial hyper fusion, or inhibition of fission may protect mitochondria from mitophagy during stress (Youle & van der Bliek, 2012).

Therefore, maintaining a balance between mitochondrial fusion and fission is critical for optimal mitochondrial structure and function, as well as the survival of neurons. For instance, mitochondrial fusion can increase the surface area of mitochondria, leading to greater rate of ATP synthesis and reducing the threshold for activating apoptosis (Merrill et al., 2011). Mitochondrial fission, on the other hand, helps disperse damaged mitochondria fragments for lysosomal degradation through mitophagy as well as helps to distributes and "dilutes" oxidatively damaged or mutated mitochondrial DNA (Archer, 2013). Mitochondrial fusion is well regulated by several large mechanoenzymes including Optic atrophy type 1 (Opa1), Mitofusin-1 (Mfn1), and Mitofusin-2 (Mfn2), while the fission pathway involves proteins like Dynamin-related protein 1 (Drp1), Mitochondrial fission factor (MFF), mitochondrial dynamics protein of 49 kDa (Mid49), and mitochondrial dynamics protein of 51 kDa (Mid51) (Youle & van der Bliek, 2012). Mitochondrial fission proteins such as Drp1 is regulated by posttranslational modifications such as ubiquitination, SUMOylation, O-GlcNAcylation, acetylation, S-Nitrosylation, including phosphorylation. For instance, PKA phosphorylates residue 637 of Drp1, which inhibits fission. In contrast, PKC and ERK2 can phosphorylate Drp1 at different sites to promote fission (Kashatus et al., 2015; Merrill & Strack, 2014). Mechanistically, PKA inhibits Drp1-mediated fission by inhibiting the formation of large oligomeric complexes of Drp1 at the outer mitochondrial membrane (OMM) and thereby increases levels of cytosolic Drp1, preventing pathological activation. Fused mitochondria increase resilience of neurons to damaged mtDNA, decrease cytochrome c release, and provides neuroprotection (Youle & van der Bliek, 2012). Inhibiting either fusion or fission leads to significant impairment of mitochondrial function (Chan, 2020).

How does PKA modify and govern mitochondrial structure/function in neurons? PKA is a small serine/threonine kinase that can activate or inhibit signaling pathways by phosphorylating several protein substrates on serine or threonine residues. The PKA holoenzyme comprises of R and C subunits, where an R-subunit dimer binds to two C-subunits to form R2C2. The biochemical and functional properties of PKA holoenzymes are primarily determined by the R-subunits. Two classes of R-subunits, RI and RII, with α and β subtypes exhibit tissue-specific expression patterns. While RIα and RIIα are broadly expressed, RIβ and RIIβ are mainly expressed in certain tissues, such as the brain. RIβ is found in hippocampal interneurons, but not RIIβ. RIβ is found in the Purkinje cells and granular cell layer, while RIIβ is mainly expressed in the soma of Purkinje cells and is detected at lower levels in their dendrites. RIβ is abundant in the cerebellar glomerulus, while RIIβ is more concentrated in the axons (Ilouz et al., 2017). Aside from the cytosolic compartment, PKA can be localized to organelles by binding to A-Kinase Anchoring Proteins (AKAPs). For instance, PKA can be targeted to mitochondria by tethering to Dual Specificity AKAP1 (D-AKAP1). Once targeted to mitochondria, PKA can phosphorylate multiple protein substrates on the outer mitochondrial membrane (OMM) such as dynamin-related protein 1 (Drp1), Translocase of the Outer Membrane of 20kDa (TOM20) or phosphorylate different subunits of complex proteins to regulate mitochondrial fission, mitochondrial import and electron transport chain activity respectively. For instance, PKA can phosphorylate subunit of complex I to increase electron flow through complex I subunit (NDUFS4) and also the level of reactive oxygen species (ROS) in the mitochondria (Rasmo & Technikova-Dobrova, 2012). PKA also plays a critical role in mitochondrial biogenesis by activating the transcription factor CREB, by phosphorylating at serine 133,

leading to the activation of PGC-1$\alpha$ a master regulator of mitochondrial biogenesis (Fernandez-Marcos & Auwerx, 2011). PGC-1$\alpha$ increases the number of mitochondria in cells, promoting neuronal energy demands and maintaining proper functioning.

Mitochondria are extremely dynamic by travelling all around the cell and move to distal sites within neurites. The mitochondrial trafficking pathway is regulated by PKA via phosphorylation of Miro2, a specific adaptor protein to the motor proteins, which controls the transportation of organelles such as the mitochondria and signaling endosomes (Course & Wang, 2016). The physiological implications of PKA-mediated phosphorylation of Miro2 is the induction of anterograde movement of mitochondria to areas of high energy demand. By increasing mitochondrial transport to dendrites, through this physiological process, it increases the amount of mitochondria in dendrites and ensures that high energy demands are met, preventing cellular damage and dysfunction. In addition, anterograde mitochondrial trafficking in neurons is facilitated by a complex of motors, adaptors, and anchor proteins such as Miro1, Miro2, Trafficking Kinesin Protein 1 (TRAK1), Trafficking Kinesin Protein 2 (TRAK2), kinesin, dynein/dynactin, and syntaphilin and it is regulated by the balance between motors and anchors (Course & Wang, 2016). In neurons PTEN-induced kinase 1 (PINK1) and PKA participate in a similar neuroprotective signaling pathway to maintain dendrite connectivity and regulate mitochondrial function and structure (Das Banerjee et al., 2017). Loss of PINK1 leads to impaired mitochondrial trafficking and reduced dendrite outgrowth, whereas increasing the endogenous level of PKA in the mitochondria via transiently overexpressing, A kinase anchor protein 1 (D-AKAP1)/PKA, can restore mitochondrial trafficking and content in PINK1-deficient

primary cortical neurons. Mechanistically, PKA phosphorylates the mitochondrial adaptor protein Miro2 to stimulate mitochondrial movement in dendrites, and under oxidative stress, PINK1 stimulates mitochondrial trafficking within dendrites to increase mitochondrial content leading to enhance neuroprotection of dendrites against oxidative stress (Das Banerjee et al., 2017).

How do mitochondria regulate brain metabolism? Mitochondria are organelles that produce ATP, the primary source of cellular energy, through cellular respiration termed oxidative phosphorylation (OXPHOS). They also participate in anabolic pathways, providing specific Krebs cycle components for the synthesis of non-essential amino acids, lipids, and nucleotides. Glycolysis in the cytosol produces pyruvate and ATP, which is converted to acetyl CoA in the mitochondria (Ferrer, 2009). The Krebs cycle oxidizes acetyl CoA to produce $CO^2$ and reduced coenzymes such as NADH, succinate, and $FADH_2$, which are electron carriers that supply electrons and protons to complex proteins of the ETC to facilitate the synthesis of ATP (Trigo et al., 2022). Changes in mitochondria, energy metabolism, voltage-dependent anion channel, and lipid rafts contribute to the depletion of energy in neurons as seen in Alzheimer's disease (Ferrer, 2009). Mitochondria sense the energetic demands of synaptic activity in the brain and act as a buffering system during high-frequency synaptic transmission, taking up excess $Ca^{+2}$ and releasing it gradually to maintain the synapse by fine-tune $Ca^{+2}$ signals (Faria-Pereira & Morais, 2022).

While the influence of BDNF on mitochondrial structure and function has been established the specific molecular mechanisms underlying how this neurotrophic factor regulates

mitochondrial physiology was yet to be determined. What are the physiological implications of BDNF regulating mitochondrial function in neurons? *In vivo*, studies have shown that exogenous BDNF can prevent detrimental excitotoxicity in rats by promoting the recruitment of additional mitochondria to focal sites of excitotoxicity in retinal ganglion cells (Schuettauf et al., 2004). This neuroprotective mechanism modulated by BDNF ensures a balance of energy supply and demand in the brain by facilitating bidirectional trafficking of mitochondria towards sites of high energy demand which experience high levels of oxidative stress. Therefore, the proper distribution of mitochondria is critical for maintaining healthy neuronal function, as disruptions can lead to neurological disorders (Markham et al., 2014). BDNF plays a key role in regulating mitochondrial trafficking, thus serving as a crucial factor in maintaining neuronal homeostasis and preventing excitotoxicity (Swain et al., 2023). Dysregulation of Trkβ can lead to neuronal death in excitotoxicity induced by ischemia (Vidaurre et al., 2012)

Recent evidence has demonstrated that exogenous BDNF can influence brain metabolism by regulating the electron transport chain in mitochondria. *In vitro*, exogenous treatment of cultured mouse primary cortical neurons with BDNF has been found to have a significant impact on cellular metabolism by enhancing both oxidative phosphorylation and glycolysis in neurons (Maryann et al., 2023; Swain et al., 2023). The precise molecular mechanisms through which BDNF upregulates mitochondrial function, and whether Protein Kinase A is involved in regulating the activity of the electron transport chain (ETC), are not yet fully understood and require further investigation. BDNF has been found to affect brain mitochondrial respiration through neurotrophin signal transduction pathways

and the B-cell lymphoma 2 (Bcl-2)/ B-cell lymphoma-extra-large (Bcl-xL) system, specifically targeting complex I, and protecting against ibotenate-induced excitotoxicity via the MEK-MAPK pathway. Inflammatory cytokines can also block or modulate BDNF's effect on energy metabolism, potentially impacting neuronal plasticity, pathological changes, and neurodegenerative disorders (Markham et al., 2014).

Astrocytes protect neurons from iron overload and oxidative stress-induced damage, and enhanced astrocyte-neuron interactions are essential for nuclear factor erythroid 2-related factor 2 (Nrf2) regulation. Nrf2 activation in astrocytes is important for protecting neurons against oxidative damage caused by neurotoxins, and BDNF has been shown to activate Nrf2, the BDNF-TrkB.T1-p75NTR-ceramide signaling pathway mainly activates the PKCζ-CK2-Nrf2 pathway during the light/rest phase in rodent astrocytes. (Ishii et al., 2019). Additionally, glutamate release and activation of group I metabotropic glutamate receptors contribute to Nrf2 activation in astrocytes. The investigation of the complex interaction between BDNF and mitochondrial cellular metabolism has the potential to unveil valuable insights into the regulation of energy production in the body and may lead to more effective treatments for metabolic disorders and neurodegenerative diseases (Ishii et al., 2019).

How does BDNF and mitochondria impact and modify memory? Memory is facilitated by BDNF, which regulates synaptic plasticity. Synaptic plasticity is the capacity of synapses to strengthen or weaken their connections over time in response to neuronal activity which impact learning and memory. This physiological process is complex and highly

coordinated as it requires an increase in the activity of multiple ser/thr kinases and an increase in the trafficking of post-synaptic receptors, scaffold proteins, and messenger RNAs to dendrites as well as localized synthesis of proteins in dendrites, and synaptic terminals. An increase in neuronal activity is initially facilitated by the activation of N-methyl-D-aspartate (NMDA) receptors and maintained by the activation of α-amino-3-hydroxy-5-methyl-4-isoxazolepropionic acid (AMPA) receptors which then activates Long Term Potentiation (LTP). LTP is the persistent reinforcement of synapses, that is dependent on recent activity patterns by activating downstream serine/threonine kinases including PKA, Phosphoinositide 3-kinase (PI-3K) and others. LTP and hippocampus-dependent learning can modulate the synthesis, and maturation of BDNF as well as its extracellular release, while defects in BDNF expression result in defective LTP and memory formation (Zheng et al., 2009). The D-AKAP1/PKA pathway also plays a role in memory, as it regulates synaptic plasticity through cAMP signaling (C. X. Zheng et al., 2016). Further research is needed to understand the transport and regulation of different mRNAs and the relative contributions of local translation and protein transport in BDNF regulation. Additionally, the impact of dendritic transcripts and BDNF-induced signals on protein and mRNAs targeting of activated synapses must be examined as well (Leal et al., 2014). Memory impairment and comorbidity with neuronal pathologies, including dementia, are associated with BDNF, highlighting its importance in maintaining cognitive function.

Mitochondria, which modify their location and function in dendrites and axons, play a critical role in synaptic plasticity and energy production for dendritic remodeling (Cheng et al., 2010). The maintenance of dendritic structures and dendritic trees heavily relies on

mitochondria, which supply the critical energy in the form of ATP. Additionally, mitochondria play a crucial role in the discharge of synaptic vesicles (Cheng et al., 2010; Smith et al., 2016). ROS, which have a signaling function in synaptic plasticity and development, require further research to understand their effects on synapse homeostasis (Faria-Pereira & Morais, 2022).

Mitochondria have an effect in neurodegenerative diseases. Mitochondrial dysfunction and morphological changes are often observed in neurodegenerative disorders, leading to reduced ATP production, decreased membrane potential, and increased oxidative stress. Disrupted transport and impaired fission/fusion regulation are observed in various disorders such as AD, Huntington's disease (HD), and Amyotrophic lateral sclerosis (ALS). Mutations in PINK1 and PARKIN (a 465-amino acid residue E3 ubiquitin ligase) are associated with PD, while mutant amyloid precursor protein (APP) in AD neurons exhibit enhanced Parkin mediated mitophagy (Faria-Pereira & Morais, 2022). Synaptic mitochondrial dysfunction is commonly observed in these neuronal disorders. Compensatory energy boosting mechanisms have been observed in surviving neurons in postmortem studies of PD and ALS patients. Therapeutic strategies to delay some neurodegenerative diseases at onset focus on restoring mitochondrial function, especially in patients with genetic mitochondrial disorders (Faria-Pereira & Morais, 2022).

How does BDNF and mitochondria affect Parkinson's disease? Parkinson's Disease (PD) is a neurodegenerative disorder that is primarily caused by mutations in Pink1 and Parkin genes, which are involved in mitochondrial degradation through mitophagy (Chan, 2020). These mutations lead to impaired mitochondrial structure and function, which can result in

impaired neurotransmitter release and increased susceptibility to stress. Moreover, excessive calcium uptake by mitochondria has been linked to calcium overload and neurodegeneration in PD (Trigo et al., 2022). Dysfunctional Pink1 or Parkin can contribute to neuronal death, by failing to isolate and remove the damaged mitochondria, leading to PD pathogenesis. In addition to mitochondrial dysfunction, other factors are involved in PD pathogenesis. DJ-1 (park7) mutations have also been associated with inherited PD (Cheng et al., 2010). BDNF and D-AKAP1/PKA pathways play crucial roles in neuroplasticity and neuronal health. Therefore, the dysregulation of these signaling pathways contribute to PD pathogenesis, especially PKA signaling and deregulation of CREB translocation to the nucleus, decreased PKA activity in neurotoxin models, also shows that BDNF is decreased in Parkinson's disease (Dagda & Chu, 2009). Halting the motility of damaged mitochondria can provide neuroprotection, and restoring mitochondrial function is a promising therapeutic strategy to delay the onset of PD (Course & Wang, 2016).

How does BDNF and mitochondria affect Alzheimer's disease? BDNF is dysregulated in AD, with reduced BDNF mRNA and protein levels are observed in the hippocampus and frontal cortex (Lima Giacobbo et al., 2019). This can lead to impaired neuroplasticity and contribute to cognitive decline (Cheng et al., 2010; Dagda & Das Banerjee, 2015). Trkβ receptor signaling is implicated in various neurological disorders, including Alzheimer's and Huntington's disease, as well as psychiatric disorders such as depression and anxiety (Gupta et al., 2013). Dysregulation of Trkβ signaling by decreased levels of BDNF can contribute to the pathogenesis of these diseases. Mitochondrial dysfunction is a hallmark

of AD, with Amyloid beta (Aβ) accumulation directly impacting mitochondrial structure and function. This can lead to alterations in fission/fusion, mitochondrial transport balance, and increased ROS generation, ultimately leading to neuronal degeneration (Ferrer, 2009). D-AKAP1/PKA signaling pathways are involved in regulating mitochondrial function in neurons, and disruptions in this pathway may contribute to mitochondrial damage in neurodegenerative diseases such as Alzheimer's Disease, D-AKAP1 levels are reduced in 5X-FAD mouse model of Alzheimer's disease. (Tania Das Banerjee et al., 2021; Merrill & Strack, 2014).

This dissertation aims to bridge the conceptual gaps between BDNF and mitochondria by investigating the molecular mechanisms underlying BDNF's regulation of mitochondrial physiology, including oxidative phosphorylation, and dynamics of fusion and trafficking. It also aims to explore other mechanisms by which BDNF promotes neuroprotection and examine the role of mitochondrial PKA activity, modulated by BDNF, in protecting neurons in an in vitro model of Alzheimer's disease. As presented in my dissertation, the collective published and unpublished data that I garnered in Dr. Dagda's research laboratory for the past five years suggest that BDNF can modulate mitochondrial function through the cyclic AMP pathway, leading to the downstream activation of PKA. This activation increases the level of D-AKAP1 which leads to an increase in the activity of mitochondrially-localized PKA (D-AKAP1/PKA), resulting in highly interconnected and mobile mitochondria that can traffic to dendrites and show increased capacity to produce ATP through OXPHOS. An increase in PKA in the mitochondrion may serve as a new protective mechanism that neurons employ to withstand a high level of stress induced by

promoting mitochondrial fusion, increasing OXPHOS, mitochondrial-derived ATP, and glycolysis, and increasing the transport of mitochondria to dendrites to presumably facilitate the provision of energy and antioxidants that dendrites require to maintain their complex dendritic trees and structures (See graphical abstract below). Therefore, by promoting an increase in the content of mitochondria to dendrites via exogenous BDNF, mitochondria can provide the necessary energy in the form of ATP and a level of antioxidants (superoxide dismutase and catalase) to protect dendrites from retraction and eventual destruction elicited by a high level of ROS induced toxic insults. While it has been shown that BDNF influences mitochondrial structure and function (Markham et al., 2004), the molecular mechanisms by which this neurotrophic factor regulates mitochondrial physiology remains elusive. In the following chapters of my dissertation, I will provide scientific evidence that delineates the molecular mechanisms by which PKA activity enhanced by BDNF governs mitochondrial structure, function and mobility in neurons as observed in **chapter** 2, and how enhanced PKA activity can impact neuronal survival and protect mitochondria in an *in vitro* model of Alzheimer's disease.

## Graphical Abstract: BDNF & Mitochondria relationship

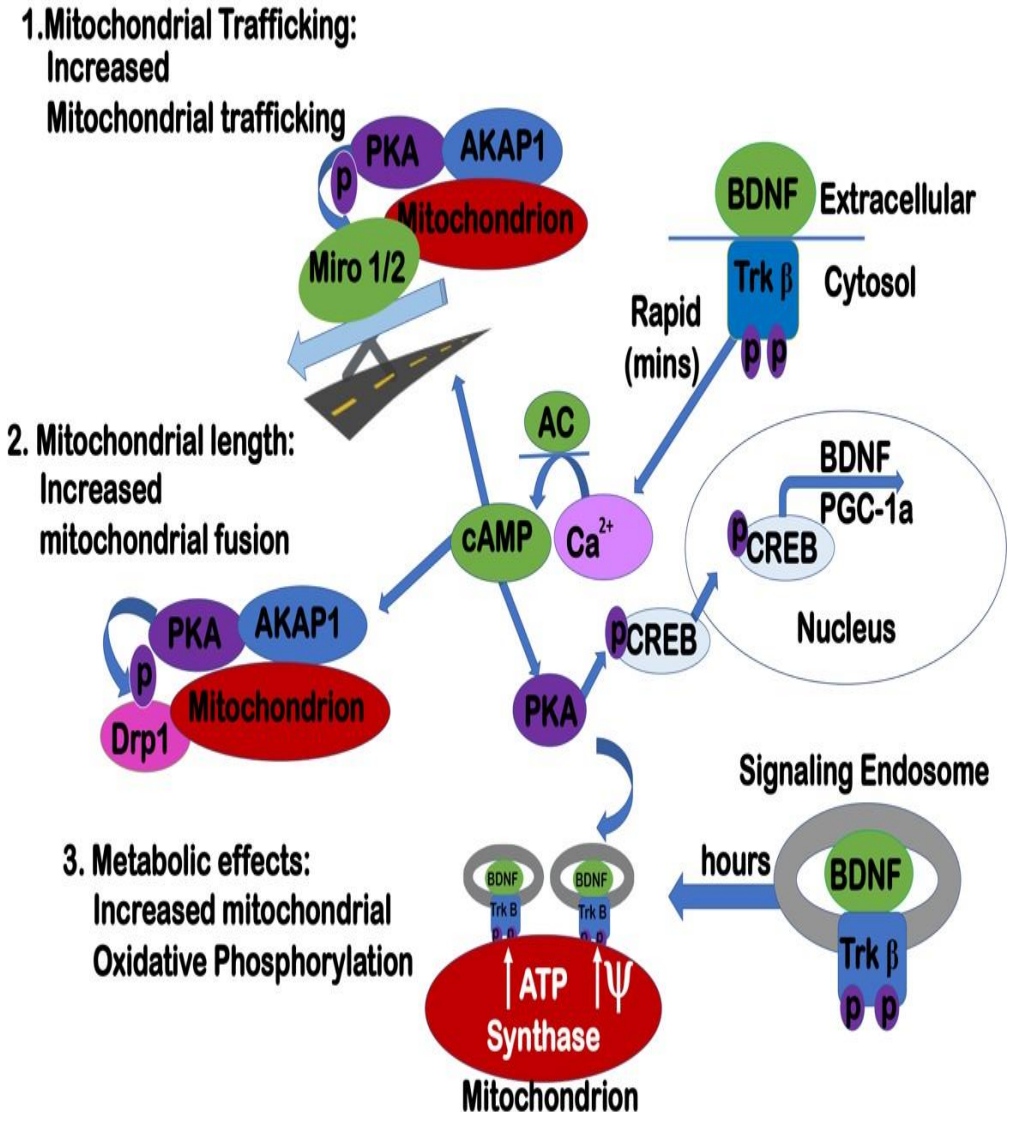

## Chapter II

## Title: BDNF Regulates Mitochondrial Physiology and function in Neurons through PKA-Dependent Mechanisms


### Abstract

Brain derived neurotrophic factor (BDNF) stimulates dendrite outgrowth and synaptic plasticity by activating downstream protein kinase A (PKA) signaling. Recently, BDNF has been shown to modulate mitochondrial respiration in isolated brain mitochondria, suggesting that BDNF can modulate mitochondrial physiology. However, the molecular mechanisms by which BDNF stimulates mitochondrial function in neurons remain to be elucidated. Like BDNF, enhanced PKA activity within mitochondria has been shown to foster dendrite outgrowth, promote mitochondrial trafficking, and enhance oxidative phosphorylation. In this study, we surmised that BDNF binds to the Trkβ receptor and translocates to mitochondria to govern mitochondrial physiology in a PKA-dependent manner. Translocation assays through confocal microscopy and biochemical sub-cellular fractionation assays confirm the localization of the Trkβ receptor to mitochondria. The translocation of the Trkβ receptor to mitochondria was significantly enhanced upon treating primary cortical neurons with exogenous BDNF, leading to rapid PKA activation. Showing a direct role of BDNF in regulating mitochondrial structure/function, time-lapse confocal microscopy in primary cortical neurons showed that exogenous BDNF enhances mitochondrial fusion, increases mitochondrial trafficking, and mitochondrial content within dendrites, which led to increased oxidative phosphorylation and glycolysis. Mechanistically, the effects of BDNF on mitochondrial physiology require activation of

PKA as treating primary cortical neurons with a pharmacological inhibitor of PKA or transiently expressing constructs that target an inhibitor peptide of PKA (PKI) to the mitochondria abrogated the effects of BDNF on mitochondrial structure and movement. In addition, biochemical assays showed that BDNF stimulates PKA-mediated phosphorylation of Drp1 and Miro-2 to promote mitochondrial fusion and elevate mitochondrial content in dendrites, respectively. These physiological effects induced by BDNF were associated with increased resistance to oxidative stress induced by rotenone. Overall, this study revealed novel molecular mechanisms of BDNF-mediated neuroprotection and "Mito-protection" which involves enhancing mitochondrial health and the bioenergetic landscape of neurons.

## Introduction

BDNF, a member of the neurotrophin family, plays a critical role in regulating neuronal function, development, and survival (Reichardt, 2006). BDNF is initially synthesized as a precursor protein in the endoplasmic reticulum and is processed to pro-BDNF by cleaving the signaling peptide. The terminal domain of pro-BDNF is then further cleaved by plasmin to generate the mature, 13kDa active form of BDNF (Lessmann & Brigadski, 2009). While pro-BDNF binding to the p75 receptor is primarily implicated in apoptosis, the mature form of BDNF exerts its neurotrophic effects by binding to Tropomyosin receptor kinase β (Trkβ) (Costa et al., 2018). Activation of Trkβ by BDNF leads to receptor dimerization, kinase activation, and autophosphorylation on specific tyrosine residues, such as Tyr-670/674/675/785 (Middlemas et al., 1994). The phosphorylated and activated Trkβ receptor recruits several intracellular adaptor proteins, including Shc2, via SH2 domains,

initiating multiple signaling cascades such as Ras/MAPK-ERK pathway, PI-3 kinase (PI3-K) pathway, and phospholipase C (PLC) pathway. These pathways are involved in various neuronal processes, such as growth, maintenance, survival, dendrite outgrowth, and differentiation (Ahmed & Prigent, 2017; Reichardt, 2006; You et al., 2010). Moreover, BDNF also functions as a self-amplifying signal to promote neuronal growth by inducing Trkβ-dependent activation of protein Kinase A (PKA). This triggers the synthesis and secretion of additional BDNF, further augmenting BDNF function. In its inactive state, PKA is a tetrameric holoenzyme consisting of two catalytic subunits and two regulatory subunits (Zhang et al., 2012). When cyclic AMP, the second messenger, binds to the catalytic subunits of PKA, the PKA holoenzyme rapidly dissociates, leading to the downstream phosphorylation of various substrates, including cyclic AMP response binding element protein (CREB), a transcription factor. Phosphorylated CREB at serine 133 then translocates from the cytosol to the nucleus to activate several pro-survival and pro-differentiation transcription programs in neurons (Quinn, 2002). PKA is a crucial player in maintaining various neuronal functions in the mitochondria, including bioenergetics, neuronal development, neurotransmission, and mitochondrial homeostasis (Cao et al., 2011; Ould Amer & Hebert-Chatelain, 2018; Piccini et al., 2015; Zhang et al., 2019). The regulation of PKA signaling is well organized and compartmentalized, as it forms a complex with scaffolding proteins, such as A-kinase anchoring protein (AKAP), to target subcellular domains. Localized PKA signaling in the mitochondria is amplified through the association of PKA with D-AKAP1, the murine homolog of human Dual specificity AKAP1. This interaction leads to the PKA-mediated phosphorylation and inhibition of dynamin-related protein (Drp1), a mitochondrial fission modulator that stabilizes the

mitochondria and supports neuronal survival (Merrill & Strack, 2014). Research has demonstrated that when Drp1 is phosphorylated by PKA, it increases the ability of neurons to withstand toxic insults like staurosporine, $H_2O_2$, and rotenone (Merrill et al., 2011). Mitochondria not only function as energy hubs by generating ATP through oxidative phosphorylation, but also sequester $Ca^{+2}$ and synthesize critical regulatory molecules such as reactive oxygen species (ROS), which can trigger differentiation of neurons and immune system cells, and are crucial for maintaining synaptic plasticity in neurons (Giorgi et al., 2018). In addition, proper functioning of the neuronal network requires the trafficking of mitochondria throughout the neuron and their recruitment to regions with high metabolic demands. Miro-2, a mitochondrial adaptor protein, is phosphorylated by PKA, resulting in increased anterograde mitochondrial movement towards dendrites and retrograde movement towards the soma (Das Banerjee et al., 2017). It has been demonstrated that when the concentration of $Ca^{+2}$ increases in the cytoplasm and axons, Miro-1 is broken down, leading to a halt in mitochondrial transport in axons (Nguyen et al., 2021). Another crucial factor in synaptic plasticity is BDNF, which boosts neuronal activity that is dependent on synaptic strength through long-term potentiation (Aicardi et al., 2004; Lu et al., 2008). BDNF is responsible for the increased transcription of pro-survival programs such as B-cell lymphoma 2 (Bcl2) mRNA level (Guan et al., 2019), tyrosine hydroxylase (TH), local dendritic mRNAs (Leal et al., 2014), tissue plasminogen activator (tPA) (Pang et al., 2004), synaptic markers, vesicles, and other PKA-modulated proteins via CREB.

Although BDNF is known to activate various signaling pathways within the cell membrane and cytosolic compartments upon binding to Trkβ, recent evidence suggests that it also has

a direct physiological impact on mitochondrial structure and function. Specifically, studies have demonstrated that BDNF can increase the respiratory coupling efficiency of neurons, thereby regulating mitochondrial efficiency and promoting ATP synthesis. For instance, in an *in vitro* synaptosome-mitochondrial preparation, BDNF was shown to enhance the respiratory control index of rat brain mitochondria (Markham et al., 2014; Markham et al., 2004). Additionally, BDNF can stimulate mitochondrial biogenesis by activating mitogen-activated protein kinases (MAPKs) and CREB, which enhances peroxisome proliferator activated receptor gamma coactivator 1-alpha (PGC-1α) promoter activity. This process is critical for the formation and maintenance of hippocampal dendritic spines and synapses (Cheng et al., 2012). On the other hand, activation of PGC-1α and secreted Irisin has been shown to increase BDNF release in the hippocampus (Wrann et al., 2013). Another study reported that BDNF can activate mitophagy through the HIF-1 α/BNIP3 signaling pathway in endothelial cells (Jin et al., 2019). Despite the growing evidence suggesting that BDNF plays a role in regulating mitochondrial function and dendrite health, the exact molecular mechanisms underlying this regulation remain unknown. In this study, we present novel findings that demonstrate how exogenous BDNF treatment can lead to the translocation of Trkβ to mitochondria, thereby promoting neuronal maintenance through the stimulation of mitochondrial trafficking, dynamics, and bioenergetics. Moreover, we report for the first time the molecular mechanisms by which BDNF regulates mitochondrial trafficking, dynamics, content, and bioenergetics through the activation of PKA signaling and the subsequent phosphorylation of OMM-localized substrates, including Drp1 and Miro2.

## Materials and methods

**Culture of primary cortical neurons**: Primary cortical neurons were prepared from wild-type (WT) E15 C57BL/6 mouse embryos as previously described (Soman et al., 2021). Briefly, the E15 embryos were individually extracted, dissected from the embryonic sac, and placed into separate wells containing dissection media [DMEM (Thermo Fisher Scientific, Waltham, MA), 5% FBS (Sigma-Aldrich, St. Louis, MO), and 0.5mM Glutamax (Thermo Fisher Scientific, Waltham, MA)]. The intact whole brain was extracted from the severed head of the E15 embryos. The cortices were micro-dissected from the brain and placed into ice-cold plating media [Neurobasal media (Thermo Fisher Scientific, Waltham, MA), 2% FBS, 2% B27 (Thermo Fisher Scientific, Waltham, MA), 0.5mM Glutamax, 25µM Glutamic acid (Sigma-Aldrich, St. Louis, MO), 100 U/ml penicillin/streptomycin (Thermo Fisher Scientific, Waltham, MA)] and mechanically dissociated with repeated pipetting (12-15 times) with a 1mL pipettor. The cell density was determined using a hemocytometer, and subsequently, primary cortical neurons were plated on poly-L-Lysine (P4832; Thermo Fisher Scientific, Waltham, MA) coated sterile cell culture plates [Lab-Tek™ IV Chamber Slides (0.5ml media/well)- 2 X $10^6$ cells/mL; 12 well plate (0.5ml media/well)- 2 X $10^6$ cells/mL; 6 well plate (2ml media/well)- 3.5 X $10^5$cells/mL] in pre-warmed plating media. The plates containing primary cortical neurons were maintained at 37°C, 5% $CO_2$ / 95% humidity in a cell culture incubator. Approximately 1/3$^{rd}$ of the culture medium was then changed every three days and replaced by fresh serum-free maintenance media [Neurobasal media (Thermo Fisher Scientific, Waltham, MA), 2% B27 (Thermo Fisher Scientific, Waltham, MA), 0.5mM Glutamax (Thermo Fisher Scientific, Waltham, MA)].

**Transfection**: DNA plasmids that encode RFP targeted to mitochondria (Mito-RFP) and C-terminally tagged GFP to Trkβ (Trkβ -GFP) were purchased from (AddGene plasmid #83952, Trkβ mEGFP was a gift from Ryohei Yasuda), C-terminally GFP tagged inhibitor of PKA targeted to the OMM (Mito-PKI-GFP) were provided by Dr. Stefan Strack (University of Iowa, Department of Pharmacology). For primary cortical neurons grown in Lab-Tek™ IV Chamber Slides, 1µg of DNA plasmid was diluted in OPTIMEM media (Thermo Fisher Scientific, Waltham, MA) and mixed with Lipofectamine 2000 (Thermo Fisher Scientific, Waltham, MA) at a final concentration of 1%. Cells were subsequently treated with combined and diluted DNA: Lipofectamine mixture. 24hrs. following transfection, up to 2/3rd of the media was changed with pre-warmed maintenance media.

**Extraction of mitochondria from brain tissue**: WT mice were perfused using PBS supplemented with glucose for the prevention of blood clots and to clear the brain tissue from serum albumins. The brain was weighed, and 200mg of tissue was dissected and used for mitochondrial isolation. The brain tissue was homogenized with a Dounce homogenizer (10-15 times) in ice-cold mitochondrial isolation buffer [3mM HEPES (pH 7.4), 210mM Mannitol, 70mM Sucrose, 0.2mM EGTA; Add 1 ml mitochondrial isolation buffer /0.1 g of tissue] supplemented with protease inhibitor cocktail and 40mg bovine serum albumin without forming bubbles. Following homogenization, the homogenate was separated into multiple Eppendorf tubes on ice and centrifuged 4ºC at 700 x g for 10 min, the supernatant was collected, whereas the resulting pellet was saved as the whole lysate fraction. The homogenized lysate was transferred to ice cold Eppendorf tubes and centrifuged at 600 x

g for 10 min at 4°C. The supernatant was collected and transferred to new Eppendorf tubes and the pellet was stored as nuclear fraction which was labeled as lipid phase for Western blots. The supernatant was then centrifuged at 15,000 x g for 15 min at 4°C for subcellular fractionation, and the subsequent supernatant was transferred to new Eppendorf tubes and labeled as cytoplasmic fraction. The pellet was washed several times (3-5X) with mitochondrial isolation buffer and centrifuged at 15,000 x g for 15 min at 4°C. The pellet, being the mitochondrial fraction, was labeled and resuspended in storage buffer and stored at -80°C.

**Western blotting and $Mn^{2+}$ Phos-tag™ SDS-PAGE**: Primary cortical neurons were harvested and lysed on ice using lysis buffer [50mM Tris-HCl, 150mM NaCl, 0.25% SDS, 1mM EGTA, 1mM EDTA, 1% Triton X, 10mM NaF, 1mM dithiothreitol, 0.5mM $NaVO_3$, 1X protease inhibitor cocktail (Roche, Basel, Switzerland)]. Cell lysates were then centrifuged for 15min at 13,000 x g, and the resulting supernatants were transferred to sterile 1.5 mL microcentrifuge tubes. The protein amount in cell lysates was determined by employing the Pierce BCA protein assay kit per manufacturer's instructions (Thermo Fisher Scientific, Waltham, MA). Sample buffer [5% Mercaptoethanol in 4X Laemmli buffer (Bio-Rad Laboratories, Hercules, CA)] was added to each of the cell lysate samples and boiled for 5 min at 90°C. Proteins were then resolved in SDS/PAGE electrophoresis by using polyacrylamide gels composed of various acrylamide percentages, per the molecular weight of the proteins of interest to be analyzed (7.5%, 10%, 12.5%). The separated proteins were then transferred onto a PVDF membrane using a semi-dry transfer system (BioRad Laboratories, Hercules, Ca) at 250 mA for 45min. The PVDF membrane

was then blocked in TBST [20mM Tris, pH 7.5, 150 mM NaCl, 0.05% Tween 20 (v/v)] containing 5% skimmed milk or with 2-5% BSA for 2hrs. at RT with gentle shaking on an orbital rocker. The PVDF membranes were then incubated overnight at 4°C with primary antibodies. Following incubation with primary antibodies, the PVDF membranes were rinsed in TBST and subsequently incubated with the respective horseradish peroxidase (HRP)-conjugated secondary antibodies for 2hrs. at RT. Chemiluminescence substrate kit SuperSignal™ Western Blotting Substrate was used to detect immunoreactive proteins and were visualized by a detector [ChemiDoc™MP Imaging System (170-8280) Bio-Rad Laboratories, Hercules, CA]. Densitometric analysis of immunoreactive bands in technical replicates of each protein marker of interest was performed by using NIH ImageJ (version 1.44-1.50i) software (NIH, Bethesda, MD) as previously published (Tania Das Banerjee et al., 2021; Soman et al., 2021). The integrated density for each immunoreactive band of interest was normalized to β-tubulin. $Mn^{2+}$/Phos-tag™ was employed for analyzing the phosphorylation of endogenous proteins-Miro-2 and Drp1 as previously published but with the following modifications (Das Banerjee et al., 2017). The major difference from the conventional SDS/PAGE electrophoresis pertains to the preparation of the acrylamide gel with the addition of $Mn^{2+}$/Phos-tag. Also, following electrophoresis, the gels were treated with 10mM EDTA to remove $Mn^{2+}$ for efficient transfer.

**Immunocytochemistry**: PFA-fixed primary cortical neurons were immunolabeled as previously described (Das Banerjee et al., 2017), but with the following minor modifications. Briefly, dissociated cultured primary neurons were fixed in 4% PFA and then permeabilized with PBST (PBS supplemented with 0.3% Triton X 100) for 15min.

Subsequently, cells were blocked in 2.5% BSA for 1hr., incubated in primary antibodies overnight at 4°C, washed four times in PBST (5-10 min/wash), and subsequently incubated in applicable secondary antibody for 1hr. at room temperature. Primary cortical neurons were then counter-stained with 4′,6-diamidino-2-phenylindole (DAPI) (Molecular Probes, Eugene, CA) at a concentration of 1.25 µg/ml and stored for imaging.

**Image acquisition and analysis**: Epifluorescence microscopy: EVOS-FL Cell Imaging System (Thermo Fisher Scientific, Waltham, MA) with a 40X objective. The images were analyzed using Image J software and compatible plugin-Neuron J (Erik Meijering, Biomedical Imaging Group Rotterdam, Netherlands).

**Mitochondrial trafficking**: To study mitochondrial trafficking, primary cortical neurons were transfected with 0.5 µg Mito-RFP for 24hrs. Up to 12-15 transfected primary cortical neurons were imaged for mitochondrial transport analysis. Transfected primary cortical neurons were identified by the red fluorescence emitted from Mito-RFP expression as well by their characteristic elongated axons and dendritic arbors that are noticeable by the "bleed through" extra-mitochondrial fluorescence emitted by Mito-RFP expression. The movement of mitochondria was recorded via live-cell imaging, using a Leica spinning disk confocal microscope containing a Plan-Apochromat 100X/oil objective. The mitochondrial movement was recorded every 10 seconds for four minutes. Kymographs were analyzed using Image J v 1.44 (Bethesda, MD, USA) and compatible plugin 'Multiple Kymograph' (J. Rietdorf, A. Seitz, EMBL, Heidelberg). In brief, the movement of mitochondria was characterized as 'anterograde' if mitochondria moved away from the cell body, and

'retrograde' for movement toward the cell body. Hence, to assign the direction of moving mitochondria for each neuron of interest in a consistent manner, the 'movement tracks' of mitochondria were always traced from left to right of the cell body. Mitochondrial velocity and distance were assessed for at least 50–70 mitochondria per neuron, for 6–7 transfected primary cortical neurons per condition.

**Translocation studies**: Primary cortical neurons were co-transected with Mito-RFP and Trkβ -GFP (1:1 plasmid ratio) for 24hrs. in Lab-Tek™ IV chambered slides. Live-cell imaging was performed using a Leica spinning disk confocal microscope or an Olympus Fluoview1000 laser-scanning confocal microscope running Fluoview FV10-ASW software (Olympus Corporation, Waltham, MA, USA, RRID:SCR_014215), using a × 60 oil objective plus digital zoom. The translocation of Trkβ-GFP puncta to mitochondria labeled with Mito Tracker Red or with Mito-RFP was analyzed in at least 15-17 transfected primary cortical neurons by using ImageJ plugin Coloc2 program and manually by counting the number of yellow puncta (Dagda et al., 2008). Given that Trkβ is localized to the outer mitochondrial membrane, mitochondria that were decorated or delineated with Trkβ-GFP but did not completely colocalized were counted as associated structured but included in the analysis. In addition to counting the mean number of Trkβ-GFP puncta per neuron, the mean number of Trkβ puncta that translocated to mitochondria was calculated within the dendrites or soma of neurons.

**Analyzing bioenergetics:** The effect of BDNF on the bioenergetic status of primary cortical neurons was analyzed by studying oxidative phosphorylation (OXPHOS) and

glycolysis using Seahorse XF24 Extracellular Flux Analyzer (Agilent, Santa Clara, CA). In brief, primary cortical neurons were plated (75,000 cells/well) in poly-L-Lysine pre-coated 24 well XF cell culture plates and exposed to BDNF (35ng/well, 2hrs.), ANA12 (200nM, 2hrs.) and H89 (1µM, 2hrs.) respectively which were injected from one of the injection ports into the wells (quadruplicate wells) via the Seahorse XF24 Extracellular Flux Analyzer. Cells were subsequently washed with pre-warmed XF assay media. After washing 3 x, cells were further incubated in the respective media (37 °C, 1 hr.) in a $CO_2$-free incubator to further purge $CO_2$ and allow temperature/pH equilibration before each set of measurements in the metabolic analyzer. Each plate contained four wells that were not seeded with neurons which served as blank controls. The real-time oxygen consumption rates (OCRs), which is an indicator of OXPHOS, and extracellular acidification rates (ECARs), which is an indirect measurement of glycolysis, were monitored by quantifying the following parameters: the non-mitochondrial oxygen consumption (the OCRs measured following injection with rotenone and antimycin-A), the basal respiration (the last OCR measured prior to exposing cells to the ATP synthase inhibitor oligomycin), the maximal respiration (the maximum OCR rate measurement obtained following exposure of cells with the mitochondrial uncoupler FCCP), the proton ($H^+$) leak (the residual OCRs measured following oligomycin injection minus the OCRs obtained following rotenone/antimycin A injection), the ATP production (the baseline OCRs minus the OCRs obtained following exposing cells to oligomycin injection), and the mitochondrial reserve capacity (the maximal OCR minus the basal OCR). At the end of the Seahorse experiment, to allow a comparison among biological replicates, the data was normalized by cell number, as further described below. Immediately after the assay, the primary cortical neurons were

fixed using 4% paraformaldehyde. Post fixation, the primary neurons were treated with DAPI and imaged using ImageXpress Nano high content automated microscope, to quantify cell counts for each well of the tissue culture plate as previously described (Soman et al., 2022). The metabolic parameters of the assay basal and maximal respiration, proton leak, and ATP production through oxidative phosphorylation—were calculated by using the Agilent/Seahorse XF Report Generator software and expressed as OCR in pmol/min and normalized to the cell counts obtained by using the ImageXPress Nano system. The results are illustrated as means ± standard error from at least three to six independent experiments performed in triplicate.

**Assaying mitochondrial membrane potential:** TMRM (tetramethyl rhodamine methyl ester) assay was employed to evaluate the effect of BDNF treatment on mitochondrial membrane potential. Whole brain isolated mitochondria were plated on a 96 black well plate at 15µg per well. The mitochondria were treated with FCCP (20µM) negative control, malic acid (5mM) positive control and BDNF (100ng/50ul,150ng/50ul) for time respectively, and loaded with TMRM (200nM) and incubated for 45 mins at RT. A plate reader was used to measure fluorescence at 573 to 590 nm wavelength.

**Mitochondrial reactive oxygen species imaging in primary cortical neurons:** Primary cortical neurons were seeded on 4-well chamber slides (Lab-Tek) at a density of 75,000 neurons per well. The experimental conditions consisted of a control group, a rotenone treatment group, and a rotenone treatment combined with a BDNF treatment group. At 5 DIV, the neurons were treated with BDNF (100ng/ml) for 1hr. Subsequently, the neurons

were treated with 0.5 µM rotenone for 1 hr. to induce mitochondrial reactive oxygen species production. Finally, the neurons were incubated with 1 µM MitoSox ((Mitochondrial Superoxide Indicators, Invitrogen) for 20 mins, followed by DRAQ5 nuclear staining. The maintenance media was exchanged with fresh phenol red-free maintenance media prior to imaging. The images were acquired using an Olympus Fluoview1000 laser-scanning confocal microscope running Fluoview FV10-ASW software (Olympus Corporation, Waltham, MA, USA, RRID:SCR_014215), using a × 40 X oil objective.

**Statistical analysis:** Unless indicated otherwise, results are expressed as mean ± SEM from three independent experiments. Data were analyzed by Student's t-test (two-tailed) for pairwise comparisons, whereas multiple group comparisons were made by performing a One-way ANOVA followed by Bonferroni-corrected Tukey's test and Dunnett's multiple comparison test, using the GraphPad Prism software (version 6.0). P-values less than 0.05 were considered statistically significant.

## Results

### BDNF receptor Trkβ localizes to mitochondria.

While it has been shown that BDNF influences mitochondrial structure and function (Markham et al., 2004), the molecular mechanisms by which this neurotrophic factor regulates mitochondrial physiology remains elusive. Given that BDNF stimulates mitochondrial movement (e.g., mitochondrial motility in axons) and Trkβ complexes have been reported to localize to mitochondria, we wanted to investigate the molecular

mechanisms by which BDNF regulates mitochondrial structure/function in the dendrites and the soma of neurons. Here, we hypothesized that BDNF regulates mitochondrial structure and function by promoting the early translocation of Trkβ to the mitochondria in neurons. To test this hypothesis, we transiently transfected primary cortical neurons with a plasmid that expresses a C-terminally GFP-tagged Trkβ via Lipofectamine-mediated transfection, in the absence and presence of exogenous treatment with recombinant human BDNF and tracked the localization of Trkβ -GFP in live neurons via confocal microscopy. Indeed, we observed that a significant proportion of Trkβ -GFP puncta translocated with mitochondria under basal conditions (Fig. 1 A-E). Furthermore, in the presence of BDNF, we noticed that some of the Trkβ-GFP puncta either colocalized with mitochondria or surrounded mitochondria by forming distinct fluorescent rings that engulfed red fluorescent mitochondria within dendrites and soma (Fig. 1A); hence, given these distinct phenotypes, these GFP puncta that surrounded mitochondria, without showing perfect colocalization, were counted "translocation" events along with colocalized puncta within neurons. By quantifying the mean number of translocation events per neuron, we observed that exogenous treatment of BDNF for 4hrs. in the primary cortical neurons significantly elevated the translocation of Trkβ to mitochondria in dendrites and the soma compared to untreated neurons (Fig. 1A-C). A less pronounced, non-significant increase in the mean number of translocation events in the dendrites and soma were observed at a later time point (24hrs.) of BDNF treatment (Fig. 1D-E). In the presence of ANA12, a pharmacological inhibitor of Trkβ receptor, we noted that BDNF treatment for 4 hrs. was unable to significantly increase translocation of Trkβ to mitochondria in the dendrites or the soma suggesting that binding and activation of Trkβ is required for its translocation to

the mitochondrion. It is worth noting that the significant increase in the mean number of translocation events in neurons treated with exogenous BDNF is not due to an increase in the total number of Trkβ-GFP puncta as the mean number Trkβ-GFP puncta in the dendrites or soma per neuron was not significantly increased in neurons exposed to BDNF (Suppl. Fig. 1). Overall, our data suggest that exposing neurons to BDNF increases the translocation of Trkβ receptor to mitochondria, a physiological event that requires the binding of BDNF with Trkβ (Fig. 1B, 1D). In addition, this data is consistent with a previous report that Trkβ colocalizes with mitochondria under basal conditions (Markham et al., 2004). To confirm the presence of endogenous Trkβ within the cytosolic and mitochondrial compartments, we isolated mitochondria from the whole brains of 4-month-old mice by subcellular fractionation and immunoblotted for endogenous Trkβ receptor and mitochondrial markers. In brief, we observed that Trkβ predominantly localizes in isolated mitochondria relative to the cytosolic compartment, whereas a significant fraction remains in the lipid fraction, consistent with the localization of Trkβ within cell membranes (Fig. 1F; Suppl. Fig. 1). Overall, these observations show that Trkβ localizes to mitochondria, and its translocation can be enhanced via functional activation of the receptor by BDNF.

**BDNF promotes mitochondrial fusion in dendrites in a PKA-dependent manner.**

In primary mouse embryonic fibroblasts (MEFs), mitochondrial fusion is a protective mechanism against oxidative stress, given that the increased surface area of mitochondria is associated with decreased probability in the release of apoptotic factors, including cytochrome c (Gomes et al., 2011). Mechanistically, PKA increases mitochondrial fusion by phosphorylating S637 on Drp1 (Kim et al., 2019) and thereby restricting mitochondrial

fission. We hypothesized that BDNF activates downstream PKA signaling to regulate mitochondrial structure/function in neurons. Indeed, we observed that exogenous treatment of BDNF in primary cortical neurons rapidly stimulates PKA activity within 5-15 minutes of treatment (Suppl. Fig. 2) and concomitantly increased the endogenous levels of the PKA scaffolding protein D-AKAP1 as measured by Western blot analyses of cell lysates from SH-SY5Y neuroblastoma cells treated with exogenous recombinant BDNF, indicating that BDNF mediates enhanced localized PKA activity at the mitochondria presumably by increasing the endogenous levels of D-AKAP1 (Suppl. Fig. 3). Next, we hypothesized that BDNF influences mitochondrial remodeling by stimulating PKA-mediated phosphorylation of Drp1 to inhibit its fission activity. In contrast, impeding PKA function is expected to terminate BDNF mediated mitochondrial fusion within dendrites. To test this hypothesis, primary cortical neurons were treated with exogenous BDNF at two time points (4 and 24 hrs.) and transfected with the following panel of plasmids to decrease PKA activity: PKI-GFP (C-terminally GFP tagged plasmid coding for Protein Kinase Inhibitor peptide), OMM-PKI-GFP (also known as Mito-PKI-GFP for the purposes of this paper, PKI targeted to the outer mitochondrial membrane via a TOM20 leader sequence), and mitochondrially targeted RFP (Mito-RFP) for assaying mitochondrial length and distribution using live-cell imaging with a confocal microscope. In brief, we observed that BDNF treatment significantly increased mitochondrial length in dendrites compared to control (Fig. 2B) in a bimodal manner. While exposing primary cortical neurons with 50ng/mL BDNF was able to significantly increase mitochondrial length (Fig. 2B), treatment with a higher concentration of BDNF (75ng/mL) did not significantly increase mitochondrial length showing a bimodal effect. In addition, we observed that treatment of

BDNF 4hrs. (Fig. 2C) or 24hrs. (Fig. 2D) significantly increased mitochondrial length of dendritic mitochondria, but not when PKI, a specific endogenous inhibitor of PKA, or Mito-PKI-GFP, was transiently expressed in primary cortical neurons (Suppl. Fig. 4). Overall, these observations show that BDNF increases mitochondrial length in a PKA-dependent manner.

**BDNF promotes mitochondrial length via phosphorylation of Drp1.**

Thus far, our data suggest that the ability of BDNF to increase mitochondrial length is PKA dependent (Fig. 2, Suppl. Fig. 2, Suppl. Fig. 3). Given that PKA-mediated fusion of mitochondria is associated with PKA mediated phosphorylation of Drp1 at serine 637 (mouse) (J Thomas Cribbs & Stefan Strack, 2007), we hypothesized that BDNF promotes mitochondrial fusion by enhancing PKA mediated phosphorylation of Drp1 and thereby restricting mitochondrial fission. To test this hypothesis, primary cortical neurons were treated with exogenous recombinant human BDNF and co-transfected with either wild-type (WT) Drp1 or a PKA phosphorylation site resistant mutant of Drp1 (with Drp1-S656A), and with Mito-RFP plasmids 48hrs. post-transfection, the cells were analyzed for mean length and distribution of mitochondria within dendrites (mitochondrial content, as defined by the percentage of a consistent length of a dendrite occupied by mitochondria) of neurons through live cell imaging with a confocal microscope (Fig. 3A). Briefly, while exogenous treatment with BDNF alone increased mitochondrial length compared to control cells, BDNF treatment (4hrs.) partially increased the mean mitochondrial length and mitochondrial content in the presence of WT-Drp1-GFP, but not when Drp1-S656A-GFP was expressed (Fig. 3B, 3C). The data suggest that mitochondrial fission induced by

transient expression of both GFP tagged Drp1 constructs can counteract the mitochondrial fusion stimulating effects of BDNF. It is worth noting that the abilities of the Drp1 (S656A) to completely negate the effects of BDNF in increasing mitochondrial length were not attributed to differences in expression of the individual plasmids in transiently transfected primary cortical neurons as both plasmids are expressed to similar levels as noted by their GFP fluorescence (Suppl. Fig. 5). Mechanistically, the data indicates that BDNF promotes mitochondrial fusion in dendrites via PKA mediated phosphorylation of Drp1 at S637. To biochemically verify that exogenous treatment of primary cortical neurons with BDNF promotes mitochondrial fusion via phosphorylation of Drp1, we employed Phos-Tag™-mediated identification of phosphorylated proteins by performing an SDS-PAGE of cell lysates extracted from primary cortical neurons treated with exogenous human recombinant BDNF. Indeed, we observed that BDNF significantly increased the phosphorylation of Drp1 (Fig. 3D-E) within 4hrs. of treating primary cortical neurons as evident by the presence of a higher molecular weight species of Drp1. However, co-treatment of BDNF with ANA12, a pharmacological inhibitor of Trkβ, significantly reduced the ability of BDNF to phosphorylate Drp1, indicating that the BDNF mediated phosphorylation of Drp1 requires binding and activation of its cognate receptor (Trkβ). By using a phospho-specific antibody for the PKA site in Drp1 (S637), we were able to confirm that exogenous treatment of primary cortical neurons with BDNF increased the ratio of phosphorylated Drp1 relative to total Drp1 but not in the presence of ANA12 (Suppl. Fig. 6). Mechanistically, these observations show that BDNF-mediated mitochondrial fusion and increased mitochondrial content (as defined by the percentage of a consistent length of

a dendrite occupied by mitochondria) in dendrites involves PKA mediated phosphorylation of Drp1 at serine 637.

**BDNF increases anterograde and retrograde mitochondrial trafficking in dendrites.** Mitochondria are dynamic organelles that undergo fission and fusion events but also traffic to areas of high energy demand, specifically in the dendrites and axons of neurons, to aid in functions such as calcium sequestering and to supply ATP (Bartolák-Suki et al., 2017; Pallafacchina et al., 2018; Sheng et al., 2012). In PINK1-deficient neurons, pharmacological and molecular approaches that enhance PKA activity within mitochondria can reverse mitochondrial pathology within dendrites induced by loss of endogenous PINK1, including reversing mitochondrial fission, loss of mitochondrial content in dendrites, decreased transmembrane potential while restoring mitochondrial trafficking in dendrites (Dagda et al., 2011; Das Banerjee et al., 2017). Given that enhanced PKA activity regulates mitochondrial trafficking, and content in dendrites, we hypothesized that BDNF modulates mitochondrial trafficking in dendrites via downstream activation of PKA. To test the hypothesis, we transiently transfected primary cortical neurons with Mito-RFP in the absence and presence of exogenous human BDNF, analyzed the trafficking and distribution of mitochondria by employing a spinning disc confocal microscope, and quantified mean velocity of moving mitochondria by analyzing kymographs assembled from stacks of epifluorescence images (Fig. 4A). In brief, we observed that exogenous treatment of primary cortical neurons with BDNF for 24hrs. significantly increased both anterograde and retrograde movement in dendrites when compared to untreated neurons (Fig. 4B, 4C). Interestingly, exposing primary cortical neurons to a higher concentration of

BDNF (75ngs/ml) did not significantly enhance mean mitochondrial velocity compared to 50ngs/ml of BDNF (Fig. 4B, 4C). Overall, these observations show that BDNF enhances mitochondrial trafficking in a bi-directional manner in dendrites.

**BDNF increases anterograde and retrograde mitochondrial trafficking in a PKA dependent manner.**

Next, to determine the extent that BDNF regulates mitochondrial trafficking by enhancing PKA activity (Suppl. Fig. 2), primary cortical neurons were treated with exogenous recombinant human BDNF and co-transfected with either PKI-GFP (C-terminally GFP tagged plasmid coding for protein kinase inhibitor peptide), or with OMM-PKI-GFP (mitochondrial targeted PKI), to inhibit PKA in the cytosolic or mitochondrial compartments respectively, and with Mito-RFP (RFP targeted to mitochondria) to label mitochondria. By performing time lapse spinning disc confocal microscopy, we observed that primary cortical neurons (Fig. 5A) treated with BDNF for 4 hrs., significantly increased mitochondrial anterograde movement, but this effect is transient as it is not significant at 24hrs. following treatment (Fig. 5B), consistent with our mitochondrial trafficking data shown in Figure 4. However, co-expression of PKI or of Mito-PKI significantly blocked the ability of BDNF in enhancing anterograde or retrograde mitochondrial movement (Fig. 5A, 5C). Overall, our observations show that bi-directional increase of mitochondrial trafficking in the dendrites is modulated by BDNF via PKA.

**BDNF increases mitochondrial trafficking through PKA mediated phosphorylation of Miro-2.**

Next, we investigated the molecular mechanisms by which BDNF regulates mitochondrial trafficking and content within dendrites. We have previously shown that mitochondrial PKA (D-AKAP1/PKA) phosphorylates the mitochondrial adaptor protein Miro-2 to stimulate bi-directional mitochondrial trafficking and mitochondrial content within dendrites (Das Banerjee et al., 2017). To this end, we hypothesized that BDNF enhances bi-directional mitochondrial trafficking and content via PKA-mediated phosphorylation of Miro-2. To test our hypothesis, primary cortical neurons were treated with exogenous recombinant human BDNF in the presence or absence of ANA12, a pharmacological inhibitor of Trkβ, and analyzed for the phosphorylation of Miro-2 by performing Western blot/Phos-tag assays. Given that commercial antibodies that recognize the PKA phosphorylation sites in Miro-2 are currently not available, performing Western blot/Phos-tag assays is a well validated biochemical alternative to analyze the ability of BDNF, and other pharmacological compounds, to phosphorylate Miro-2. In brief, we observed that exogenous treatment of primary cortical neurons with BDNF for 4hrs. rapidly increased the phosphorylation of Miro-2 (Fig. 6A, 6B) as noted by the presence of higher molecular weight species detected with an anti-Miro-2 antibody. However, BDNF-mediated phosphorylation of Miro-2 was abolished in the presence of ANA12 indicating that BDNF promotes phosphorylation of Miro-2 by coupling with the Trkβ receptor (Fig. 6A, 6B). Next, to determine whether the ability of BDNF to increase mitochondrial content within dendrites requires PKA activity, primary cortical neurons were co-transfected with PKI-GFP or GFP-OMM-PKI, and with Mito-RFP to visualize dendritic mitochondria by time

lapse confocal microscopy. In brief, we observed that mitochondrial content (% of dendrites occupied by mitochondria) in the dendrites was increased significantly with 4hrs. BDNF treatment but not when PKI or Mito-PKI was co-expressed (Fig. 6C-D), suggesting that BDNF increases mitochondrial content by stimulating PKA activity within mitochondria. In another set of experiments, we transiently transfected primary cortical neurons with Mito-RFP and treated the neurons with exogenous BDNF, in the presence or absence of H89, a pharmacological inhibitor of PKA. Briefly, consistent with our transient transfection data (Fig. 6C-D), we observed that pharmacological inhibition of PKA by treatment of primary cortical neurons with H89 ceased the ability of BDNF to induce mitochondrial trafficking within dendrites (Fig. 6E, 6F). Overall, our collective imaging data shows that BDNF enhances bi-directional mitochondrial trafficking and content within dendrites in a PKA-dependent manner, presumably via mitochondrial PKA-mediated phosphorylation of Miro-2.

**BDNF increases bioenergetics in live neurons and in isolated mitochondria.**

Determining the bioenergetic status of neurons is a representative measurement of neuronal health (Theurey et al., 2019). BDNF mimetics can enhance mitochondrial respiration and mitochondrial biogenesis in skeletal muscles suggesting that BDNF directly regulates mitochondrial function (Wood et al., 2018). Given that BDNF regulates mitochondrial morphology, content and trafficking within dendrites in a PKA dependent manner (Fig. 2, Fig. 5) and the fact that exogenous BDNF can increase complex I activity in mitochondria isolated from brain-derived synaptosomes (Markham et al., 2004), we next hypothesized that exogenous treatment of primary cortical neurons with BDNF increases oxidative

phosphorylation in a PKA dependent manner and by binding to the Trkβ receptor. To test this hypothesis, primary cortical neurons plated on the Seahorse XF24 tissue culture plates were treated with exogenous BDNF at different time points in the presence or absence of H89 (pharmacological inhibitor of PKA), with/without ANA12 (pharmacological inhibitor of Trkβ) or co-treated with BDNF. Mitochondrial respiration and glycolysis were then measured by using an XF24eBioAnalyzer as previously published (Grigoruţă et al., 2020; Lujan et al., 2016; Soman et al., 2022). In brief, we observed exogenous treatment of primary cortical neurons with BDNF rapidly and significantly elevated oxygen consumption rates (OCRs) after 2hrs. of treatment. Specifically, exogenous treatment of primary cortical neurons with BDNF significantly increased both basal OCRs (Fig. 7A, 7C) and ATP-linked OCRs (Fig. 7B), while having no significant effects on maximal OCRs, or proton leak-associated OCRs (Fig. 7D, 7E). Unlike treatment with BDNF alone, treatment of BDNF with ANA12 did not significantly increase either basal or ATP-linked OCRs (Suppl. Fig. 7). On the other hand, co-treating primary cortical neurons with H89 modestly reduced both basal and ATP linked OCRs suggesting that BDNF enhances OXPHOS in manner that does not require global PKA activity (Fig. 7B-C). Although ATP linked OCRs is a proxy of ATP production, the data suggest that BDNF may positively influence ATP production through the ATP synthase. In contrast, we observed that co-treating primary cortical neurons with ANA12 completely negated the effects of BDNF in stimulating basal or ATP-dependent OCRs, suggesting that BDNF regulates mitochondrial respiration by binding and activating Trkβ receptor. Interestingly, we observed that exogenous treatment of primary cortical neurons with BDNF significantly elevated basal glycolysis (Fig. 7F, 7G) while only a non-significant effect was observed for maximal

glycolysis as analyzed by measuring the extracellular acidification rates (ECARs) (Fig. 7H). These data suggest that BDNF affects the overall bioenergetic states of neurons by enhancing both glycolysis and OXPHOS. To complement the mitochondrial respiration assays and to further corroborate the effects of BDNF on mitochondrial physiology, we measured the effects of treating isolated mitochondria derived from 4-month-old wild-type mice on transmembrane potential by using a multimode plate reader. In brief, whole brain mitochondria were co-treated with the red, potentiometric fluorescent dye TMRM to fluorescently quantify the mitochondrial transmembrane potential and with either exogenous recombinant BDNF (5 min.), treated with malic acid as a positive control for enhancing transmembrane potential, or with FCCP as a negative control to collapse transmembrane potential. The mean TMRM fluorescence was kinetically measured for up to 1hr. at 579/590 nm by using a multimode plate reader. In brief, we observed that exogenous treatment of isolated brain mitochondria with both 100ng/50uL of BDNF enhanced the TMRM fluorescence at mitochondrial membrane compared to untreated mitochondria. Indeed, treatment of isolated mitochondria with 100ng/50µL, but not with 150ng/50µL of BDNF, enhanced TMRM fluorescence in a time-dependent manner in a similar manner as treatment with malic acid (Fig. 7I). Therefore, in addition to remodeling mitochondria and trafficking in dendrites (Figs. 2-6), our collective bioenergetics data shows that exogenous BDNF directly modulates mitochondrial function via the Trkβ receptor (Suppl. Fig. 7), which can localize to mitochondria (Fig. 1).

**BDNF regulates mitochondria and protects dendrites from oxidative stress.**

Exogenous BDNF is a strong neuroprotective neurotrophin as evident by its ability to reduce or delay neurodegeneration in genetic and chemical models of Parkinson's disease (PD) and against a myriad of other toxic insults (Bifrare et al., 2005; Colucci-D'Amato et al., 2020; Jiao et al., 2016; Palasz et al., 2020). Like BDNF, elevating PKA signaling in either the mitochondrial (Tania Das Banerjee et al., 2021) or cytosolic compartments can protect neurons from apoptosis induced by multiple toxic insults (Almeida et al., 2005). To this end, we hypothesized that exogenous treatment of primary cortical neurons with BDNF protects dendrites and mitochondria against oxidative stress induced by rotenone, a complex I inhibitor used to chemically model PD *in vivo* and in cultured primary neurons (Merrill et al., 2011). To test this hypothesis, primary cortical neurons were treated with exogenous BDNF and with rotenone at 20nM, a dose known to induce dendrite degeneration without causing overt cell death for 24hrs. (Das Banerjee et al., 2017). Following treatments, primary cortical neurons were fixed and stained with antibodies specific MAP2B to label dendrites and with TOM20 to label mitochondria respectively. The extent of dendrite loss was measured by analyzing for mean dendrite length of MAP2B positive structures, and for mitochondrial loss by measuring the mean intensity of somatic and dendritic mitochondria labeled with anti-TOM20 antibodies. In brief, while rotenone drastically reduced dendrite length and mitochondrial content in primary cortical neurons as expected (Fig. 8A-C), co-treatment of primary cortical neurons with exogenous recombinant BDNF significantly reversed both the loss of dendrites and of mitochondria induced by rotenone treatment (Fig. 8A, 8C). Rotenone is a neurotoxin and a complex I inhibitor used to chemically model Parkinson's disease in cultured primary cortical and

midbrain dopamine neurons and *in vivo* sporadic models of PD. Rotenone can elicit an increase in the level of mitochondrial derived superoxide by blocking the electron flow from complex I to complex II (Sherer et.al., 2003). To identify the molecular mechanisms by which BDNF protects dendrites from rotenone mediated toxicity, we surmised that exposing neurons to pretreatment with BDNF may reduce the level of superoxide generated by dendritic mitochondria when exposed to complex I inhibitor rotenone. To measure the level of superoxide, we stained untreated live primary cortical neurons or treated (with BDNF or pretreated with BDNF and rotenone), with the red fluorescence permeable dye MitoSox. The superoxide levels were analyzed by confocal microscopy and ROS levels were measured by image analyses of the integrated density of MitoSox stained neurons and normalized to the number of DRAQ5-stained nuclei per epifluorescence field. In brief, we observed that pre-treating primary cortical neurons with BDNF for 4 hrs. efficiently reduced the level of superoxide induced by rotenone to the same extent as untreated cells (Fig. 8 D-E). Overall, these observations show that BDNF not only can significantly reverse the loss of dendrites, a measure of early stages of neurodegeneration, but can also protect mitochondria against overt oxidative stress induced by complex I inhibitor of mitochondria.

## Discussion

Over the past two decades, a wealth of scientific data has identified canonical physiological roles of BDNF, when bound to the Trkβ receptor, which include promoting synaptic plasticity, dendrite outgrowth, and neuronal survival in numerous brain regions including

the cerebral cortex, hippocampus, olfactory bulb, basal forebrain, mesencephalon, brainstem and spinal cord (Bathina & Das, 2015; Lipsky & Marini, 2007; Shen et al., 2018). Although the canonical roles of BDNF are associated with touting signaling pathways in the cytosol and cell membrane, novel non-canonical roles of BDNF in other compartments have been identified including modulating different aspects of mitochondrial behavior and function (Markham et al., 2014; Marosi & Mattson, 2014). For instance, BDNF modulates mitochondrial trafficking of proteins and mRNA in dendrites (Righi et al., 2000), increases mitochondrial trafficking in the axons (Adachi et al., 2005), and regulates oxidative phosphorylation via modulating mitochondrial complex 1 and IV activity (Markham et al., 2004). PINK1, a dual localized mitochondrial/cytosolic kinase, interacts with PKA to stimulate intracellular levels of BDNF levels and its extracellular secretion to maintain neuronal functions (Soman et al., 2021). Pharmacological stimulation of PINK1 by treating neurons with kinetin has been shown to remodel dendrite morphology via regulation of PKA (Soman et al., 2021). In that particular study, we showed that the PINK1 PKA signaling axis modulates BDNF synthesis, maturation and its extracellular release to regulate dendrite outgrowth in neurons. Furthermore, PINK1 and PKA work in succession to drive mitochondrial morphology, content, trafficking to dendrites, and ultimately dendrite remodeling (Das Banerjee et al., 2017; Soman & Dagda, 2021). Previously, transient transfections studies in primary neurons have shown that PKA-mediated phosphorylation of Drp1 at S637 inhibits its ability to fragment mitochondria (Dagda et al., 2011), thereby allowing pro-fusion modulators like Mitofusin 1 and 2 (MFN ½) and optic atrophy 1 (OPA1) to fuse the outer mitochondrial membranes (OMM) (Zorzano et al., 2010), and inner mitochondrial membranes (IMM) respectively of

mitochondria to promote mitochondrial fusion (J Thomas Cribbs & Stefan Strack, 2007). Overall, these studies raised the possibility that physiological functions of BDNF, which can be modulated by a mitochondrial targeted kinase (PINK1) and PKA, include regulating signaling pathways in the mitochondrion to enhance neuronal health and survival. Here, for the first time, we show that BDNF regulates multiple aspects of mitochondrial behavior and function including mitochondrial trafficking in dendrites (Fig. 4), mitochondrial shape (Fig. 2), and mitochondrial bioenergetics (Fig. 7), leading to augmented mitochondrial health in neurons, a reduction in oxidative stress and dendrite loss (neurodegeneration) induced by the complex I inhibitor rotenone (Fig. 8). In addition, we have shown that Trkβ receptor, upon activation by exogenous BDNF, rapidly and dynamically translocates from the cell membrane and localizes at mitochondria as assessed by confocal microscopy in live and in fixed neurons (Fig. 1; Supplementary Fig. S1). It is plausible that Trkβ, which may compass various signaling endosomes, elicit downstream signaling cascades in the proximity of the OMM, and extended BDNF treatment (24hrs.) is required for significant translocation of Trkβ to mitochondria to influence mitochondrial mobility, structure and function, presumably by increasing the endogenous levels of D-AKAP1, a mitochondrial-localized scaffold of PKA which redirects the endogenous pool of PKA from the cytosol to the mitochondrion (Suppl. Fig. 3). However, we recognize that studies are warranted to identify the specific sub-compartment that Trkβ is localized to in the mitochondria including the OMM, IMM or matrix, and the molecular players that it is coupled to and activates within mitochondria. Additionally, our data shows that BDNF increases the fused state of mitochondria (Fig. 2) presumably by phosphorylating Drp1 in a PKA dependent manner (Fig. 3) and in a bimodal manner. However, the extent that the translocation of

Trkβ to mitochondria is required for the effects of BDNF on mitochondrial physiology requires future experimental verification. Furthermore, our collective immunocytochemical data show that BDNF promotes mitochondrial fusion of dendritic mitochondria and increased mitochondrial content via eliciting PKA mediated phosphorylation of Drp1 and increasing the endogenous levels of D-AKAP1. However, the molecular mechanism(s) by which BDNF promotes PKA mediated phosphorylation of Drp1 remains to be elucidated. It is plausible that BDNF binds to Trkβ receptors to increase its mitochondrial translocation to activate PKA, presumably by increasing the localized concentration of cyclic AMP. Indeed, it has been shown that adenylate cyclizes (AC) have been localized inside the mitochondria (Kumar et al., 2009), and BDNF-Trkβ may activate mitochondrial ACs. Similarly, it has been reported that stimulation of the mitochondrial sAC–cAMP–inner mitochondrial PKA (mt-sAC) signaling pathway increases mitochondrial respiration and ATP synthesis (Acin-Perez et al., 2009). The physiological implications of the hyper fused state of mitochondria are linked to increased resistance of neurons to oxidative stress, enhanced neuronal survival and reduced mitochondrial dysfunction as evidenced in various *in vivo* and cell culture models such as Parkinson's and Alzheimer's disease and excitotoxicity (Merrill et al., 2011; Meyer et al., 2017). Interestingly, we observed that BDNF significantly increased mitochondrial length at 25ng/ml but not at 37.5ng/ml. It is conceivable that the bi-modal effects of BDNF on mitochondrial fusion in dendrites is caused by PKA mediated phosphorylation of all the available pool of Drp1 in mitochondrial scission sites within mitochondria, especially in light of the fact that PKA mediated phosphorylation of Drp1 does not inhibit its translocation to mitochondria or assembly of constriction rings (Merrill et al., 2011; Yu et

al., 2019). However, future studies are warranted to determine the underlying mechanism by which BDNF promotes PKA-mediated phosphorylation of Drp1.

In addition to promoting mitochondrial fusion, exposing primary cortical neurons to exogenous BDNF increased mitochondrial motility in a bi-directional manner, which leads to increased mitochondrial content in dendrites. Increased mitochondrial content, as a virtue of increased anterograde transport of mitochondria to proximal and distal sites of dendrites, is necessary to provide the energy in the form of ATP to maintain dendritic arbors as evident by an increased in oxidative phosphorylation and glycolysis as assessed by performing seahorse metabolic assays in cultured neurons treated with BDNF (Fig.7). To this end, it is conceivable that increased mitochondria availability in the dendrites allows for enhanced energy production necessary for powering critical biological functions such as localized translation of proteins, calcium buffering and signal transduction (Leung et al., 2021; Sheng, 2017). Indeed, given that BDNF enhances mitochondrial fusion and content by eliciting PKA mediated phosphorylation of Drp1, our data is consistent with other published observations that PKA mediated phosphorylation of Drp1 increases the fusion and content of mitochondria in dendrites to increase the number of dendrites while reducing the number of synapses (Dickey & Strack, 2011). Mitochondrial content in dendrites is significantly increased with exposure of neurons to BDNF. It is plausible that BDNF either slows down the turnover of mitochondria (mitophagy) in dendrites and/or drives an increase in biogenesis of mitochondria. Mitochondrial turnover and biogenesis are opposing physiological processes that work in an orchestrated manner to increase the quality and health of mitochondria. Mitochondria become damaged upon buffering high amounts of calcium or experiencing high levels of oxidative stress due to increased

metabolic demand. The damaged/effete mitochondria would be sent to the soma to be degraded via mitophagy, which leads to increased mitochondrial biogenesis by employing raw, recycled biological materials/nutrients. To this end, it would be vital to study how mitophagy and mitochondrial turnover may be impacted by BDNF which leads to increased mitochondrial content in dendrites.

In addition, we observed that BDNF mediated increased mitochondrial motility in dendrites requires PKA activity in the cytosolic and mitochondrial compartments as expressing constructs that express untargeted PKI or mitochondrially targeted PKI abrogated its effects. Furthermore, our collective immunocytochemical data show that BDNF promotes mitochondrial trafficking of dendritic mitochondria and increased mitochondrial content via eliciting PKA-mediated phosphorylation of Miro-2 and increasing the endogenous levels of D-AKAP1 (Fig. S2). However, the mechanism by which BDNF promotes PKA mediated phosphorylation of Miro-2 remains to be elucidated and is recognized that this conceptual gap in our study warrants future studies. It is plausible that BDNF binding to Trkβ leads to increased mitochondrial translocation of Trkβ, increased PKA and D-AKAP1 levels and phosphorylation of Miro-2 and Drp1, which are PKA substrates. PKA-mediated phosphorylation of Miro-2 has been shown to be a molecular mechanism that drives increases mitochondrial anterograde transport in dendrites (Das Banerjee et al., 2017). In our study, we showed that exposure of primary cortical neurons to exogenous BDNF increased mitochondrial content in the dendrites but not in the presence of PKI or Mito-PKI (Fig. 6). Also, BDNF in the presence of PKA inhibitor H89 was unable to increase mitochondrial anterograde trafficking (Fig. 6). Evidently, BDNF activates mitochondrial PKA, which in turn increases Miro-2

phosphorylation leading to anterograde transport of mitochondria to the dendrites and locations of high energy demand.

BDNF enhances oxidative phosphorylation leading to increased ATP production and metabolic potential. Interestingly, in addition to increasing OXPHOS, BDNF was able to increase glycolysis. There is rationale that may explain how BDNF enhances glycolysis. Previously, other groups have shown that Trkβ was shown to interact with the dopamine receptor D1 and adenosine A2AR receptors to enhance the cAMP-PKA signaling which activates downstream effectors leading to aerobic glycolysis (Ishii et al., 2018), also as previously observed in neuronal differentiation when neural progenitor cells (NPCs) were treated with BDNF (20ng/ml) and also significantly increased the levels of PGC-1a (X. Zheng et al., 2016), a protein known to upregulate hundreds of genes in glycolysis in cardiac cells (Rowe et al., 2010). In other skeletal muscle models, BDNF was shown to affect the muscle fiber program by increasing fast twitch glycolytic muscle which is a way to treat muscle degeneration pathologies (Delezie et al., 2019). Furthermore, pharmacological inhibition of Trkβ by treating neurons with ANA12 shunts oxidative phosphorylation and glycolysis, leading to the concept that active Trkβ has a direct effect on mitochondrial bioenergetics. Here, we showed that BDNF modulates mitochondrial bioenergetics, presumably to increase ATP production, as shown by an increase in ATP synthase derived OCR and increased mitochondrial energy capacity which can be compensatory mechanisms by which neurons elicit to meet instances of high “energy currency” (Fig. 7). However, the molecular mechanisms leading to enhanced bioenergetic flux following Trkβ activation through BDNF is not clear, and further studies delineating

functional roles of BDNF in regulating electron transport chain are warranted. Thus far, the treatment of primary neurons with exogenous BDNF depends on downstream activation of PKA to modulate mitochondrial structure/function, and this concentration of BDNF is associated with neuroprotective effects against oxidative stress. In the rotenone model of neurodegeneration, exogenous BDNF exerted both a reduction in the loss of dendrites and mitochondria in neurons exposed to high levels of oxidative stress induced by the complex I inhibitor rotenone (Fig. 8). In this *in vitro* chemical model of Parkinson's disease, the neuroprotective effects of BDNF on dendrites is consistent its ability in reducing the levels of mitochondrial derived superoxide induced by rotenone in BDNF-treated neurons (Fig. 8C-D). Furthermore, it is conceivable that BDNF increases the bioenergetic landscape of neurons by enhancing the activities of complex I and IV (Markham et al., 2004). Overall, our study shows that exogenous BDNF, by enhancing PKA mediated phosphorylation of OMM localized substrates (Drp1 and Miro-2), can modulate mitochondrial structure and mitochondrial health, effects associated with increased neuronal survival induced by oxidative stress. Given that the levels of BDNF, PKA activity and mitochondrial dysfunction play an etiological role in various brain-degenerative disorders, our work has implications in Parkinson's disease, Alzheimer's disease, and other brain-related diseases. Overall, our study expands on the canonical model of BDNF mediated neuroprotection by remodeling mitochondria and enhancing mitochondrial health in dendrites by inducing the following sequence of molecular events in neurons: 1- Binding of BDNF to Trkβ, 2- activation of PKA (5-15 minutes), 3 - increased ox/phos levels including basal and ATP synthase-derived OCR, (15 mins-2 hrs.) and glycolysis, 4- increased translocation to mitochondria (4-24 hrs.), 5-increased D-AKAP1 levels (24-48 hrs.) post treatment with

BDNF, 6- then increased PKA-mediated phosphorylation of Drp1 and MFN leading to increased mitochondrial length (24hrs.), 7- trafficking and content in dendrites (24hrs.). 8- Finally, BDNF-mediated enhanced mitochondrial health is associated with increased resistance to oxidative stress and increased neuronal survival (Fig. 9).

**Figure legends**

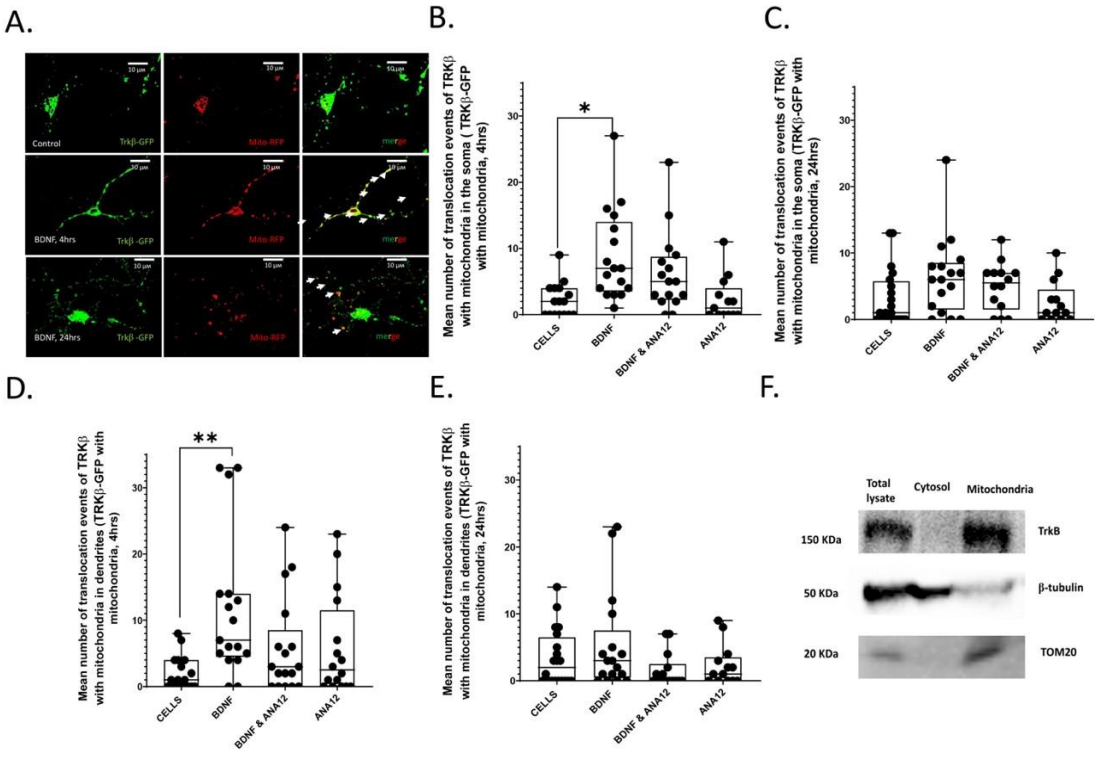


Fig. 1

**Figure 1. Trkβ receptor translocates to dendritic mitochondria of primary cortical neurons in response to BDNF treatment.**

Representative epifluorescence images of primary cortical neurons transfected with Mito-RFP (48hrs.) and Trkβ-GFP (48hrs.) and treated with exogenous recombinant human BDNF (50ng/ml cell culture media, 4hrs & 24hrs.). scale bar = 10 microns. The bar graph in **(B)** depicts the mean (±SEM) of Trkβ -GFP translocation events in the dendrites with mitochondria following treatment with BDNF (50ng/ml, 4hrs.). The bar graph in **(C)** depicts the mean (±SEM) of Trkβ-GFP translocation events in the dendrites with mitochondria after BDNF treatment (50ng/ml, 24hrs.). The bar graph in **(D)** depicts the mean (±SEM) of Trkβ-GFP translocation events in the soma with mitochondria after BDNF

treatment (50ng/mL, 4hrs.). The bar graph in **(E)** depicts the mean (±SEM) of Trkβ-GFP translocation events in the soma with mitochondria after BDNF treatment (50ng/ml, 24hrs.). (Means ±SEM, *: $p<0.05$ vs. Control, **: $p<0.05$ vs. Control, number of events per neuron, 13-17 transfected primary cortical neurons per condition, N=4 experiments/ condition, One-way ANOVA, post-hoc Tukey's test. The data suggests that exposing primary cortical neurons to exogenous BDNF increases the translocation of Trkβ-GFP with Mito-RFP-labeled mitochondria at 4hrs. post treatment and mitochondrial translocation of Trkβ-GFP saturates at 24hrs. treatment of BDNF. **(F)** Representative Western blot of endogenous Trkβ in mitochondrial fractions isolated from whole brains extracted from 10-month-old *wt* mouse. The membrane was stripped and re-probed for TOM20, an OMM-localized mitochondrial marker, to verify the purity of mitochondria relative to the cytosolic and lipid compartments. The representative WB suggests that a fraction of endogenous Trkβ is localized in the mitochondrial compartment.

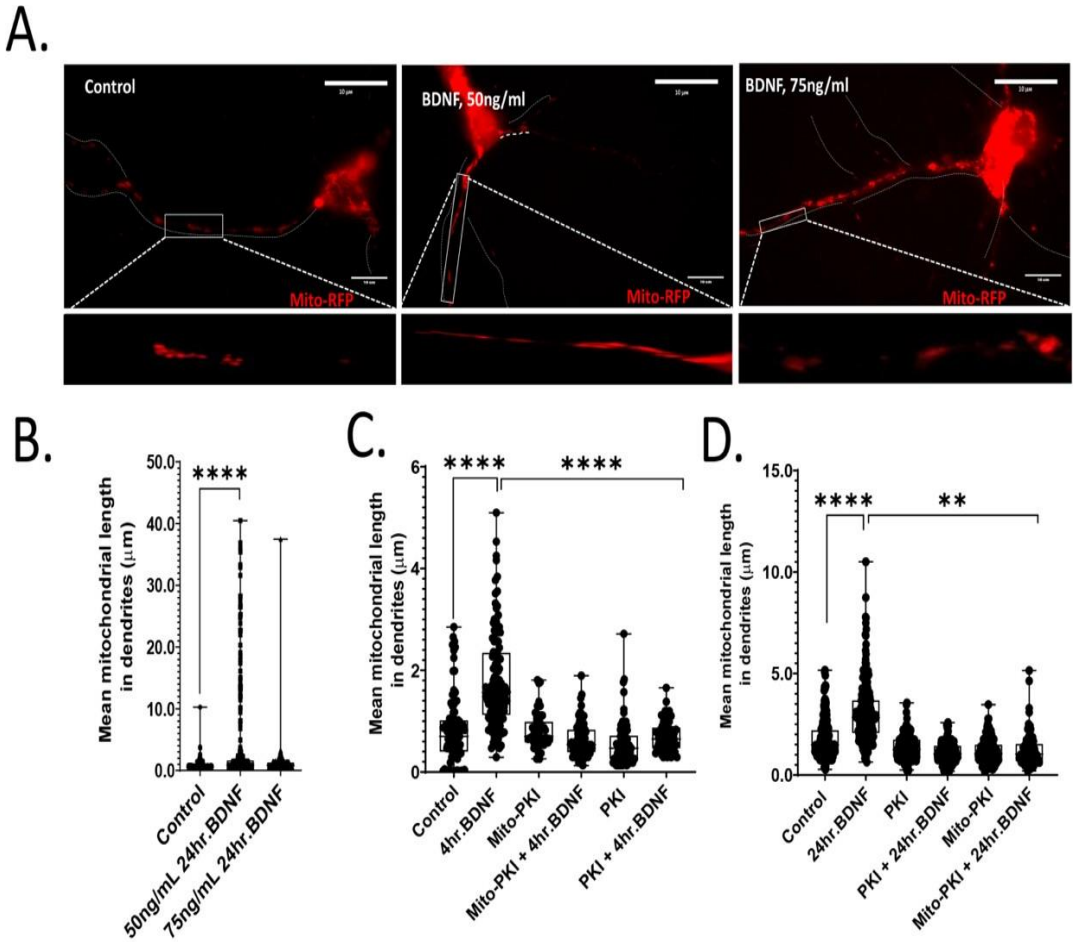


Fig. 2

**Figure 2. BDNF promotes mitochondrial fusion in a PKA-dependent manner**. **(A)** Representative epifluorescence image of a primary cortical neuron transfected with Mito-RFP (48hrs.) and treated with exogenous recombinant human BDNF (50ng/ml, 24hrs.), scale bar = 10 microns. The bar graph in **(B)** depicts the mean (±SEM) of mitochondrial length as a measure of mitochondrial fusion in dendrites of primary cortical neurons. The bar graph in **(C)** depicts the mean (±SEM) of mitochondrial length in neurons following transient transfection of GFP-tagged protein kinase A inhibitor peptide (PKI-GFP) or OMM targeted-PKI (Mito-PKI-GFP) to inhibit PKA with and without exogenous

recombinant human BDNF (50ng/ml, 4hrs.) treatment. The bar graph in **(D)** depicts the mean (±SEM) of mitochondrial length in neurons after transfection of PKI-GFP or Mito-PKI-GFP, with and without treatment with exogenous recombinant human BDNF (50ng/ml, 24hrs.). In brief, the data shows that BDNF (50ng/ml, 4 & 24hrs.) increased mitochondrial length, but not in primary cortical neurons co-transfected with the PKA inhibitor PKI. For B-D, (****: $p<0.0001$ vs. control, ***: $p<0.0001$ vs. 4hrs. or **: $p<0.001$ vs. 24hrs. BDNF, n=100-200 mitochondria/condition from at least 13-17 primary cortical neurons per condition, One-way ANOVA, post-hoc Tukey's test, N=3 experiments/ condition)

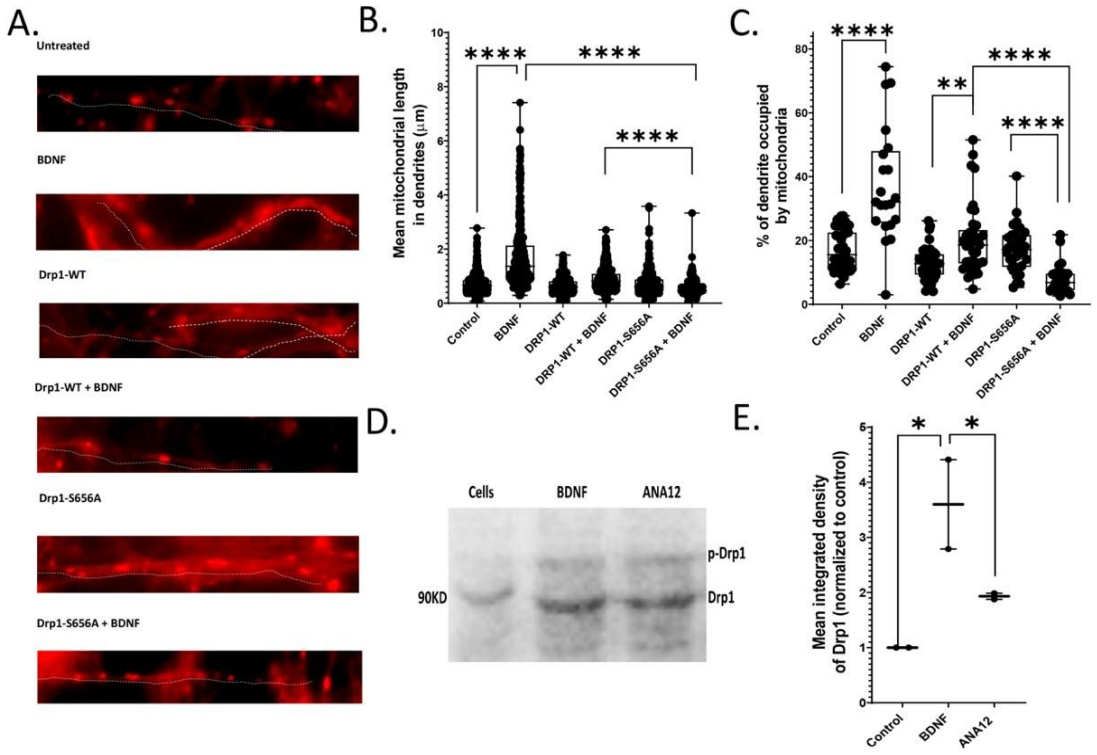


Fig. 3

**Figure 3. BDNF promotes mitochondrial length through phosphorylation of Drp1. (A)** Representative epifluorescence images of primary cortical neurons transfected with Mito-RFP (48hrs.) and treated with exogenous recombinant human BDNF (50ng/ml, 24hrs.), in the presence or absence of transient expression of GFP tagged Drp1-WT (Drp1-WT-GFP) & phosphorylation resistant (S656A)-mutant Drp1(Drp1-S656A-GFP) for 72hrs., scale bar = 10 microns. Transfected primary cortical neurons were identified based on GFP fluorescence with their elongated axons and complex dendritic arbors. The bar graph in **(B)** depicts the mean (±SEM) of mitochondrial length as a measure of mitochondrial fusion in dendrites. BDNF treatment was unable to increase mitochondrial length in the presence of the mutant Drp1-S656A-GFP. The bar graph in **(C)** depicts the mean (±SEM) of

mitochondrial content in primary cortical neurons after exposure to exogenous recombinant human BDNF or transient transfection with the indicated plasmids. In brief, BDNF was partially able to rescue mitochondrial content when Drp1-WT was co-expressed but not by mutant Drp1-S656A-GFP, **(D)** Representative Phos-tag Western blot of phosphorylated-Drp1 and total Drp1 in cell lysates extracted from Primary cortical neurons treated with BDNF (50ng/ml, 24hrs.) & ANA12. The representative Western blot image suggests that exposing primary cortical neurons to exogenous BDNF increases the PKA-mediated phosphorylation of Drp1 leading to increased mitochondrial length. (**E**) Densitometric analysis of the Phos-tag Western blot data shown in (D) on the phosphorylation status of Drp1 normalized to Drp1. For B, (****: $p<0.0001$ vs. control, ****: $p<0.0001$ vs. BDNF, for C , (****: $p<0.0001$ vs. control, **: $p<0.01$ Drp1-WT vs. BDNF, ****: $p<0.0001$ Drp1-S656A vs. BDNF, n=100-200 mitochondria/condition from at least 13-15 transfected primary cortical neurons per condition, One-way ANOVA, post-hoc Tukey's test, N=3 experiments/ condition), For E (*:$p<0.05$ vs. control, N=3 experiments, One-way ANOVA, Tukey's test, N=3 experiments/ condition).

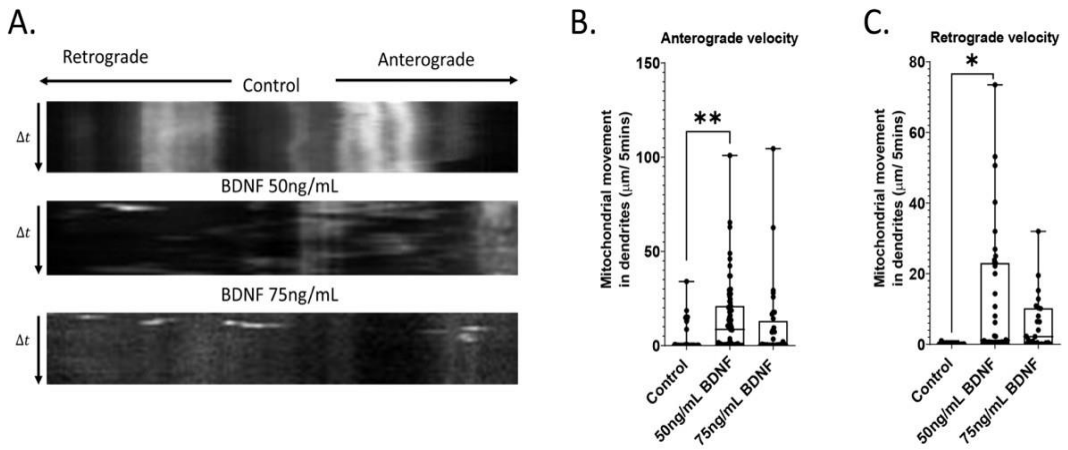


Fig. 4

**Figure 4. Exogenous recombinant BDNF treatment increases anterograde and retrograde mitochondrial trafficking to dendrites. (A)** Representative kymographs assembled from untreated primary cortical neurons treated with BDNF at 50ng/ml or 75ng/ml, for 24hrs. The data shows that exogenous administration of BDNF can significantly increase bi-directional movement of mitochondria (μm, x-axis) over a period of five minutes (min., y-axis). The bar graph in **(B)** depicts the mean (±SEM) mitochondrial anterograde velocity (μm/10s) in dendrites of primary cortical neurons in response to exogenous recombinant human BDNF (50ng/ml, 75ng/ml, 24hrs.) treatment. The graph in **(C)** depicts mean (±SEM) retrograde velocity of mitochondria in dendrites of primary cortical neurons in response to exogenous recombinant human BDNF (50ng/ml, 75ng/ml, 24hrs.) treatment. The data shows that treating neurons with 50ng/ml BDNF increases anterograde and retrograde trafficking when compared to control. For B (**: $p<0.01$ vs. Control), for C (*: $p<0.05$ vs. Control), n = 20-40 moving mitochondria/condition from at least 13-18 transfected primary cortical neurons per condition, One-way ANOVA, Tukey's test, N=3 experiments).

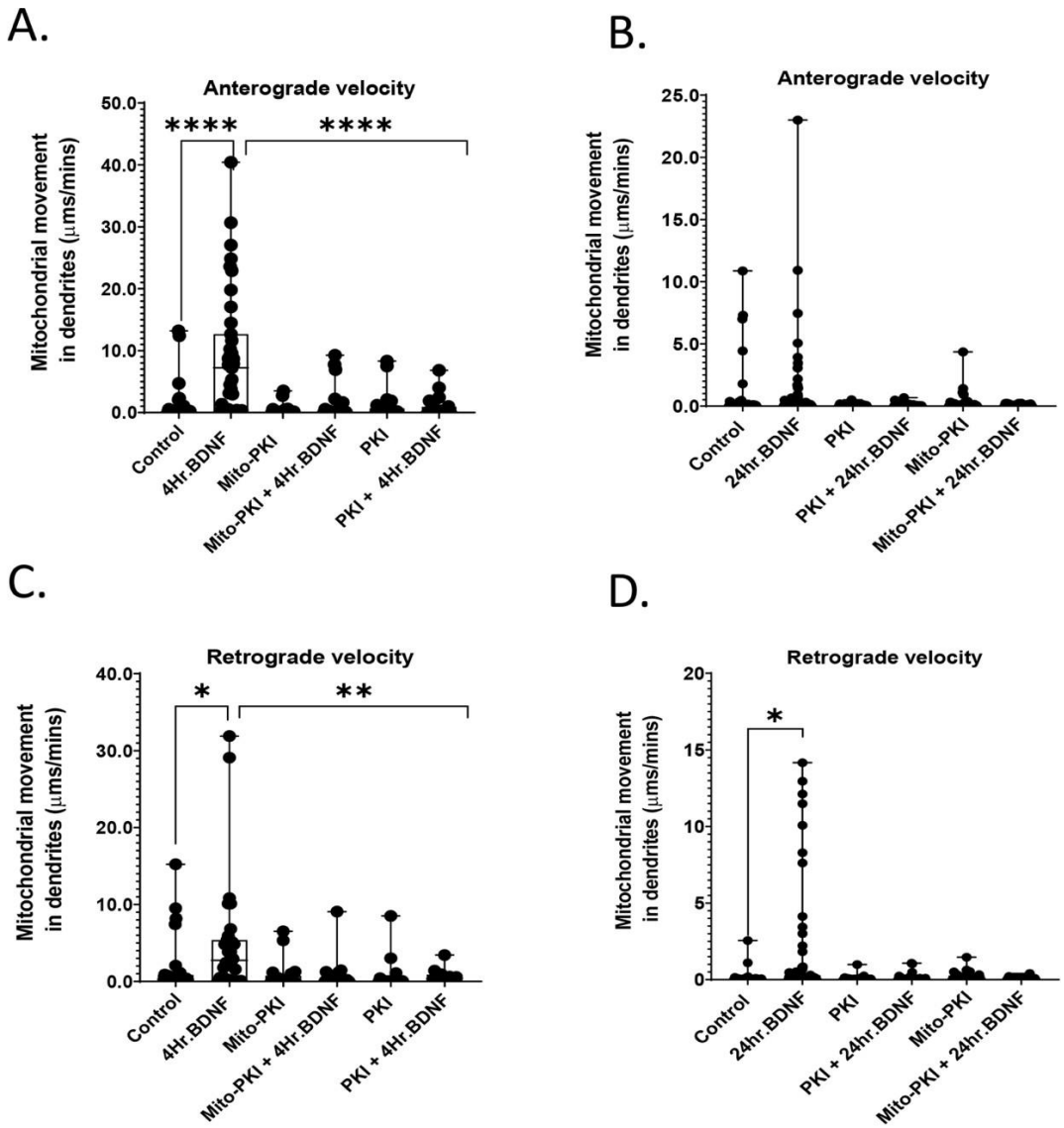


Fig. 5

**Figure 5. BDNF treatment increases anterograde and retrograde mitochondrial trafficking in dendrites in a PKA-dependent manner**. The graph in (A) depicts the mean (±SEM) of mitochondrial anterograde trafficking (μm/10s) in dendrites of primary cortical neurons.

transfected with Mito-RFP (48hrs.) and treated with exogenous recombinant human BDNF (50ng/ml, 4hrs.), in the presence or absence of transient expression of Mito-PKI-GFP &

PKI plasmids when compared to untreated transiently GFP transfected control. The graph in (B) depicts the mean (±SEM) mitochondrial anterograde trafficking (μm/10s) in dendrites of primary cortical neurons transfected with Mito-RFP (48hrs.) and treated with exogenous recombinant human BDNF (100ng/ml, 24hrs.), in the presence or absence of transient expression of Mito-PKI-GFP & PKI plasmids when compared to untreated transiently GFP transfected control. The graph in (C) depicts the mean (±SEM) mitochondrial retrograde trafficking (μm/10s) in dendrites of primary cortical neurons transfected with Mito-RFP (48hrs.) and treated with exogenous recombinant human BDNF (50ng/ml, 4hrs.), in the presence or absence of transient expression of Mito-PKI-GFP & PKI plasmids when compared to untreated transiently GFP transfected control. The graph in (D) depicts the mean (±SEM) mitochondrial retrograde trafficking (μm/10s) in dendrites of primary cortical neurons transfected with Mito-RFP (48hrs.) and treated with exogenous recombinant human BDNF (50ng/ml, 24hrs.), in the presence or absence of transient expression of Mito-PKI-GFP & PKI plasmids when compared to untreated transiently GFP transfected control. For A-D (*: $p<0.05$, ****: $p<0.0001$, vs. GFP control, **: $p<0.01$, ****: $p<0.0001$, vs. BDNF n = 20-40 moving mitochondria/ condition from at least 13-17 transfected primary cortical neurons per condition, one-way ANOVA, Tukey's test, N=3 experiments).

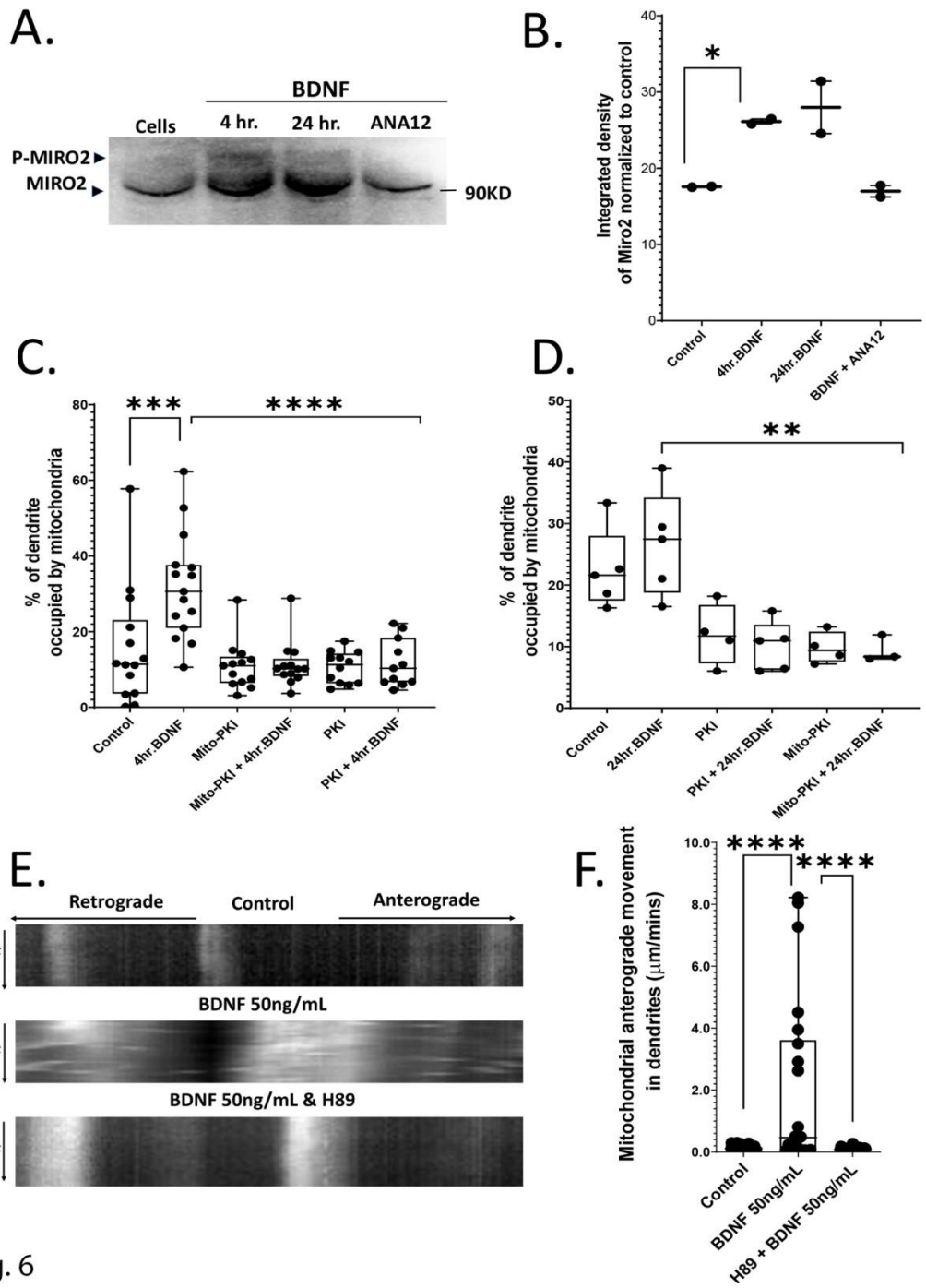


Fig. 6

**Figure 6. Exposure of primary cortical neurons with BDNF enhances mitochondrial content in dendrites through PKA. (A)** Representative Phos-tag western blot for Miro-2 in lysates extracted from primary cortical neurons after treatment with 50ng/ml BDNF for

4 and 24hrs. The bar graph in **(B)** shows the means ±SEM of densitometric analysis of the immunoreactive bands for Miro-2 at the indicated conditions and normalized to control. BDNF treatment significantly increases the phosphorylation of Miro-2. The graph in (C) depicts the mean (±SEM) of mitochondrial content in dendrites of primary cortical neurons transfected with Mito-RFP (48hrs.) and treated with exogenous recombinant human BDNF (50ng/ml, 4hrs.), in the presence or absence of transient expression of Mito-PKI-GFP & PKI plasmids when compared to untreated transiently Mito-RFP transfected control. The graph in (D) depicts the mean (±SEM) of mitochondrial content in dendrites of primary cortical neurons transfected with Mito-RFP (48hrs.) and treated with exogenous recombinant human BDNF (50ng/ml, 24hrs.), in the presence or absence of transient expression of Mito-PKI-GFP & PKI plasmids when compared to untreated transiently Mito-RFP transfected control. Mitochondrial content is defined by the percentage of a defined segment of a dendrite occupied by mitochondria. An appropriate level of mitochondrial content is an indication that dendrites have a sufficient number of mitochondria to maintain dendrite length as previously validated by our research group. **(E)** Representative kymograph of mitochondrial movement in primary cortical neurons treated with BDNF (50ng/ml, 24hrs.), BDNF (50ng/ml, 24hrs.) co-treated with H89 (0.5µM, 24hrs.) and untreated control, exhibiting significantly increased bi-directional movement of mitochondria (µm, x-axis) over a period of five minutes (min., y-axis) with BDNF treatment but does not with PKA inhibitor H89 co-treatment. The graph in **(F)** depicts the mean (±SEM) anterograde movement of mitochondria in dendrites of primary cortical neurons treated with BDNF (50ng/ml, 24hrs.), BDNF co treated with H89 (0.5µM, 24hrs.) when compared to Mito-RFP transfected control. In brief, the data shows that when

compared to untreated Mito-RFP transfected control, treatment of primary cortical neurons with BDNF increased anterograde trafficking but not in neurons co-treated with the PKA inhibitor H89 (0.5μM). For B, C, D, F (*: $p<0.05$, ***: $p<0.001$, ****: $p<0.0001$ vs. control, **: $p<0.01$, ****: $p<0.0001$ vs. BDNF, n = integrated density, n = percent of dendrite occupied by mitochondria, n = 20-40 moving mitochondria in anterograde direction, from at least 13-17 primary cortical neurons per condition, one-way ANOVA, post-hoc Tukey's test, N=3 experiments,).

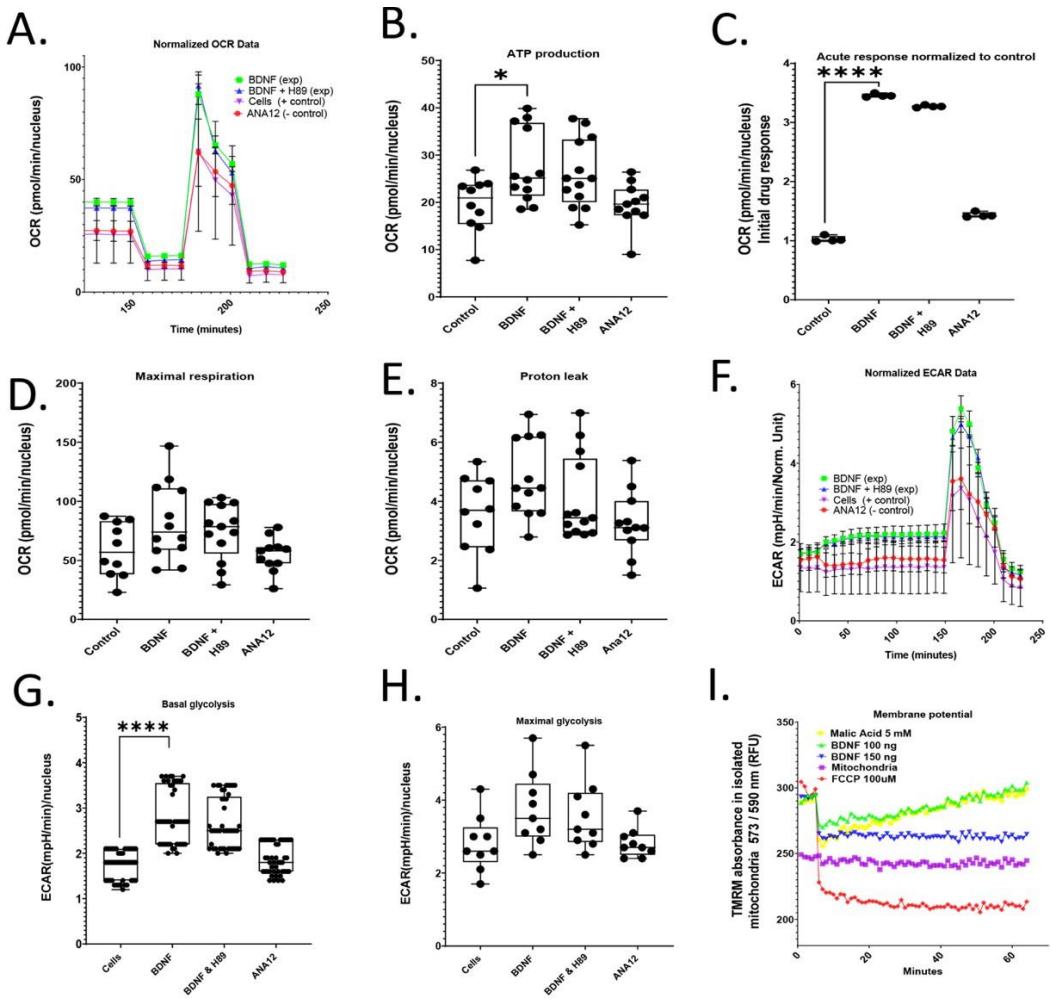


Fig. 7

**Figure 7. BDNF increases oxidative phosphorylation in live primary neurons and in isolated mitochondria**.

A representative Seahorse oxygraph in primary cortical neurons treated with exogenous BDNF (75ng/ml, 2hrs.) followed by treatment with oligomycin (oligo), FCCP and rotenone (rot) to measure ATP-dependent, maximal, and mitochondrial-dependent OCRs respectively at the specified time points. **(B)** compiled graph showing mean basal (acute) OCRs in primary cortical neurons treated with exogenous BDNF and the indicated

treatments. **(C)** compiled graph of maximal mean OCRs in primary cortical neurons following exposure to FCCP. The graph shows BDNF increases mitochondrial production of ATP. **(D)**. **(E)** graph of OCR shows BDNF increased proton leak compared to Trkβ inhibitor ANA12. **(F)** graph of a representative experiment shows the mean ±SEM extracellular acidification rates (ECARs), a proxy of glycolysis, in neurons treated with BDNF (75ng/m; 2hrs.). The data shows that exposing neurons with BDNF treatment (75ng/ml, 24hrs.) enhanced glycolysis. **(G)** graph of ECAR shows BDNF increased Basal Glycolysis. **(H)** graph of ECAR maximal Glycolysis. For panels **(A-H)**, BDNF treatment (75ng/ml, 2hrs.), BDNF treatment (75ng/ml, 2hrs.) & H89 (0.5μM, 24hrs.), ANA12 (200nM, 24hrs.), For A-H (means ±SEM, *: $p<0.05$, ****: $p<0.0001$, vs. Control, n= 3-5 wells/condition, N=3 experiments, one-way ANOVA, Turkey's test). **(I)** Isolated mitochondria from mouse brain were treated with exogenous BDNF (100ng/50ul, 150ng/50ul, 1hr.) and the transmembrane potential ($\Delta\psi m$) was measured by employing a multimode fluorescent plate reader. The data shows that BDNF enhances $\Delta\psi m$. For some conditions, isolated mitochondria were also treated with FCCP to collapse $\Delta\psi m$ or with malic acid to enhance the transmembrane potential by stimulating complex II dependent respiration. For I (means ±SEM *: $p<0.05$, n = 3-5 wells/ condition, One-way ANOVA, Tukey's test).

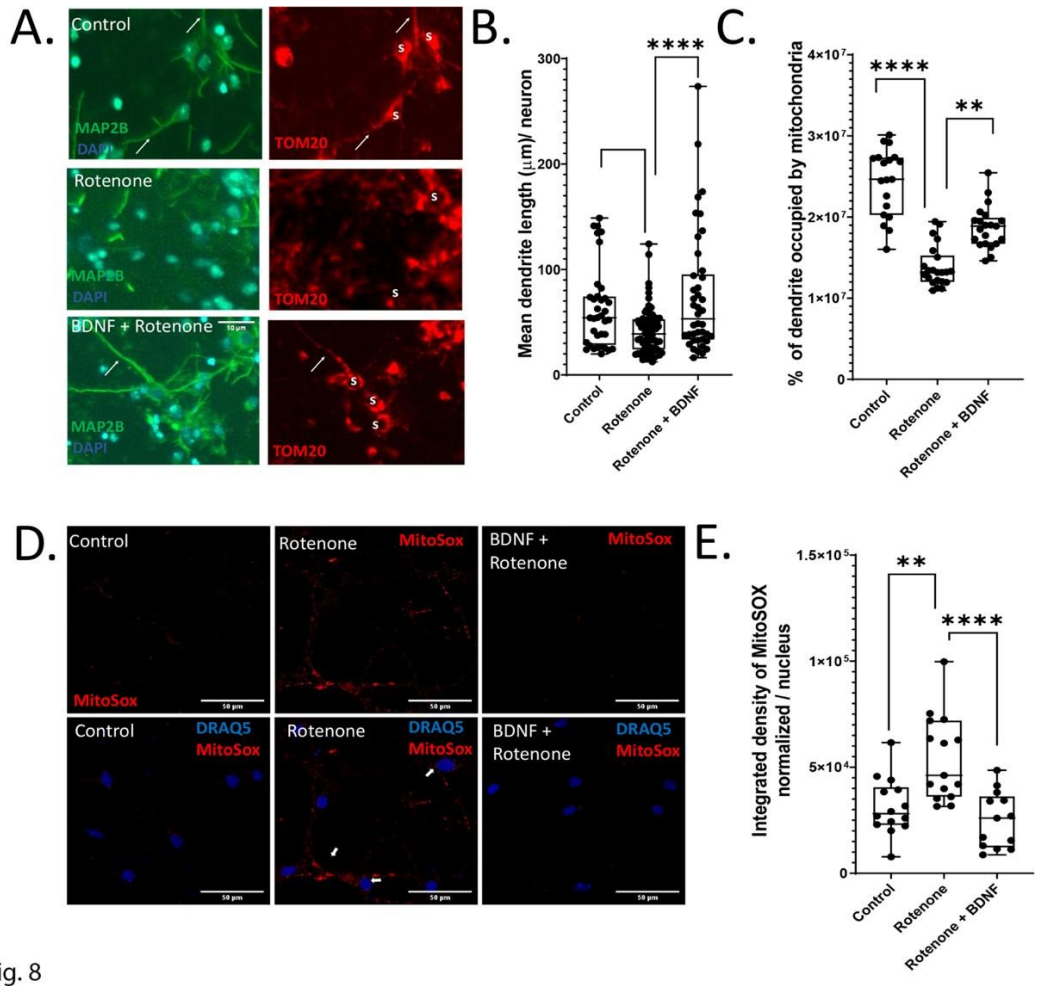


Fig. 8

**Figure 8. BDNF promotes mitochondria and protects dendrites from oxidative stress.** Representative fluorescent images of primary cortical neurons treated with exogenous recombinant human BDNF (50ng/ml, 24hrs.), rotenone (60nM, 24hrs.), BDNF (50ng/ml, 24hrs.) & rotenone (60nM, 24hrs.) and immunostained with MAP2B (1:250) and TOM20 (1:250) to label dendrites and mitochondria respectively, scale bar = 10 microns. The graph in **(B)** shows mean (±SEM) dendrite length/neuron in neurons exposed to BDNF (50ng/ml, 24hrs.) in the presence or absence of rotenone (60nM, 24hrs.) The graph in **(C)** depicts mean (±SEM) integrated density of TOM20 in primary cortical neurons exposed to BDNF (50ng/ml, 24hrs.) in the presence or absence of rotenone (60nM, 24hrs.). It was observed

that BDNF can rescue rotenone-induced loss of dendrites and of dendritic mitochondria (D) Representative fluorescent images of primary cortical neurons incubated with MitoSox for measuring mitochondrial reactive oxygen species in primary cortical neurons. The experimental conditions consisted of a control group, a rotenone (0.5 µM for 1hr.) treatment group, and a rotenone treatment combined with a BDNF (100ng/ml for 1 hour) pre-treatment group. The nucleus is stained by DRQ5. scale bar = 50 microns. The box plot graph in (E) is the graphical representation of (D) and shows enhanced mitochondrial ROS production after rotenone treatment reduced in BDNF treated neurons. In B, C and E (*: $p<0.05$, **: $p<0.01$, ****: $p<0.0001$ vs. control, vs, **: $p<0.01$, ****: $p<0.0001$ vs. rotenone, n=30-40 primary cortical neurons/condition, one-way ANOVA, Tukey's test).

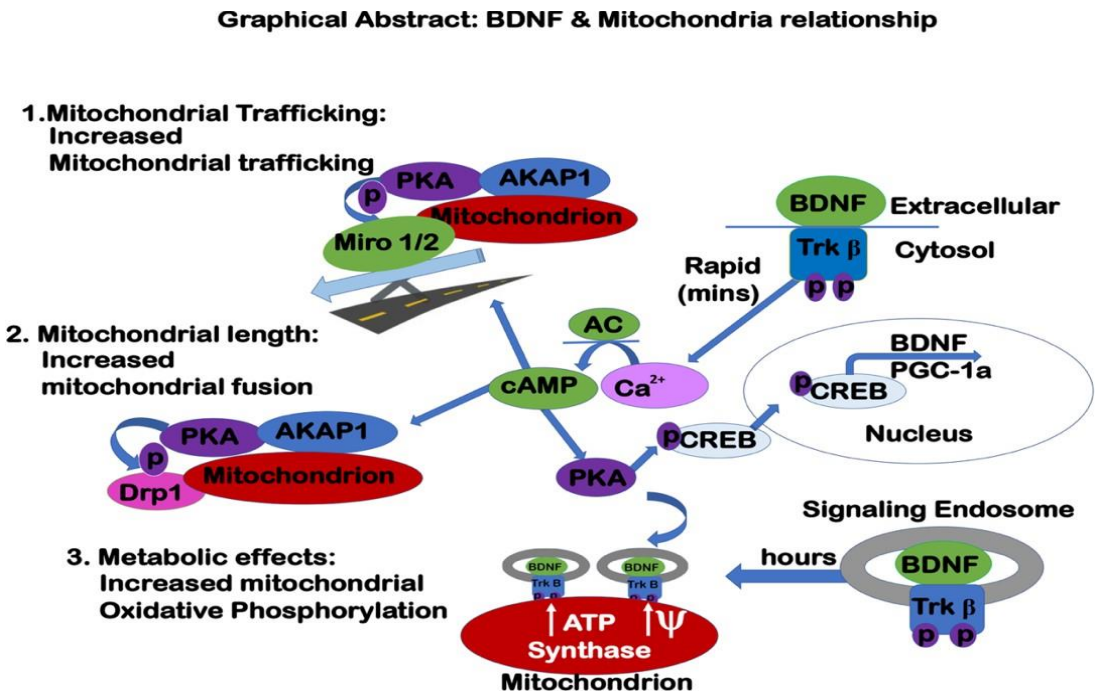


**Figure 9. Mechanistic conceptual model on the role of BDNF in regulating mitochondrial structure/function in neurons.**

The representative figure shows 1. BDNF increases mitochondrial bi-directional trafficking by increasing PKA activity of phosphorylation of Miro-2. 2. BDNF increases mitochondrial fusion and length by increasing PKA activity of phosphorylation of Drp1. BDNF increases mitochondrial metabolism by a direct interaction of Trkβ signaling endosome with the mitochondria. Our conceptual model shows the mechanisms BDNF uses to regulate mitochondrial health as follows: 1) Binding of BDNF to Trkβ, 2) activation of PKA (5-15 minutes) which may occur the cell membrane, 3) increased mitochondrial ATP levels (15mins-2hrs.), 4) then increased translocation to mitochondria (4-24 hrs.), 5) increased D-AKAP1 levels (24-48 hrs.) post treatment with BDNF, 6) then increased PKA-

mediated phosphorylation of Drp1 and MFN leading to increased mitochondrial length (24hrs.), 7) trafficking and content in dendrites (24hrs.). All responses lead to the physiological implication of increased resistance of mitochondria and dendrites to oxidative stress and increased neuronal survival.

**Supplemental Materials**

**Figure S.1**

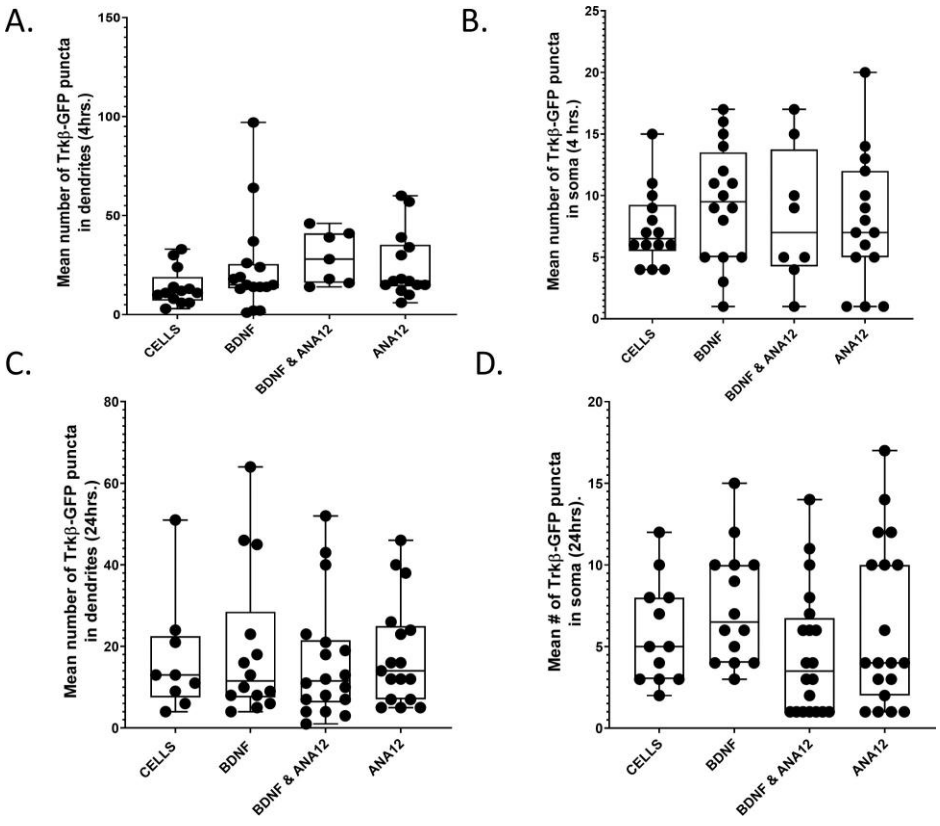


---

**Figure S.1: BDNF does not increase the mean number of Trkβ -GFP puncta in the dendrites or soma of neurons.**

The bar graph in depicts the mean (±SEM) of puncta of Trk**β**-GFP in transfected primary cortical neurons, as assessed by quantifying the puncta in the neurites (using the 3D object counter in image J) following treatment with exogenous recombinant human BDNF (50ng/ml, 4hrs.), BDNF (50ng/ml, 4hrs.) & ANA12 (200nM, 4hrs.) ANA12 (200nM, 4hrs.). **(B)** The bar graph in depicts the mean (±SEM) of puncta of Trk**β**-GFP in transfected primary cortical neurons, as assessed by quantifying the puncta in the soma (using the 3D object counter in image J) following treatment with exogenous recombinant human BDNF (50ng/ml, 4hrs.), BDNF (50ng/ml, 4hrs.) & ANA12 (200nM, 4hrs.) ANA12 (200nM, 4hrs.). **(C)** The bar graph in depicts the mean (±SEM) of puncta of Trk**β**-GFP in transfected primary cortical neurons, as assessed by quantifying the puncta in the neurites (using the 3D object counter in image J) following treatment with exogenous recombinant human BDNF (50ng/ml, 24hrs.), BDNF (50ng/ml, 4hrs.) & ANA12 (200nM, 4hrs.) ANA12 (200nM, 4hrs.). **(D)** The bar graph in depicts the mean (±SEM) of puncta of Trk**β**-GFP in transfected primary cortical neurons, as assessed by quantifying the puncta in the soma (using the 3D object counter in image J) following treatment with exogenous recombinant human BDNF (50ng/ml, 24hrs.), BDNF (50ng/ml, 4hrs.) & ANA12 (200nM, 4hrs.) ANA12 (200nM, 4hrs.). A-D (Means ±SEM, n = 13-17 neurons/condition, N=4 Experiments/ condition, one-way ANOVA, Tukey's test).

**Figure S.2**

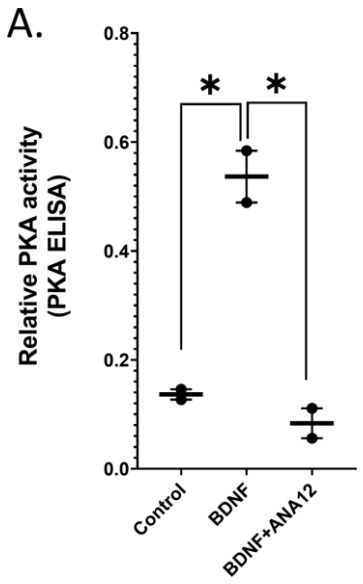


**Figure S.2: BDNF increases PKA activity.**

PKA activity was measured in cell lysates derived from untreated control, BDNF (75ng/ml, 5min.) and BDNF + ANA12 (200nm) treated primary cortical neurons. The kinase activity was determined by an ELISA kit (ADI-EKS-390A, Enzo Life Sciences, NY, USA) following the manufacturer's protocol. Relative kinase activity was calculated with the following equation: (average absorbance sample at 450 nm average absorbance blank at 450 nm) / quantity of crude protein used per assay. The representative graph suggests that BDNF but not in the presence of Trk**β** inhibitor ANA12 increases PKA activity compared to control. (Means ±SEM, *: $p<0.01$ N=3 wells/ condition, one-way ANOVA, Tukey's test).

**Figure S.3**

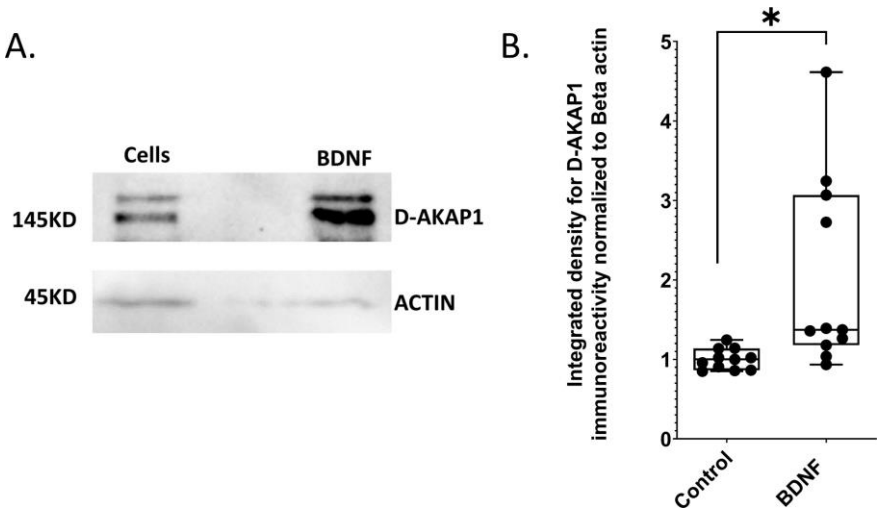


**Figure S.3: BDNF increases the endogenous level of D-AKAP1**.

Representative Western blot for D-AKAP1 and β-actin in cell lysates extracted from SH-SY5Y cells treated with BDNF (50ng/ml, 24hrs.). (B) Densitometric analysis of D-AKAP1 specific immunoreactive bands on the Western blot shown in (A) normalized to β-actin. BDNF (50ng/ml, 24hrs.) treatment in SH-SY5Y cells increased the endogenous levels of D-AKAP1. (Means ±SEM, *: $p<0.01$, n = 2-3 lanes/condition, N=4 experiments/condition, student t test).

**Figure S.4**

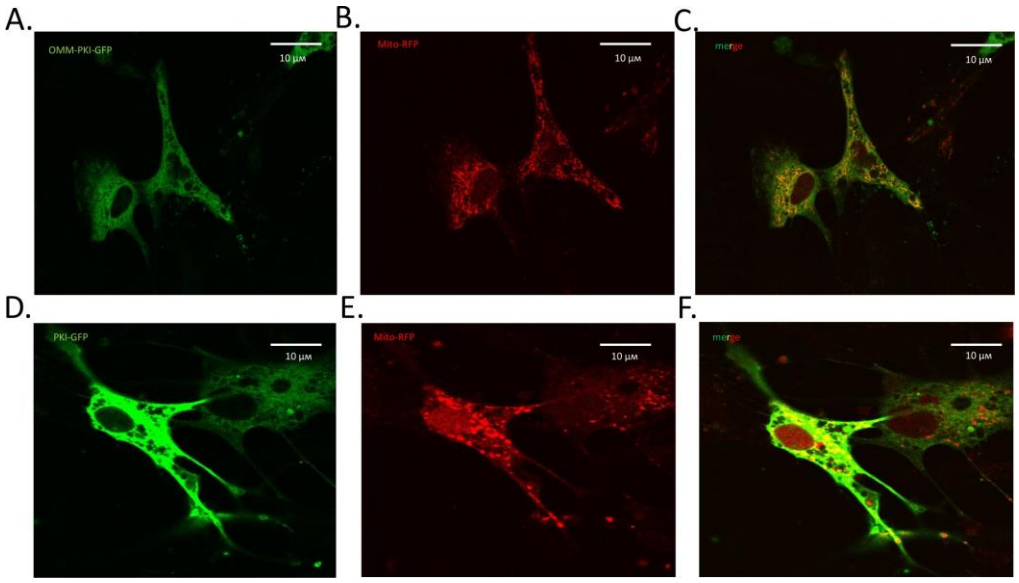


---

**Figure S.4: Co-transfection of Mito-RFP with PKI and MITO-PKI.**

Representative fluorescent images of primary cortical neurons transfected with OMM-PKI-GFP (48hrs.). scale bar = 10 microns.

Representative fluorescent images of primary cortical neurons transfected with Mito-RFP (48hrs.). scale bar = 10 microns.

Representative fluorescent images of primary cortical neurons transfected with Mito-RFP (48hrs.) and OMM-PKI-GFP (48hrs.). scale bar = 10 microns.

Representative fluorescent images of primary cortical neurons transfected with Mito-PKI-GFP (48hrs.). scale bar = 10 microns.

Representative fluorescent images of primary cortical neurons transfected with Mito-RFP (48hrs.). scale bar = 10 microns.

Representative fluorescent images of primary cortical neurons transfected with Mito-RFP (48hrs.) and Mito-PKI-GFP (48hrs.). scale bar = 10 microns.

**Figure S.5**

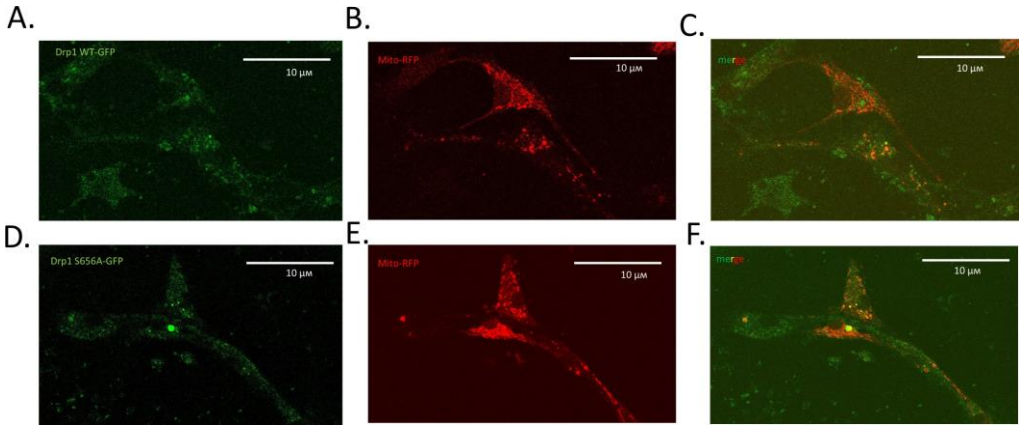


**Figure S.5: Co-transfection of Mito-RFP with Drp1-WT and Drp1-S656A**

Representative fluorescent images of primary cortical neurons transfected Drp1-WT-GFP (48hrs.). scale bar = 10 microns.

Representative fluorescent images of primary cortical neurons transfected with Mito-RFP (48hrs.). scale bar = 10 microns

Representative fluorescent images of primary cortical neurons transfected with Mito-RFP (48hrs.) and Drp1-WT-GFP (48hrs.). scale bar = 10 microns

Representative fluorescent images of primary cortical neurons transfected with Drp1-S656A-GFP (48hrs.). scale bar = 10 microns.

Representative fluorescent images of primary cortical neurons transfected with Mito-RFP (48hrs.). scale bar = 10 microns.

Representative fluorescent images of primary cortical neurons transfected with Mito-RFP (48hrs.) and Drp1-S656A-GFP (48hrs.). scale bar = 10 microns.

**Figure S.6**

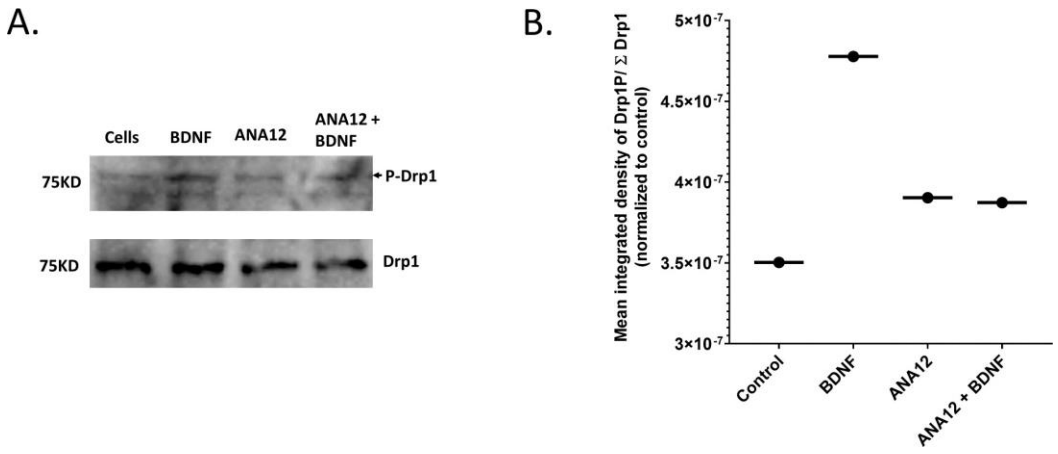


**Figure S.6: BDNF increases the phosphorylation of Drp1 but not in the presence of ANA12.**

Representative Western blot for total and phosphorylated Drp1 (Ser 637), total Drp1, and β-tubulin in cell lysates extracted from primary cortical neurons treated with BDNF (100ng/ml, 24hrs.) and ANA12 (200nM, 24hrs.). **(B)** Densitometric analysis of phosphorylated and total Drp1-specific immunoreactive bands on the Western blot shown in (A) normalized to β-tubulin. Primary cortical neurons treated with BDNF (100ng/ml, 24hrs.) increased the phosphorylation of Drp1 but not in the presence of pharmacological inhibitor of Trk**β**, ANA12 (200nM, 24hrs.).

**Figure S.7**

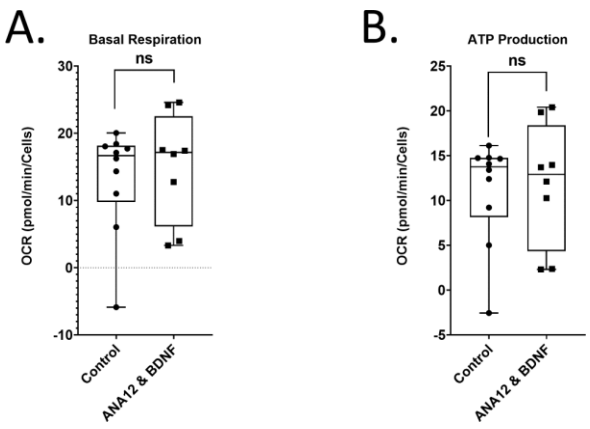


**Figure S.7: Trkβ is required for BDNF to modulate mitochondrial respiration.**

Representative graphs showing mean OCR levels in untreated control and BDNF (75ng/ml, 1hr.) + ANA12 (200nM, 24hrs.) treated primary cortical neurons. ANA12, a pharmacological inhibitor of Trk**β** inhibited BDNF's ability to enhance its response to increase basal respiration (A) and in ATP-dependent OCRs production (B). (Means ±SEM, n = 3-4 wells/ condition, N=2 experiments/ condition, student t test).

## Chapter III

## Mitochondrial PKA is neuroprotective in a cell culture model of Alzheimer's disease.


### Abstract

Alzheimer's disease (AD) is a neurodegenerative disease characterized by progressive memory loss and cognitive decline. In hippocampal neurons, the pathological features of AD include the accumulation of extracellular amyloid beta peptide (Aβ) accompanied by oxidative stress, mitochondrial dysfunction, and neuron loss. A decrease in neuroprotective Protein Kinase A (PKA) signaling contributes to mitochondrial fragmentation and neurodegeneration in AD. A decrease in neurotrophic factors like BDNF is also observed in AD; By associating with the protein scaffold Dual-Specificity Anchoring Protein 1 (D-AKAP1), PKA is targeted to the mitochondrion to promote mitochondrial fusion by phosphorylating the fission modulator dynamin-related protein 1 (Drp1). We hypothesized that: 1) a decrease in the endogenous level of endogenous D-AKAP1 contributes to decreased PKA signaling in mitochondria, and that 2) restoring PKA signaling in mitochondria can reverse neurodegeneration and mitochondrial fragmentation in neurons in AD models. Through immunohistochemistry, we showed that endogenous D-AKAP1, but not other mitochondrial proteins, is significantly reduced in primary neurons treated with $A\beta_{42}$ peptide (10μM, 24 hrs.), and in the hippocampus and cortex from asymptomatic and symptomatic AD mice (5X-FAD). Transiently expressing wild-type, but not a PKA-binding deficient mutant of D-AKAP1, was able to reduce mitochondrial fission, dendrite retraction, and apoptosis in primary neurons treated with $A\beta_{42}$. Mechanistically, the protective effects of D-AKAP1/PKA are moderated through PKA-mediated

phosphorylation of Drp1, as transiently expressing a PKA phosphomimetic mutant of Drp1 (Drp1-S656D) phenocopies D-AKAP1's ability to reduce $A\beta_{42}$-mediated apoptosis and mitochondrial fission. Overall, our data suggest that a loss of D-AKAP1/PKA contributes to mitochondrial pathology and neurodegeneration in an *in vitro* cell culture model of AD.

**Introduction**

Alzheimer's disease (AD) is a degenerative neurological disorder that is characterized by progressive memory impairment, cognitive decline, and significant behavioral changes over time. Currently, AD affects over 5.4 million Americans (Thies, 2011). At the cellular level, AD is characterized by the accumulation of amyloid beta peptide (Aβ) outside the cells and the formation of intracellular neurofibrillary tangles composed of hyper-phosphorylated tau. These pathological features result in synaptic dysfunction, mitochondrial dysfunction, loss of dendrites and axons, and eventual neuronal loss in vulnerable regions of the brain such as the hippocampus, subcortical regions, and the limbic system (Forero et al., 2006; Sheng et al., 2012) (Fassbender et al., 2001). In postmortem AD brain cortex, studies have reported visible mitochondrial fragmentation and disassembly within dendrites, and the level of BDNF and other neurotrophic factors and kinase signaling like PKA is reduced (Tania Das Banerjee et al., 2021; Saraiva et al., 1985). Mitochondria are crucial for maintaining neuronal function and survival, and their impairment has been linked to the development of neurodegenerative diseases, including AD (Dagda & Das Banerjee, 2015). Studies conducted on *in vitro* and *in vivo* models of AD have shown that mitochondria exhibit various dysfunctions, such as impaired oxidative phosphorylation (OXPHOS), overt fragmentation, decreased membrane potential, and

increased reactive oxygen species (ROS) production (Calkins & Reddy, 2011; Devi & Anandatheerthavarada, 2010; Iijima-Ando et al., 2009). Apart from mitochondrial dysfunction, global dysregulation of Protein Kinase A (PKA) signaling and PKA-modulated neurotrophic signaling have also been implicated in the pathogenesis of AD. PKA is a well-known pro-survival serine/threonine kinase that modulates various cyclic AMP-dependent cellular responses, including survival mechanisms, neuronal differentiation, synaptic plasticity, and initiation of pro-survival gene transcription programs (Dagda & Das Banerjee, 2015). PKA exists as a holoenzyme, consisting of two regulatory subunits (type I and type II) bound to catalytic subunits (α and β). Type II regulatory subunits can target the PKA holoenzyme to membrane-bound organelles, such as the endoplasmic reticulum and mitochondria, by associating with A-kinase anchoring proteins (AKAPs) (Brandon et al., 1997; Feliciello et al., 2001). PKA targeting to the outer mitochondrial membrane (OMM) occurs through the association of its regulatory subunits with three different AKAPs, namely (1) D-AKAP1, or dual-specificity kinase AKAP84/121, (2) AKAP2, and (3) the atypical G-protein Rab32 (Cardone et al., 2004; Carnegie et al., 2009; Feliciello et al., 2001). D-AKAP1, or dual-specificity kinase AKAP84/121, is expressed in most tissues, with high mRNA expression in testes and heart tissue and low levels observed in the brain ((Huang et al., 1997). D-AKAP1 complexed with PKA (D-AKAP1/PKA, also known as mitochondrial PKA) is a neuroprotective, mitochondria-directed scaffolding protein.

The outer mitochondrial membrane (OMM) can be targeted by a protein that directs the PKA holoenzyme. In neurons, PKA plays a critical role in regulating mitochondrial biology

by promoting mitochondrial interconnectivity, anterograde mitochondrial transport in dendrites, and mitophagy.(Dagda et al., 2011; Das Banerjee et al., 2017; Merrill et al., 2011; Zhang et al., 2019). Mitochondrial PKA phosphorylates the mitochondrial fission modulator Drp1 at serine 637 in human Drp1 isoform 1 (or Drp1 656 in rat homologue) to suppress mitochondrial fission and enhance neuroprotection against glutamate excitotoxicity and oxidative stress in a cell culture model of Parkinson's disease (PD). (Merrill et al., 2011; Zhang et al., 2019). It is worth noting that a reduction in PKA-mediated phosphorylation of Drp1 plays a significant role in the development of AD. AD postmortem brain tissue studies, in vitro and in vivo models of AD, have all demonstrated elevated expression of Drp1 and increased mitochondrial fission (Kim et al., 2016; Manczak et al., 2011; Manczak et al., 2018; Manczak & Reddy, 2012; Reddy, Manczak, et al., 2018). ). As mitochondrial fission is necessary to induce neuronal apoptosis, these findings suggest that decreased PKA activity at the mitochondria contributes to Drp1-mediated apoptosis and neurodegeneration. Moreover, several studies have shown that pharmacological inhibition of Drp1 activity via treatment with mdivi-1 can replicate the neuroprotective effects of D-AKAP1/PKA in cell culture and in vivo models of AD, further supporting the notion that decreased mitochondrial PKA activity is a contributing factor to the etiology of AD (Baek et al., 2017; Reddy et al., 2017).

Previous studies have reported a decrease in PKA signaling in the cytosol and nucleus in AD postmortem brain tissue and Aβ-treated neurons, but it is not yet clear if there are changes in the mitochondrial pool of PKA in AD models, and whether decreased mitochondrial PKA contributes to neurodegeneration in AD (Arvanitis et al., 2007; Dagda

& Das Banerjee, 2015; Peng et al., 2005; Pugazhenthi et al., 2011a; Wang et al., 2011), Previous work has shown that transient expression of D-AKAP1 can partially reverse the reduction in dendritic arbors and mitochondrial defects caused by a loss of endogenous PINK1, a kinase mutated in Parkinson's disease (Das Banerjee et al., 2017; Merrill et al., 2011). Enhancing PKA signaling in the mitochondrion can reduce mitochondrial fission, restore oxidative phosphorylation, reverse loss of transmembrane potential, block increased levels of mitochondrial superoxide, and suppress overt mitochondrial turnover in PINK1-deficient neuroblastoma cells (Dagda et al., 2011). Previous studies have shown that Aβ-treated neurons exhibit impaired mitochondrial functions regulated by D-AKAP1/PKA (Manczak et al., 2011; Manczak et al., 2018; Manczak & Reddy, 2012; Saraiva et al., 1985), we hypothesized that treating mouse primary neurons with $A\beta_{42}$ would reduce D-AKAP1 expression, thereby disrupting mitochondrial PKA signaling. To investigate whether Aβ42 treatment affects D-AKAP1 expression and mitochondrial PKA signaling, we treated primary mouse neurons with Aβ42 and found a significant reduction in endogenous D-AKAP1 expression in these cells, as well as in the cortex and hippocampus of young and middle-aged 5X-FAD mice, a transgenic mouse model of AD that recapitulates clinical symptoms of AD (Eimer & Vassar, 2013; Girard et al., 2014; Youmans et al., 2012). Furthermore, we discovered that transient expression of D-AKAP1 or a phosphomimetic mutant of Drp1 (Drp1-S656D) protected against Aβ42-mediated reductions in dendritic length, mitochondrial content, mitochondrial fission, and apoptosis. Therefore, our findings suggest that besides cytosolic/nuclear PKA signaling alterations, the disruption of mitochondrial PKA signaling plays a critical role in driving AD pathogenesis in a cell culture model of AD (Arvanitis et al., 2007; Dagda & Das Banerjee,

2015; Wang et al., 2011). The data presented in this chapter demonstrates the functional implications of increased PKA activity, Drp1-mediated phosphorylation, and D-AKAP1 in an in vitro model of Alzheimer's disease (AD). Specifically, the findings suggest that increased PKA activity and D-AKAP1 levels in mitochondria, induced by exogenous BDNF (as discussed in Chapter 2), can protect mitochondria from beta-amyloid toxicity by promoting fusion through inhibiting Drp1 and can also protect dendrites by increasing PKA activity and mitochondrial content.

## Materials and Methods

### Plasmids

Plasmids encoding OMM-targeted GFP (OMM-GFP), the murine cDNA of wild-type D-AKAP1 or a mutant version that is deficient for binding PKA fused to GFP (D-AKAP1-ΔPKA-GFP; I310P, and L316P), wild-type rat Drp1 and GFP-tagged forms of rat Drp1 (S656A and S656D) plasmids which co-express single hairpins RNA that reduce the level of endogenous rat Drp1 while co-expressing mutant forms of Drp1 that are resistant to knockdown by Drp1shRNAs (J. T. Cribbs & S. Strack, 2007), were generously provided by Dr. Stefan Strack (Department of Pharmacology, University of Iowa). To interrogate the role of PKA in the mitochondrion on neuronal survival in models of AD, it is worth noting that wild-type and PKA binding deficient constructs GFP tagged D-AKAP1 only comprise of the first 525 amino acids and lack the C-terminal domain regions which are required to promote mitochondrial biogenesis. Predesigned stealth siRNAs targeting murine D-AKAP1 were purchased from Life Technologies and prepared as 50μM stocks.

**Cell Culture**

Primary cortical neurons were prepared as previously described (Dagda et al., 2011; Dagda et al., 2014), and used to investigate the effects of β amyloid, estrogen and PKA on neuron-specific processes. All experiments involving mice were performed in accordance with ARRIVE guidelines and were approved by the University of Nevada, Reno's Institutional Animal Care and Use Committee (IACUC, Protocol # 00572). In brief, primary cortical neurons were prepared from timed-pregnant female E17 wild type C57BL/6 (JAX:000664) mice. Per transfection experiment, approximately 32 million total primary cortical cells derived from 8 embryos were plated at a density of 175,000 cells per well. Primary neurons were transfected with the indicated plasmids (0.75µg/well in 4-well LabTekII slides), or with NTsiRNA control or D-AKAP1 siRNAs (20-30 pmols/well in 4-well LabTekII slides), for 72 hours using Lipofectamine at a final concentration of 0.07% as previously described (Dagda et al., 2011; Dagda et al., 2014). After 3 days, two-thirds of the media was exchanged with fresh Neurobasal Media (Gibco/Invitrogen, Carlsbad, CA) containing B27 and 0.75mM L-glutamine. At 5 days in vitro (DIV), primary cortical neurons were transiently transfected with the different plasmids for three days, prior to performing immunocytochemical analysis of mitochondrial morphology, mitochondrial transport, and dendrite length in neurons treated with estrogen (30nM-48hrs) or A$\beta_{42}$ (10µM, 24hrs) at 6 DIV.

**Antibodies**

The following antibodies were used: goat anti-GFP (1:1000) (Rockland Cat# 600-101-215, RRID:AB_218182), mouse anti-human MAP2A/2B (1:500) (Millipore, Cat# MAB378,

RRID:AB_94967), rabbit anti-cleaved caspase3 (1:1000) (Cell Signaling Technology Cat# 9661, RRID:AB_2341188), rabbit anti-β-tubulin (1:2000) (Abcam Cat# ab56889, RRID:AB_2142629), rabbit anti-human D-AKAP1 (1:500) (Santa Cruz Biotechnology Cat# sc-2378, RRID:AB_634813), mouse anti-beta-amyloid 1-42 antibody (Millipore Sigma Cat# AB5078P), Abcam, rabbit anti-TOM20 (1:250) (Santa Cruz Biotechnologies), Alexa 488 and Alexa 546 (1:1000) (Molecular Probes Cat# A-21202, RRID:AB_141607, Cat# A-11010, RRID:AB_143156).

**Crude mitochondrial Isolations**

Crude mitochondrial fractions were isolated from whole brains derived from 6-month-old 5X-FAD mice, B6SJL-Tg (APPSwFlLon,PSEN1*M146L*L286V)6799Vas/Mmjax), or B6SJLF1/J (non-transgenic control) by using differential centrifugation techniques as previously published (Dagda et al., 2011; Dagda et al., 2014) but with the following modifications applied for isolating mitochondria from brain tissue. In brief, approximately 700 milligrams of minced whole brain tissue extracted from mice transcardially perfused with saline was processed for disruption by using an autoclaved glass dounce homogenizer and pestle in 3 mL of cold extraction buffer. The homogenate was transferred into a centrifuge tube in 30-40 mL of cold extraction buffer and centrifuged at 700 x g for 4 min. The supernatant was transferred into a new tube and centrifuged at 700 x g for 10 min. at 4°C to remove the nuclei of unbroken cells. The supernatant was then centrifuged at 10,000 x g for 15 min. at 4°C, and the resulting pellet was resuspended and “washed” up to three times in cold extraction buffer twice, then centrifuged at 10,000 x g for 15 min. at 4°C. The

final pellet was resuspended in approximately 100 µl of mitochondrial storage buffer (ingredients) prior to being processed downstream for Western blots (see below).

**Western Blot**

Proteins (1% TritonX-100 with protease/phosphatase inhibitors) from cell lysates or from cytosolic or crude mitochondrial fractions derived from 6-month-old 5X-FAD mice were resolved on 10% Tris-HCl polyacrylamide gels as previously described (R. K. Dagda et al., 2009) with the following modifications. Following 1D electrophoresis and transfer of proteins to PDVF by using the semidry transblot system (Biorad), immunoblotting for D-AKAP1 and TOM20 were determined in cell lysates by incubating the PDVF membranes with rabbit anti-TOM20 (1:1000) and with rabbit anti-D-AKAP1 (1:1000) antibodies overnight at 4°C. PVDF membranes were incubated with the appropriate secondary antibodies conjugated to horseradish peroxidase (1:5,000; Amersham/GE Healthcare) in 5% milk in TBS containing 0.1% Triton X-100 (TBST), then analyzed by film detection of chemiluminescence.

**Quantification of apoptosis**

Primary cortical neurons were transfected with OMM-GFP, D-AKAP1-GFP, D-AKAP1-ΔPKA-GFP, Drp1-WT-GFP or Drp1-S656D-GFP at 4DIV. At 5DIV, cultures were treated with A$\beta$42 (10µM, 24 h.) to induce cytotoxicity. Post-treatment, neurons were fixed with 4% PFA, blocked in 1% goat serum for 1 hr., permeabilized for 20 minutes in PBS containing 0.1% Triton X-100, and then immunostained for GFP and for cleaved caspase-3 by incubating with rabbit-anti GFP (1:500) and with mouse anti-caspase 3 (1:1000) for

24 hours at 4°C. The fixed cells were then incubated prior to incubating with fluorescently labeled secondary antibodies (goat anti-rabbit Alexa 488 and donkey anti-mouse Alexa 546; Life Technologies) at 1:1000 dilution for 2 hrs. at room temperature. The cells were then sequentially washed in PBS and counterstained with DAPI (1.25μg/ml) to visualize nuclei. Cells were imaged at 25°C using an EVOS-FL microscope Life Technologies) equipped with EVOS Light cubes specific for GFP (excitation/emission of 470/510 nm), RFP (excitation/emission of 531/593 nm), and Cy5 (excitation/emission of 628/692 nm), at magnifications of ×20 (numeric aperture 0.45) or ×40 (numeric aperture 0.60). Apoptosis was analyzed by quantifying the percentage of transfected, MAP2B-positive neurons that contained fragmented or pyknotic nuclei, a hallmark of late-stage apoptosis (Figure 5). The percentage of GFP-positive cells with condensed or fragmented nuclei was analyzed using well-validated methods (Dagda et al., 2011; Merrill et al., 2011). To obtain statistically sound and robust data and given that only ~1% of primary neurons were transfected, it was necessary to scan the whole well for all GFP-positive neurons (~40-70 transfected neurons per well) and quantify nuclear fragmentation in real-time, as opposed to analyzing a set of representative immunofluorescence images. This method of quantification precluded the need to save a representative set of images. Also, please note that the individual conducting the nuclear fragmentation analysis was blinded to all the experimental conditions.

**Immunofluorescence and Live Cell Imaging**

For neurite length measurements, primary cortical neurons were fixed with 4% paraformaldehyde (PFA), permeabilized in PBS containing 0.1% Triton X-100 (PBST), blocked in PBS containing 2% bovine serum albumin, and immunolabeled for GFP, MAP2B and TOM20 to identify transfected neurons, dendrites and mitochondria respectively in transfected cells by incubating with the appropriate primary antibodies (see Antibody section) at 4°C overnight. Fixed cells were then washed extensively in PBS, incubated with secondary antibodies (goat anti-rabbit Alexa 488, donkey anti-mouse Alexa 546; chicken anti-goat Alexa 648, Life Technologies), and counterstained with 1.25µg/ml DAPI to visualize nuclei. Immunolabeled cells were imaged by using an EVOS-FL Cell Imaging System, equipped with EVOS Light cubes specific for GFP (Ex/Em of 470/510) and RFP (Ex/Em of 531/593), at a magnification of 20× (0.45NA).

Neurite lengths were analyzed by using the NIH Image J plug-in program 'NeuronJ' (Erik Meijering, Biomedical Imaging Group Rotterdam, Netherlands) as previously described (Das Banerjee et al., 2017). Neurite length was assessed for at least 25–30 neurons per experiment. Mitochondrial content (percentage of dendrite length occupied by mitochondria) and length of mitochondria within dendrites was assessed using the line tool of Image J as previously described (Dagda et al., 2014). For some assays, and in order to more robustly image dendrites in a non-biased manner (Fig. 5b, Fig.5 C), dendrites were imaged in primary cortical neurons seeded in 96-well plates by using the Neurite module of an ImageXPress Nano (Molecular Devices) imager system. In brief, the mean dendrite length per cell was assessed from 16 regions of interest per well, and from at least 3 wells per condition by using the Neurite Outgrowth Module of MetaXPress high content imaging

software. Overall, approximately 10,000 neurons or more per condition, imaged at 10X magnification. The number of branches and mean dendrite length per neuron was normalized to the number of cell bodies as measured by counting the number of nuclei stained with DAPI in the same regions of interest analyzed.

**Immunohistochemistry and Image Analyses**

Immunohistochemical analyses for endogenous D-AKAP1 in neurons was performed in cortical and hippocampal tissue obtained from non-transgenic control and 5X-FAD homozygous mice to determine abundance of endogenous D-AKAP1 in young vs. aged mice. In brief, whole brains were extracted from 2 and 6-month-old transcardially perfused non-transgenic controls and 5X-FAD mice. The hippocampus and cortex were micro dissected and incubated in decreasing concentrations of sucrose (30 to 10%) overnight at 4 °C, sliced with a temperature-controlled cryostat at 20 µm per slice, mounted on glass slides, blocked in 2% BSA, and co-immunostained for D-AKAP1 (rabbit anti-human, BD Biosciences), for mitochondria (human anti-mouse TOM20, Santa Cruz Biotechnologies), for amyloid beta (mouse anti-beta-amyloid 1-42, Millipore Sigma), and for MAP2B (mouse-anti human, Millipore SIGMA) to identify neurons. The brain slices were then incubated in goat anti-rabbit Alexa 488 and co-incubated with goat anti-mouse Alexa 546 secondary antibodies. The mean integrated intensity of D-AKAP1 (green channel) in MAP2B-positive neurons were analyzed from 4-5 brain slices from 4 mice per group by using NIH Image J (version 1.44, Bethesda, MD). To determine whether alterations in the level of endogenous D-AKAP1 in neurons is due to changes in the level of mitochondria, we used NIH Image J version 1.42 (Bethesda, MD) to analyze mitochondrial content in the

soma of neurons by calculating the percentage of the cytosolic area of the soma containing TOM20-positive mitochondria from 4-5 brain slices from 4 mice per group.

**Statistical Analysis**

Unless indicated otherwise, results are expressed as mean ± S.E.M. from at least three independent experiments. Data was analyzed by performing Student's t test (two-tailed) for pairwise comparisons. Multiple group comparisons were done by performing one- or two-way ANOVA followed by Bonferroni-corrected Tukey's post hoc test. P values less than 0.05 were considered statistically significant.

**Results**

A decrease in PKA-modulated signaling pathways is implicated in AD pathogenesis, as reviewed in [(Dagda & Das Banerjee, 2015)]. Given that enhanced Drp1 activity and decreased PKA-mediated phosphorylation of Drp1 plays a role in AD pathophysiology (Kim et al., 2016; Manczak et al., 2011; Manczak et al., 2018; Manczak & Reddy, 2012; Reddy, Yin, et al., 2018), we hypothesized that PKA signaling in the mitochondrion is altered in Aβ (1-42) -treated primary cortical neurons, a well-accepted cell culture model of AD that faithfully recapitulates mitochondrial dysfunction, enhanced mitochondrial fission, and impaired mitochondrial trafficking upstream of neurodegeneration in primary neurons and neuronal cells (Cha et al., 2012; Nilsen et al., 2006; Reddy, Yin, et al., 2018). To this end, we analyzed endogenous levels of D-AKAP1 in A$_{42}$ -treated mouse primary cortical neurons. Single cell immunocytochemical analysis of D-AKAP1 revealed a robust, significant reduction in the number of primary neurons expressing D-AKAP1 (also known

as D-AKAP1 to refer to the murine homologue of D-AKAP1) in response to exposure to $A\beta_{42}$, as compared to vehicle-treated primary cortical neurons (Fig.1a, Fig.1b). This reduction is specific and is not due to a decrease in mitochondrial number, as treatment of primary cortical neurons with A$\beta_{42}$ does not alter levels of TOM20, an OMM-localized mitochondrial protein, in neuronal soma or dendrites. To further corroborate the loss of D-AKAP1 in an *in vivo* model of AD, we then examined the level of endogenous D-AKAP1 in both young, asymptomatic (~2 months) and in symptomatic, middle aged (6 months) 5X-FAD mice. The 5X-FAD mouse model of AD harbors five different familial AD-associated mutations in the Amyloid Precursor Protein (APP) gene and two mutations within the Presenilin1 (PSEN1) gene, leading to mitochondrial dysfunction accompanied by rapid and high levels of intraneuronal $A\beta_{42}$ accumulation after 2 months of age (Eimer & Vassar, 2013; Girard et al., 2014; Youmans et al., 2012). In addition, 5X-FAD mice promptly develop severe Aβ and tau pathology, including impaired hippocampal long-term potentiation, hippocampal and cortical neurodegeneration, and cognitive deficits, as seen in humans with AD (Eimer & Vassar, 2013; Girard et al., 2014; Youmans et al., 2012). Immunohistochemical analysis of the dentate gyrus of the hippocampus and of the cortex from asymptomatic young or symptomatic middle-aged 5X-FAD mice revealed a significant decrease in the endogenous level of D-AKAP1 but not of TOM20 (Fig. 1c, Fig 1d; Supplementary Fig. 1). In 6.5-month-old 5X-FAD mice, the decrease in endogenous D-AKAP1 coincided with an increase in the deposition of Aβ in the hippocampus (Fig. 1c, Fig. 1d). These observations suggest that the decrease in endogenous D-AKAP1 is not an epiphenomenon of neurodegeneration as 2-month-old 5X-FAD mice do not develop significant neurodegeneration, nor did we detect any significant amount of β amyloid

deposition in the cortex or hippocampus of these mice by IHC (data not shown). Furthermore, consistent with decreased endogenous D-AKAP1 in neurons, Western blot analyses of mitochondria isolated from whole brains from 6-month-old 5X-FAD mice revealed a significant decrease in endogenous levels of D-AKAP1 compared to non-transgenic control mice (Fig. 1e). Consistent with our IHC data, Western blot analysis showed that young, asymptomatic 2-month-old 5X-FAD mice, had a significant decrease in endogenous D-AKAP1 but not TOM20 in the cortex (Supplementary Fig. 2), implying that reductions in D-AKAP1 may precede overt pathology. Overall, our data show that D-AKAP1 levels are significantly reduced in a cell culture model and an *in vivo* model of AD, ultimately suggesting that PKA signaling in the mitochondria may contribute to AD pathology.

Given that the level of endogenous D-AKAP1 is significantly reduced *in vitro* and *in vivo*, we next sought to determine the extent to which restoring mitochondrial PKA signaling via transient expression of D-AKAP1 can block the Mito-toxic and neurotoxic effects of $A\beta_{42}$. We evaluated three morphometric parameters (dendrite length, mitochondrial morphology, and dendritic mitochondrial content) to evaluate the ability of D-AKAP1 to protect against $A\beta_{42}$-mediated neurotoxicity. Indeed, our data show that transient expression of D-AKAP1 fused to GFP (amino acids 1-525) - a shorter form of D-AKAP1 which lacks the KH and Tudor domains required to stimulate mitochondrial biogenesis by associating and redirecting mRNA to mitochondria (Ginsberg et al., 2003; Rogne et al., 2006) but contains the PKA binding site and validated to phosphorylate Drp1 at serine 637 in neuronal cells (Dagda et al., 2011) was able to significantly prevent the reduction in mean dendrite length

and mitochondrial fragmentation in primary neurons exposed to $A\beta_{42}$. In addition, given that our GFP tagged D-AKAP1 constructs lack the C-terminal region containing the KH and Tudor domains required to stimulate mitochondrial biogenesis, our data suggest that the neuroprotective effects of D-AKAP1 are dependent on its ability to bind PKA and not likely due an enhancement of mitochondrial biogenesis. In addition, the ability of D-AKAP1 to protect dendritic and mitochondrial structures against $A\beta_{42}$ requires its association with PKA, as transiently expressing a PKA-deficient mutant of D-AKAP1 (I310P, L316P, D-AKAP1-PKA) was unable to prevent the dendritic retraction and mitochondrial fission observed in control neurons expressing OMM-GFP only (Fig. 2a, Fig. 2b, Fig. 2c). While treating primary neurons with A42 had causes significant mitochondrial fragmentation and retraction of dendrites, only a non-significant decrease in mitochondrial content was observed with a 24 hr. A42 treatment of primary neurons suggesting that A42 treatment promotes mitochondrial fission without depleting dendritic mitochondria at 24 hrs. (Fig. 2d). In addition, transient expression of D-AKAP1-GFP had a non-significant increase on mitochondrial content in dendrites (dendritic mitochondria) compared to beta amyloid-treated primary neurons, as assessed by immunostaining for TOM20 and for MAP2B to identify dendrites (Fig. 2d). Our data suggest that the neuroprotective abilities of mitochondrial PKA are restricted to maintaining a level of mitochondrial structure and dendrite network stability in the Aβ cell culture model of AD reported in this manuscript.

Next, we sought to determine the molecular mechanism by which D-AKAP1 protects dendrites and mitochondrial structure in the *in vitro* Aβ model of AD. It has been shown

by other research groups that PKA-mediated phosphorylation of Drp1 at S637 (S656 is the rat homologue) promotes mitochondria interconnectivity by inhibiting Drp1 activity, reduces oxidative stress, can induce an increase in dendritic length, and increases mitochondrial content in dendrites (Dagda et al., 2011; Dickey & Strack, 2011)). To this end, we hypothesized that restoring endogenous levels of D-AKAP1 will prevent neurodegeneration in primary cortical neurons treated with $A\beta_{42}$. To address this hypothesis, primary cortical neurons were transiently transfected with an empty vector, a phosphomimetic mutant of Drp1 (Drp1-S656D), or with Drp1. When exposed to an acute dose of $A\beta_{42}$ (10 μM, 24 hr.), immunohistochemical analysis revealed that primary cortical neurons expressing Drp1-S656D, but not wild-type Drp1, showed significantly increased dendritic length and decreased mitochondrial fragmentation compared to OMM-GFP expressing primary neurons treated with $A\beta_{42}$ (Fig. 3a., Fig. 3b., Fig. 3c). These data suggest that D-AKAP1 /PKA protects dendritic and mitochondrial structures by phosphorylating Drp1 on S656. Consistent with the ability of D-AKAP1 to increase dendritic mitochondrial content (Dickey & Strack, 2011), transient expression of the phosphomimetic mutant, but not wild-type Drp1, robustly increased mitochondrial content in dendrites under basal conditions and in $A\beta_{42}$-treated neurons, and blocked β-amyloid mediated reduction in mitochondrial content (Fig. 3d). Next, we surmised that D-AKAP1 /PKA can protect primary cortical neurons against β-amyloid-mediated apoptosis by phosphorylating Drp1. Indeed, transient expression of D-AKAP1 efficiently blocked neuronal apoptosis induced by $A\beta_{42}$ (Fig. 4). Moreover, consistent with its pro-apoptotic role, transient expression of Drp1 alone increased neuronal apoptosis in untreated neurons (Fig. 4). Transient expression of the phosphomimetic mutant, but not of wild-type Drp1,

partially blocked apoptosis induced by exposure to $A\beta_{42}$. Unexpectedly, transient expression of the PKA-deficient mutant of D-AKAP1 (D-AKAP1-$\Delta$PKA) robustly increased neuronal apoptosis under basal conditions (untreated) and exacerbated apoptosis in $A\beta_{42}$-treated primary neurons. Consistent with other published studies (Zhang et al., 2019), our data suggest that D-AKAP1 -$\Delta$PKA acts in a dominant negative manner to outcompete endogenous D-AKAP1, thereby enhancing neuronal apoptosis in the absence of oxidative stress (Fig. 4).

Exposure of neurons to estrogen has also been shown to activate PKA signaling pathways and confer "Mito-protective" effects in neurons (Sarkar et al., 2015). Like PKA, estrogen supplementation has been shown to exert robust neuroprotective effects in cell culture and *in vivo* models of AD. To this end, in an effort to further determine the mechanism of neuroprotection of D-AKAP1/PKA in the cell culture model of AD, we sought to determine whether enhancing the activity of mitochondrial PKA phenocopies the neuroprotective ability of estrogen. As expected, treating primary cortical neurons with $A\beta_{42}$ significantly reduced dendrite length, and induced mitochondrial fragmentation (Fig. 5a, Fig. 5b). In contrast, transient expression of D-AKAP1 or treatment with 2-estradiol completely restored dendrite length, and mitochondrial length in primary neurons treated with $A\beta_{42}$ (Fig. 5a, Fig. 5b). Consistent with its capacity to phosphorylate and thereby decrease the fission activity of Drp1, the ability of D-AKAP121 to reverse mitochondrial fission requires binding to endogenous PKA holoenzyme as transiently expressing D-AKAP1-$\Delta$PKA did not reverse mitochondrial fission induced by $A\beta_{42}$ treatment (Fig. 5b). Finally, we sought to determine whether the ability of 2-estradiol (β-estradiol) to protect against

amyloid β requires endogenous D-AKAP1. To address this question, we transfected primary cortical neurons with siRNA directed against endogenous D-AKAP1 for three days, a time point which shows significant reduction of endogenous D-AKAP1 by immunohistochemical analysis of endogenous D-AKAP1 in fixed primary cortical neurons (Fig. 5c). As previously reported, we observed that siRNA-mediated knockdown of endogenous D-AKAP1 promoted a loss of dendrites under baseline conditions (Fig, 5d), consistent with the ability of D-AKAP1/PKA to stimulate dendritogenesis. Additionally, while 2-estradiol was able to significant block the loss of dendrites in primary cortical neurons transfected with D-AKAP121siRNA and in ﷺ-amyloid treated neurons, it was unable to reverse dendrite loss induced by ﷺ-amyloid treatment in D-AKAP1siRNA-transfected primary cortical neurons (Fig. 5d). Hence, our data suggest that estrogen can compensate for the loss of endogenous D-AKAP1 by alleviating the loss of dendrites induced by loss of endogenous D-AKAP1, suggesting that estrogen is downstream and/or participates in a parallel signaling pathway with D-AKAP1. However, the observation that estrogen is unable to reverse the loss of dendrites in D-AKAP1siRNA-transfected neurons treated with β-amyloid suggest that D-AKAP121 is a critical molecular player for 2-estradiol's neuroprotective effects in the cell culture model of AD (Fig. 5d). Overall, our data show that restoring D-AKAP1 expression at the mitochondria can ameliorate the mitochondrial and neurotoxic effects of $A\beta_{42}$. In aggregate, our research shows that a significant reduction in the levels of D-AKAP1 in neurons contributes to AD pathogenesis, as restoring the levels of endogenous D-AKAP1, at least via transient transfection for three days, is sufficient to protect against the toxic effects of $A\beta_{42}$ *in vitro*.

**Discussion**

Dysregulation of global PKA is strongly implicated in the pathogenesis of AD. Indeed, previous studies in post-mortem human AD brains, as well as *in vivo* animal and *in vitro* cellular models of AD, have reported a significant decrease in nuclear translocation and PKA-mediated phosphorylation of CREB, altered levels of regulatory and catalytic subunits of PKA, and a disruption of neurotrophic signaling modulated by PKA (e.g. BDNF), as reviewed in [(Dagda & Das Banerjee, 2015)]. These studies, however, have predominantly focused on the role of dysregulated cytosolic/nuclear PKA on AD pathogenesis. Given that mitochondrial structure and function are severely impaired in AD and that PKA at the OMM plays a monumental role in modulating mitochondrial function and structure, we sought to understand how oligomerized β-amyloid affects PKA signaling in the mitochondrion. For the first time, we show here, that D-AKAP1, the scaffolding protein of PKA, is decreased in both *in vitro* and *in vivo* models of AD, suggesting that PKA signaling is decreased in mitochondria and contributes to AD pathogenesis. Mechanistically, we show that transient expression of D-AKAP1 or the phosphomimetic mutant of Drp1 (Drp1-S656D) can rescue primary cortical neurons from A$\beta_{42}$-mediated neuronal death, loss of dendrites, and mitochondrial fission, suggesting that disruption of the mitochondrial PKA signaling pathway plays a prominent role in driving Aβ-mediated mitochondrial pathology and neurodegeneration.

AKAPs comprise a large family of 50 scaffolding proteins which anchor PKA and other proteins, including protein kinases and phosphodiesterase's, to defined subcellular locations (Brandon et al., 1997; Feliciello et al., 2001). AKAP-based protein complexes

form the basis for the spatiotemporal control of cAMP signaling, and through their additional interacting domains, AKAPs can integrate cAMP signaling with other cellular signaling processes (Brandon et al., 1997; Feliciello et al., 2001). Importantly, dysregulation of AKAPs and their interactions have been implicated in cardiac pathophysiology, sperm motility and developmental defects, HIV progression, and altered synaptic transmission(Brandon et al., 1997). Here, we report for the first time a significant reduction in endogenous D-AKAP1 in the brains of hemizygous 5X-FAD mice of AD and in primary cortical neurons treated with amyloid β (1-42). In addition, we show reduced expression of D-AKAP1 in the cortices and hippocampi 5X-FAD mice at 2 months of age, an age that precedes cognitive loss (4 months) and synaptic impairment (9 months) (Fig. 1; Supplementary Fig. 1, Supplementary Fig. 2). Overall, these data indicate that loss of D-AKAP1 and disruption of its interaction with PKA is an early event that may contribute to accelerated neuropathology in this *in vivo* model of AD.

The neuroprotective role of D-AKAP1 has traditionally been thought to involve phosphorylation of the pro-apoptotic protein BAD and of the mitochondrial fission modulator Drp1 to prevent neuronal apoptosis and elicit mitochondrial fusion, respectively (Affaitati et al., 2003; Cardone et al., 2002; Merrill et al., 2011). In a genetic model of PD, we have shown that PINK1-deficient primary cortical neurons exhibit impaired mitochondrial trafficking, loss of mitochondrial content in dendrites, increased oxidative stress and overactive mitophagy (Dagda et al., 2014; Das Banerjee et al., 2017). On the other hand, enhancing mitochondrial PKA signaling reverses mitochondrial dysfunction and Drp1-dependent fission, restores mitochondrial trafficking by inducing PKA-mediated

phosphorylation of the mitochondrial adaptor protein Miro2, and blocks neurodegeneration (Dagda et al., 2011; Das Banerjee et al., 2017). Likewise, here we show that transient expression of D-AKAP1 potently protects neurons in a cell culture model of AD. Indeed, transient expression of D-AKAP1 reduced mitochondrial fission, elevated mitochondrial content, and blocked neuronal apoptosis induced by amyloid beta (Fig. 2, Fig. 3, Fig. 4, Fig. 5). Given that PKA signaling is dysregulated in models of AD and PD, the neuro and Mito protective roles of D-AKAP1 suggest that D-AKAP dysregulation and impairment of PKA signaling at the mitochondrion may be an early event in disease pathogenesis and common to several brain-degenerative disorders, including AD and PD. Furthermore, the neuroprotective role of D-AKAP1 is dependent on intact PKA activity as the PKA binding deficient mutant of D-AKAP1 (D-AKAP1-ΔPKA), was unable to rescue neurons from amyloid β-mediated toxicity or loss of dendrites and mitochondria.

We have previously reported that PKA-mediated phosphorylation of Drp1 at S656 is a mechanism by which cAMP and PKA/D-AKAP1 promote mitochondrial fusion, which enhances mitochondrial function and neuronal survival in a genetic cell culture model of PD and in a cell culture model of glutamate excitotoxicity in HT22 hippocampal progenitor cells (Dagda et al., 2011; Zhang et al., 2019). In this study, we show that transient expression of a GFP-tagged phosphomimetic mutant of Drp1 (Drp1-S656D) is sufficient to protect neurons against neurodegeneration in the Aβ cell culture model of AD. Transient expression of Drp1-S656D reduced amyloid β-mediated neuronal apoptosis, reduced mitochondrial fission and dendritic retraction to a similar extent as that conferred by transient expression of D-AKAP1 alone (Fig. 4). Hence, our data suggest that D-AKAP1

is neuroprotective by virtue of its ability to recruit PKA to the mitochondrion to phosphorylate Drp1, and thereby prevent mitochondrial fission, loss of dendrites and mitochondrial content, and neuronal death.

Like D-AKAP1/PKA, estrogens (estradiol-2) may exert direct or indirect effects on mitochondrial function and PKA signaling, which is mediated via the mitochondrially-localized estrogen receptor β. Estradiol-2 (E2), or activators of estrogen receptor β preserve mitochondrial function by maintaining mitochondrial membrane potential (Dykens et al., 2003 ; Sarkar et al., 2015). A depletion of estrogen is observed in postmenopausal women and is a significant risk factor for the development of AD, and estrogen-based hormone therapy may reduce this risk. Given that estrogen exerts Mito-protective effects as observed for D-AKAP1 (Fig. 5A) and published observations that estrogen (e.g. estradiol-2) and ligands of estrogen receptor β can activate downstream PKA signaling in the brain (Liu et al., 2008; Vitolo et al., 2002) to protect mitochondria from β amyloid toxicity (Sarkar et al., 2015), we surmised that 2-estradiol and mitochondrial PKA may interact to protect against the loss of dendrites induced by β-amyloid. Indeed, we observed that siRNA-mediated knockdown of endogenous D-AKAP1 prevented 2-estradiol from restoring dendritic networks in -amyloid treated primary cortical neurons. This implies that estrogen protects dendritic networks through a mechanism that is dependent on D-AKAP1/PKA or is mediated through the estrogen β receptor in mitochondria. These data suggest that pharmacological activation of mitochondrial PKA (D-AKAP1 /PKA), direct activation of the estrogen  receptor in mitochondria, or enhancement of D-AKAP1 levels may be therapeutic avenue alternatives to estrogen supplementation in postmenopausal

women that may reduce the risk of developing AD. Although we acknowledge that our data in figure 5D suggests that endogenous D-AKAP1 /PKA is required for estrogen to protect dendrites, we recognize that additional experiments will need to be performed in order to determine the extent to which estrogen requires PKA to protect mitochondrial structure and function from β-amyloid toxicity, and to functionally dissect the molecular mechanism by which estrogen interacts with D-AKAP1 to exert its neuroprotective effects. Finally, our results warrant future studies to identify pharmacological activators of mitochondrial PKA that can extend neuroprotection in models of AD.

**Conclusions**

In summary, our data show that a significant reduction in the level of D-AKAP1 in neurons contributes to AD pathogenesis, and that enhancing the level of endogenous D-AKAP1 is sufficient to partially or fully protect against mitochondrial pathology and neurodegeneration induced by amyloid β. Mechanistically, the neuroprotective effects of D-AKAP1/PKA phosphorylation involves PKA-mediated phosphorylation of Drp1, blocking neuronal apoptosis and to maintaining mitochondrial interconnectivity and dendritic networks.

## Figure Legends

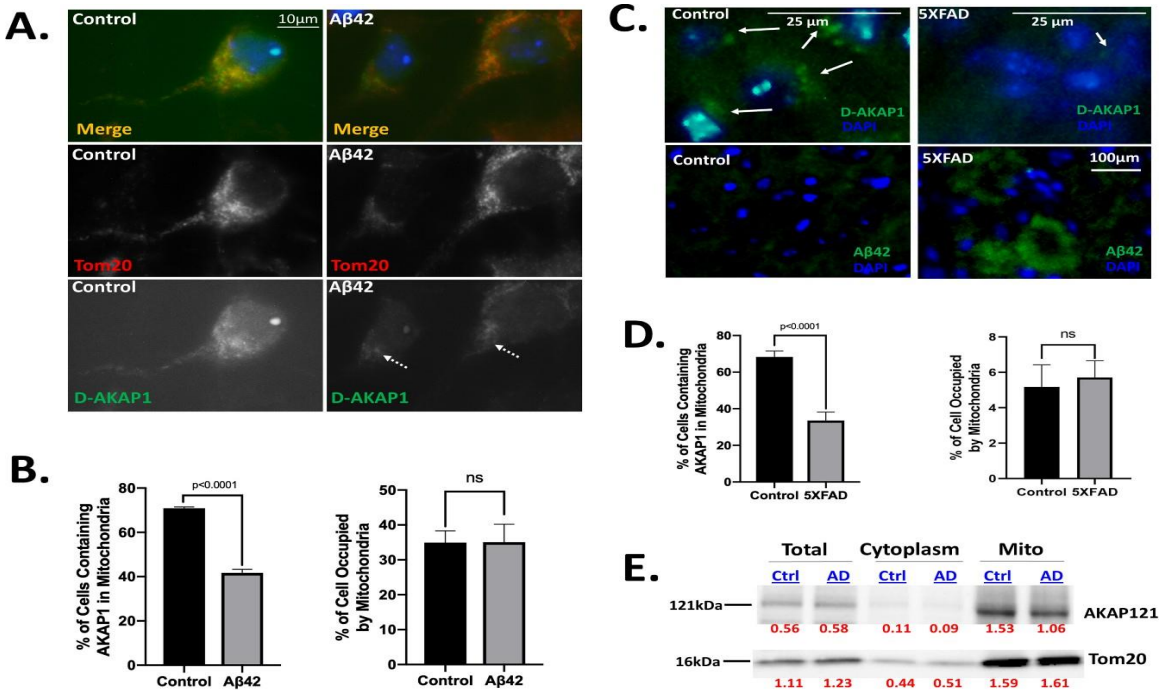


**Fig. 1** The level of endogenous D-AKAP121 is significantly decreased in mitochondria of neurons in *in vitro* and *in vivo* models of Alzheimer's disease.

**(a)** Representative epifluorescence micrographs (60X) showing decreased levels of D-AKAP1 (green channel), but not of mitochondria (TOM20, red channel), in primary cortical neurons treated with a 24-hr. dose of beta amyloid (10µM) compared to untreated primary neurons (control). White arrows point to the location of immunoreactive clusters of D-AKAP1 that colocalize with mitochondria. (**b**) Left: representative bar graph showing a compiled quantification of the percentage of cells containing D-AKAP1 in mitochondria of primary cortical neurons treated with vehicle control or with $A\beta_{42}$. The right bar graph shows a compiled quantification of the percentage of the soma occupied by mitochondria, as identified by immunostaining with TOM20, as a metric of mitochondrial

content. For both graphs, means ± SEM, derived from 250-300 primary cortical neurons from at least 10 epifluorescence microscopic fields per experiment compiled from three independent experiments (*: $p<0.05$ vs. control, Welch's t-test). (**c**) Representative epifluorescence micrographs (60X) showing a decrease in the number of neurons that immunostained with D-AKAP1 (top two panels) in hippocampal slices derived from 5X-FAD (top right and lower right panel) compared to control non-transgenic mice (top left and lower left panels). Pathological events coincide with an accumulation of $A\beta_{42}$ in neurons. White arrows point to neurons that express D-AKAP1 (green channel). (**d**) Left: representative bar graph showing a compiled quantification of the percentage of cells that contained D-AKAP1 in mitochondria of immunostained hippocampal neurons from hippocampal slices derived from 6-month-old non-transgenic control or 5X-FAD mice. The right bar graph shows a compiled quantification of the percentage of the soma occupied by mitochondria, as identified by immunostaining with TOM20, as a metric of mitochondrial content in hippocampal neurons from hippocampal slices derived from 6.6-month-old non-transgenic control or 5X-FAD mice. For both graphs, means ± SEM, derived from 4-6 brain slices from 3-4 animals per genotype (*: $p<0.05$ vs. control, Welch's t-test). (**e**) Representative Western blot of endogenous D-AKAP1 and of TOM20 from brain lysates, and of cytosolic and mitochondrial fractions derived from 6.5-month-old control non-transgenic (Ctrl) or 5X-FAD (AD) mice. Densitometric quantification of D-AKAP1-immunoreactive bands, normalized to TOM20, is shown on the bottom of the blot (red numbers). The data show that the level of endogenous D-AKAP1 is

decreased in mitochondria of 5X-FAD mice (~27% decrease) compared to non-transgenic control mice. The data show that D-AKAP1 levels are decreased in mitochondria of 5X-FAD mice (~27% decrease) compared to non-transgenic control mice. Although the AKAP121 immunoreactive bands ran at the expected molecular weight (~121kDa), please note that a slight electrophoretic shift occurred in the mitochondrial fractions relative to the corresponding cell lysates, presumably due to the different buffers that were used during the isolation of mitochondria vs. cell lysates, which may have caused the mitochondrial fraction bands to migrate modestly faster. Work done by Dr. Tania Das Banerjee.

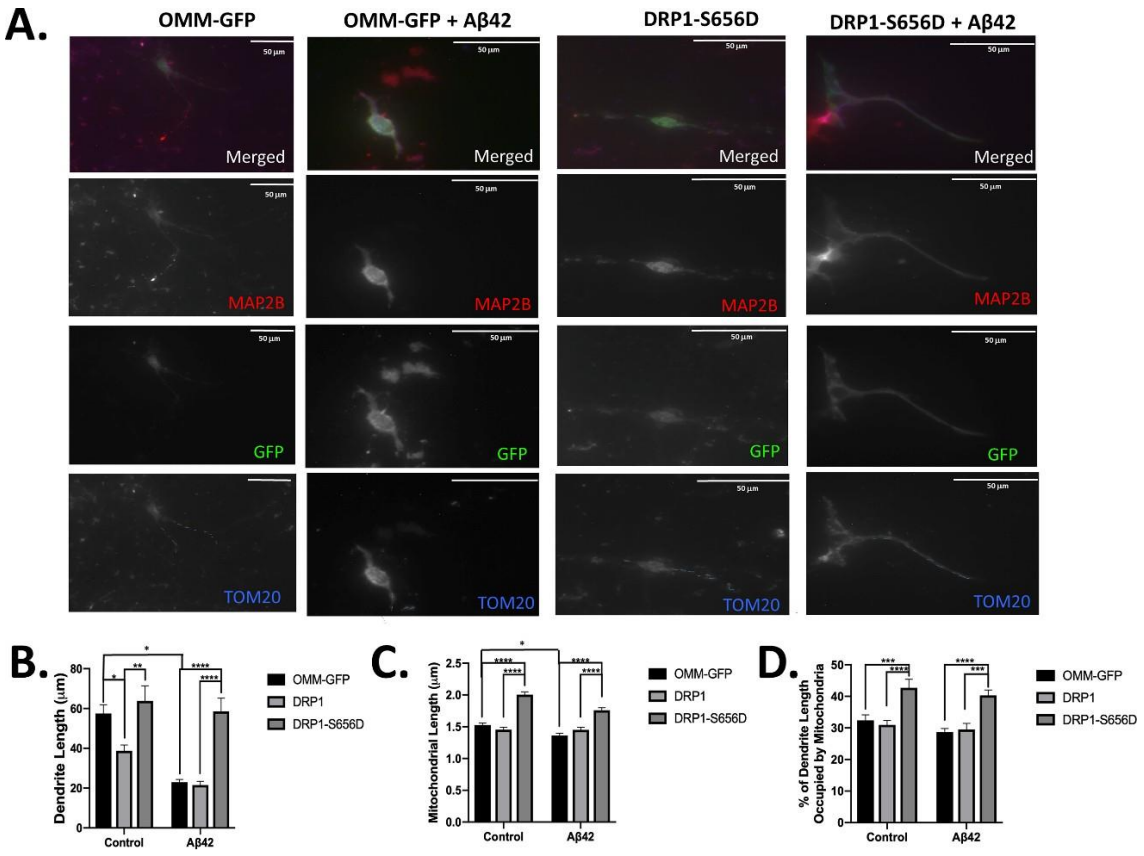


**Fig. 3** D-AKAP1/PKA protects dendrites and mitochondrial structure from $A\beta_{42}$-mediated toxicity via PKA-mediated phosphorylation of Drp1. (a) Representative epifluorescence micrographs (60X) of primary cortical neurons expressing the indicated GFP-tagged Drp1-modulating plasmids in the presence of vehicle control (DMSO) or $A\beta_{42}$. Primary neurons were immunostained for MAP2B (red) to identify dendrites, for GFP (green) to identify transfected neurons, and for TOM20 (blue) to identify mitochondria. Mitochondria inside MAP2-positive dendrites are indicated by blue dashes. Transient expression of PKA phosphomimetic mutant of Drp1 (S656D) protects dendrites and the number of dendritic mitochondria from $A\beta_{42}$-treatment compared to primary neurons expressing OMM-GFP as a control. (**b**) Bar graph shows a compiled quantification of the mean dendrite length per

neuron, as measured in MAP2B-positive neurites in primary cortical neurons treated with vehicle or with $A\beta_{42}$ (24 hr., 10µM). Means ± SEM, derived from 250-300 primary cortical neurons from at least 10 epifluorescence microscopic fields per experiment, were compiled from three independent experiments (**/***: $p<0.01$ vs. OMM-GFP or Drp1-S656D/Aβ42 in each series, *:<0.05 vs. OMM-GFP/Aβ4, Two-Way ANOVA with Tukey's post hoc test). (**c**) Bar graph shows a compiled quantification of the mean mitochondrial length of dendritic mitochondria, as identified by immunostaining with TOM20 within MAP2B-positive neurites and quantified by Image J in primary cortical neurons treated with vehicle or with $A\beta_{42}$(24 hr., 10µM). Means ± SEM, derived from 250-300 primary cortical neurons from at least 10 epifluorescence microscopic fields per experiment, were compiled from three independent experiments (**/***: $p<0.01$ vs. OMM-GFP or for Drp1-S656D/Aβ42for each series, Two-Way ANOVA with Tukey's post hoc test). (**d**) Bar graph shows a compiled quantification of the mean mitochondrial content in dendrites (% of dendrite length occupied by mitochondria), as identified by immunostaining with TOM20 within MAP2B-positive neurites and quantified by Image J in primary cortical neurons treated with vehicle or with $A\beta_{42}$ (24 hr., 10µM). Means ± SEM, derived from 250-300 primary cortical neurons from at least 10 epifluorescence microscopic fields per experiment, were compiled from three independent experiments (Two-Way ANOVA with Tukey's post hoc test). Work done by Kelly Reihl.

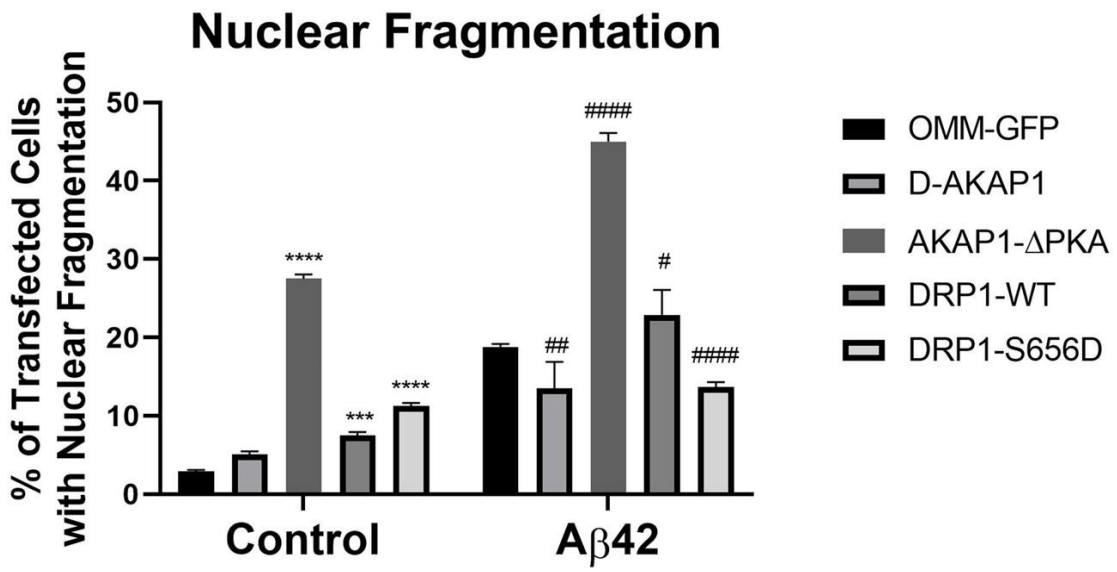


**Fig. 4** D-AKAP1/PKA decreases neuronal apoptosis induced by $A\beta_{42}$ via PKA-mediated phosphorylation of Drp1.

Bar graph showing a compiled quantification of the percentage of GFP-positive primary cortical neurons containing fragmented or pyknotic nuclei. Primary cortical neurons were treated with vehicle or $A\beta_{42}$ (24 hr., 10μM). Means ± SEM, derived from an average of 226 primary cortical neurons per construct from at least 10 epifluorescence microscopic fields per experiment, were compiled from three independent experiments (****: $p<0.0001$ vs. OMM-GFP, ##/###/####: $p<0.01$ vs. OMM-GFP/$A\beta_{42}$; Two-Way ANOVA with Tukey's post hoc test) completed experiments performed by from Kelly Reihl and Dr. Tania Das Banerjee.

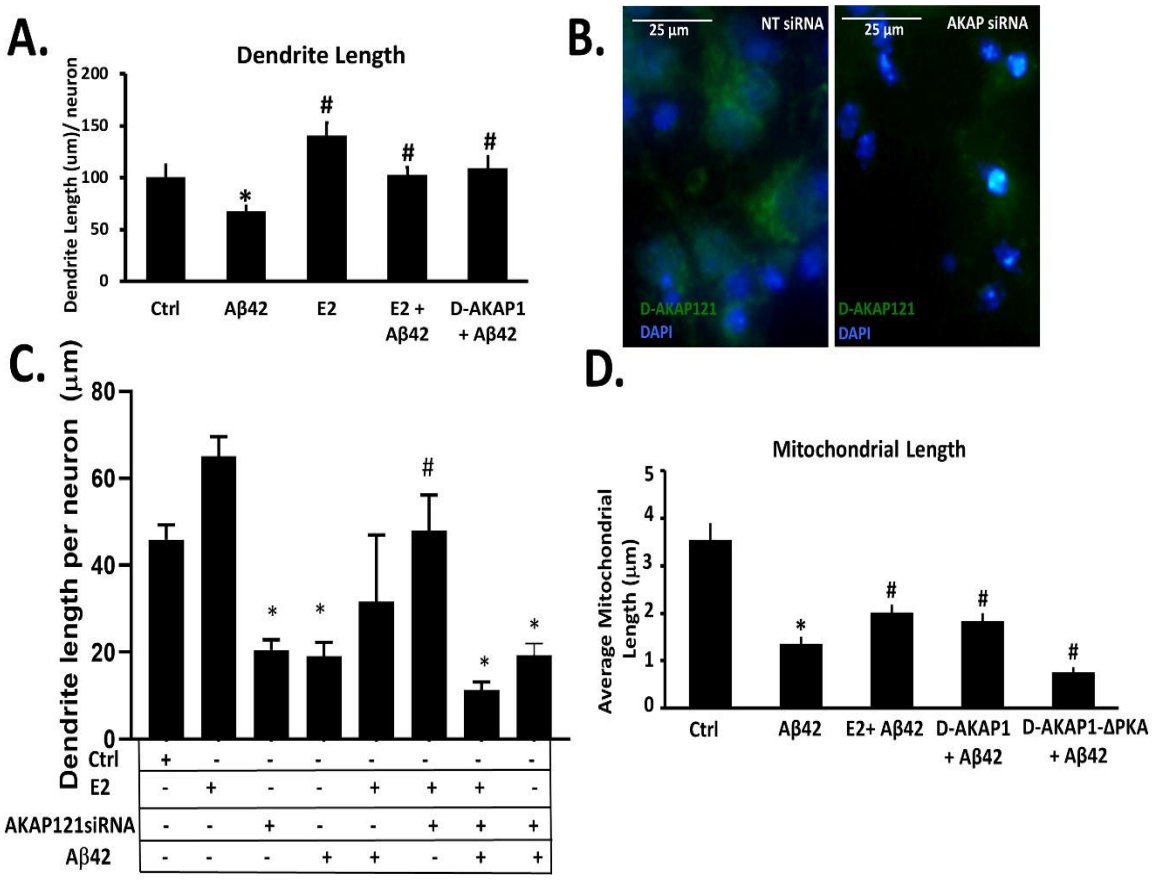


**Fig. 5** D-AKAP1/PKA exerts neuroprotection in primary cortical neurons against $A\beta_{42}$ in a similar manner as estrogen treatment.

**(a)** Representative bar graph of the mean dendrite length per neuron, as measured in MAP2B-positive neurites, in primary cortical neurons transfected with the indicated plasmids and pretreated with either vehicle or 2-estradiol in the absence or presence of $A\beta_{42}$ (24 hr., 10µM). Means ± SEM, derived from 30-35 primary cortical neurons from a representative assay of two independent experiments showing similar results (*: $p<0.05$ vs. OMM-GFP, #:$P<0.05$ VS. Aβ42 One-Way ANOVA with Tukey's post hoc test). (**b**) Representative bar graph of the mitochondrial length (µm) per neuron, as measured in TOM20-immunostained structures, in primary cortical neurons transfected with the

indicated plasmids and pretreated with either vehicle or 2-estradiol in the absence or presence of $A\beta_{42}$ (24 hr., 10μM). Means ± SEM, derived from 30-35 primary cortical neurons from a representative assay of three independent experiments showing similar results (*: $p<0.05$ vs. Ctrl; #: $p<0.05$ vs. $A\beta_{42}$, One-Way ANOVA with Tukey's post hoc test). (**c**) Representative epifluorescence micrographs of primary cortical neurons transfected with non-targeted siRNA control (NTsiRNA) or with AKAP121-specific siRNA and immunostained for D-AKAP121 (green channel) and counterstained with DAPI to visualize nuclei (blue). Primary cortical neurons transfected with AKAP121 siRNA showed a significant reduction in endogenous D-AKAP1 relative to NTsiRNA-transfected primary cortical neurons. (**d**) Representative bar graph of the mean dendrite length per neuron in 5 DIV primary cortical neurons transfected with non-targeting control siRNA (Ctrl), or with siRNA specific for endogenous D-AKAP1 (D-AKAP1siRNA) for two days prior to treating with 2-estradiol and/or $A\beta_{42}$ (24 hr., 10μM) as indicated in the table below the bar graph. Means ± SEM, derived from at least primary cortical neurons from a representative assay of two independent experiments showing similar results (*: $p<0.05$ vs. Ctrl; #: $p<0.05$ vs. $A\beta_{42}$, One-Way ANOVA with Tukey's post hoc test, n=500-2,000 imaged neurons from across 3-7 wells) research performed by Dr. Tania Das Banerjee and Maryann Swain.

**Supplemental Figures**

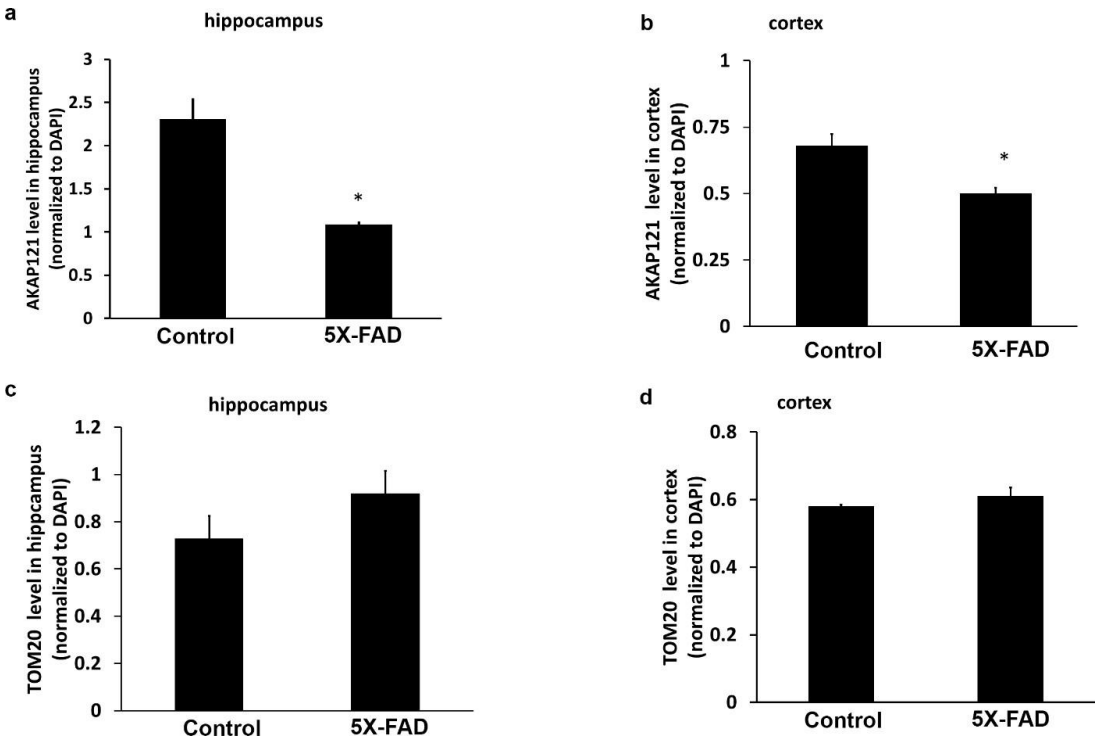


**Supplemental fig. 1** The level of endogenous D-AKAP121 is significantly reduced in the hippocampus and cortex of asymptomatic 5X-FAD mice. Immunohistochemical quantification of the level of endogenous AKAP121 in the hippocampus (**a**) or cortex (**b**) and of the OMM-localized marker TOM20 in the hippocampus (**c**) or cortex (**d**) derived from the brains of 2-month wild-type (Control) and asymptomatic heterozygous 5X-FAD. By using image-based analysis, quantification was performed by analyzing the integrated density of multiple regions of interest within each brain slice analyzed at 10X magnification and normalized to the total number of cells based on the total number of nuclei that stained for DAPI. (n=1000 neurons, 4 slices per indicated brain region, N=4 animals per genotype, Student's t-test, *: $p<0.05$). By Mariana Torres and Maryann Swain.

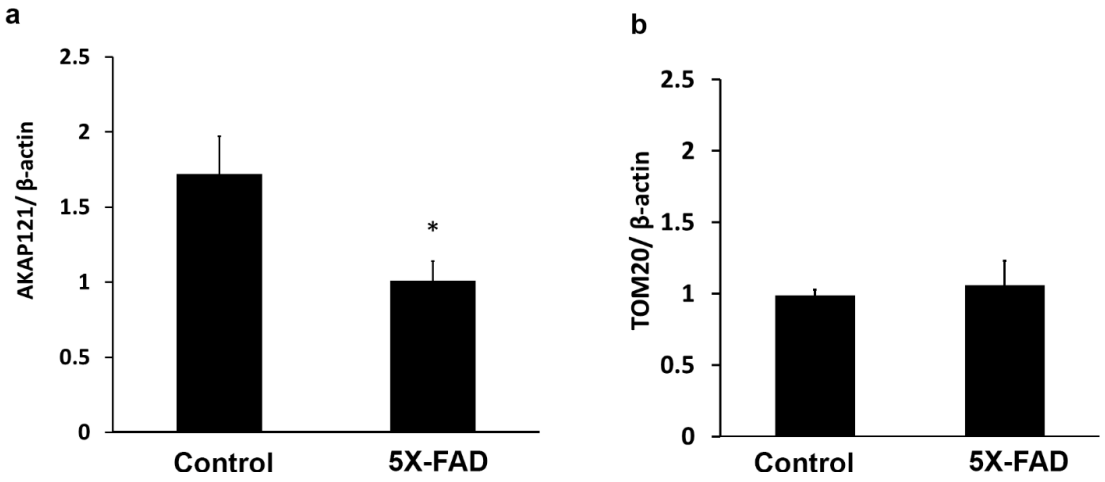


**Supplementary Fig. 2** The level of endogenous D-AKAP121 is significantly reduced in the cortex of asymptomatic 5X-FAD mice.

Western blot quantification of the level of endogenous AKAP121 (**a**) or of the OMM-localized mitochondrial marker TOM20 (**b**) from the tissue lysates derived from cortices of 2-month-old wild-type (Control) and asymptomatic, hemizygous (HET) 5X-FAD mice. The quantification was performed by analyzing the integrated density of respective immunoreactive bands of interest (~121kDa for AKAP121 and ~20kDa for TOM20) and normalized to β-actin (N= 4 animals per genotype, Student's t-test, *: $p<0.05$). Experiments by Mariana Torres and Maryann Swain.

# Chapter IV

## Multiplexing Seahorse XF$^{e}$24 and ImageXpress® Nano platforms for comprehensive evaluation of mitochondrial bioenergetic profile and neuronal morphology


### Abstract

The measurement of mitochondrial function has become imperative to understand and characterize diseases with bioenergetic variations. The advancement of automation and application of high-throughput technologies has propelled the understanding of biological complexity and facilitate drug discovery. Seahorse extracellular flux (XF$^{e}$) technology measures changes in dissolved oxygen and proton concentration in cell culture media, providing kinetic measurements of oxidative phosphorylation and glycolytic metabolism. ImageXpress® Nano is an automated fluorescent microscope with the ability to perform high-content, fast, and robust imaging in multi-well formats. In this chapter, we present a comprehensive protocol to multiplex the Seahorse XF$^{e}$24 analyzer with ImageXpress® Nano high content imaging microscope to provide a comprehensive yet rigorous profile of bioenergetics and its correlation to neuronal function. My data showed an increase in mitochondrial respiration precedes the prolonged effects of BDNF on dendrite maintenance, as evidenced by AN12's ability to abolish both the increase in dendrite length and complexity and mitochondrial respiration induced by BDNF.

## Multiplexing bioenergetics and imaging for comprehensive data

### Introduction

The mitochondrion is the primary site for essential bioenergetic processes in cells, facilitating critical processes such as oxidative phosphorylation, calcium homeostasis, ROS production, fatty acid oxidation, and the Krebs cycle (Ruben K Dagda et al., 2009; Houten et al., 2016; Soman et al., 2017). In mammalian cells, mitochondria are responsible for producing 80% of ATP for endergonic cellular functions through oxidative phosphorylation (OXPHOS), while the remaining ATP is produced anaerobically, mainly through glycolysis. Any disruptions to bioenergetic pathways can be detrimental to cellular function, leading to pathological outcomes such as neurodegeneration (Gorman et al., 2016). Oxidative phosphorylation is a catabolic process that oxidizes nutrients to establish a proton gradient, which is coupled to the electron transport chain to synthesize ATP (Papa et al., 2012). Toxins such as 1-methyl-4-phenyl-1,2,3,6-tetrahydropyridine (MPTP) can inhibit the physiological function of the Complex 1 subunit, disrupting the electron transport chain (Langston, 2017). Loss-of-function mutations in mitochondrial genes or nuclear-encoded mitochondrial proteins can also cause mitochondrial dysfunction (Alston et al., 2017). It is important to note that mitochondrial dysfunction is amplified in high energy-consuming cells such as neurons and muscle cells, and it is a hallmark of neurodegenerative diseases such as Parkinson's disease, where reduced expression and activity of the Complex 1 subunit are common (Schapira et al., 1990). Given the crucial role of mitochondrial function in healthy cells, innovative tools that assay mitochondrial function are needed to better understand the complex interplay between bioenergetic pathways and their relation to neurodegeneration (e.g., loss of dendrites, caspase-mediated

cell death, and necrosis). Although mitochondrial function can be measured through various determinants, including mitochondrial membrane potential, ATP turnover, MTT reduction, and mitochondria-derived NADPH levels, the current technique of choice is measuring oxygen consumption rates (OCRs) using dye-label techniques. This chapter describes a method for assaying mitochondrial function using Seahorse XFe technology and concurrent imaging of cells. This chapter builds upon the findings from chapters 2 and 3, which highlighted the role of BDNF in promoting neuronal survival through mitochondrial PKA mechanisms and the importance of mitochondrial dysfunction in AD pathology. The high-resolution data presented in this chapter sheds light on the temporal dynamics of BDNF's regulation of mitochondrial respiration and dendrite length. Our findings demonstrate that BDNF increases both mitochondrial respiration and dendrite length/complexity. Furthermore, treatment with AN12, a mitochondrial uncoupling agent, abrogates both effects, suggesting that an increase in mitochondrial respiration precedes the more protracted effects of BDNF on the maintenance of dendrites.

**Rationale**

Technology that measures oxygen consumption rates as a proxy of mitochondria function via the $XF^e24$ Bioanalyzer has emerged as a cutting-edge method to measure cellular bioenergetics (OXPHOS and glycolysis). However, a significant limitation of the $XF^e24$ Bioanalyzer is that mitochondrial function data derived from this instrument is not associated with the morphological data of cells, which can provide crucial scientific information to understand how extracellular stimuli, toxins, or pharmacological-active compounds affects cell viability and health(Tania Das Banerjee et al., 2021; Soman et al.,

2021). Therefore, improvising the robust XFe24 Bioanalyzer technology by combining simultaneous imaging capability to quantify morphology and expression patterns enhances the understanding of bioenergetic pathways in correlation with cellular function. In this chapter, the hypothesis that I tested is that treatment with exogenous of primary cortical neurons with exogenous human recombinant Brain Derived Neurotrophic Factor (BDNF) has an immediate effect in elevating oxidative phosphorylation, a physiological effect that precedes an increase in dendrite length/complexity induced by the neurotrophin and that requires the activation its cognate receptor (Trkβ)

**Principle and working**

In order to test this hypothesis, it was necessary to assess mitochondrial respiration and analyze neuronal morphology (dendrites and cell bodies) in the same population of neurons. To this end, I employed the $XF^e24$ Bioanalyzer (Agilent Technologies) to measure the flux of oxygen (OCR) and the flux of protons, also known as extracellular acidification rates (ECARs), as a proxy of glycolysis, in the cell medium(Chacko et al., 2014). OCRs and ECARs are key indicators of mitochondrial respiration and glycolysis, respectively (Fig. 1). The assay is performed by insulating a fraction of cell culture media (~7µl) that is generated when the fluorescent probes are lowered onto the bottom of the well to create a microchamber in the microplate well, which measure the dissolved oxygen (measured as millimeters of mercury pressure per minute) and protons (measured as the change in milli-pH units per minute) in the microchamber per well. OXPHOS consumes oxygen to make water through a four-electron reduction reaction at complex IV. The primary source of proton production in the media of cells grown in culture is lactate generated via glycolysis.

Cellular oxygen consumption and proton excretion cause a robust, measurable change to the concentrations of dissolved oxygen and free protons in the cell media measured every few seconds by employing solid-state fluorescence-based sensor probes residing 200 microns above the cell monolayer. The chamber is then unsealed (allowing baseline measurements) and re-sealed to repeat the measurement. Experiments providing a metabolic bioenergetic profile are performed by simultaneously measuring OCR and ECAR under four different conditions (basal, oligomycin, FCCP; carbonyl cyanide p-trifluoromethoxy phenylhydrazone, and rotenone/ antimycin A) in each of 20 wells of cells.

**Materials**

***For primary neuronal culture:***

**Animal:**

C57BL/6J timed pregnant (E14) mouse.

**Reagents**

Dissection media (50ml)- DMEM media supplemented with FBS: 5ml (10%), GlutaMAXTM: 500µl (0.5mM)

Plating media (50ml)- Neurobasal media supplemented with FBS: 1 ml (2%), GlutaMAXTM: 125µL(0.5mM), B27: 1ml (2%), Glutamic acid: 106µl (25 µM), Penicillin/streptomycin: 250µL (100 U/ml]

Maintenance media (50ml)- Neurobasal media supplemented GlutaMAXTM: 125µL (0.5mM), B27: 1ml.

Sterile double-distilled water

Trypan Blue stain

**Equipment**

Laminar flow cell culture hood

Dissecting macroscope with illumination

Sterile surgical tools

Sterile Agilent Seahorse $XF^e$ 24 well Cell Culture Microplate

Sterile culture dishes (60mm)

Sterile microcentrifuge tubes (0.5ml)

Sterile centrifuge tubes (15ml)

37°C Incubator with 5% $CO_2$ /95% humidity

Hemocytometer

37°C Water-bath

***For Seahorse $XF^e24$:***

**Reagents:**

Seahorse $XF^e24$ Calibrant Solution (pH 7.4)

Seahorse $XF^e24$ Extracellular Flux Assay Kit

Seahorse $XF^e24$ Run Medium - $XF^e24$ base medium/Dulbecco's Modified Eagle's Medium Base (DMEM) supplemented with 2 mM GlutaMAX™, 1 mM sodium pyruvate, 25 µM D-Glucose, were used for the Seahorse experiment. An unbuffered medium is essential for measuring changes in pH during glycolysis.

Oligomycin (Stock conc. 1mM)

FCCP (Stock conc. 300µM)

Rotenone (Stock conc. 100µM)

Antimycin A (Stock conc. 100µM)

D-Glucose

Sodium pyruvate

GlutaMAX™

**Equipment:**

Agilent Seahorse XF$^{e}$24 Bioanalyzer

pH meter

37°C Incubator without $CO_2$

37°C water-bath

***For immunocytochemistry and nuclear labeling***

**Reagents:**

Phosphate Buffered Saline (PBS) (pH 7.4)

Bovine Serum Albumin (BSA)

PBB: 0.5% BSA in PBS

Fixing solution (4% Paraformaldehyde in PBS)

Triton X-100

DAPI nuclear stain

Primary antibody (MAP2B)

Alexa Fluor–conjugated secondary antibody

***For imaging:***

ImageXpress Nano automated microscope

***For operation and data analysis:***

Wave software (Agilent Technologies) wave desktop and controller 2.6 software version 2.6.1 released April 2019

MetaXpress

GraphPad Prism

**Methods**

**Primary neuronal culture**

**Coating cell culture plates (Day-0):**

Add poly-L-lysine to each well (0.5mL/well for Agilent Seahorse XF$^e$24 well Cell Culture Microplate) and swirl gently. Incubate the plates at 37$^o$C for 2 hours. Aspirate poly-L-lysine using a sterile serological pipette and rinse each well with sterile double-distilled water. Allow plates to air dry inside the laminar flow cell culture hood.

**Culturing primary cortical neurons (Day-1):**

Collect acclimatized E15 timed pregnant mouse (C57BL/6) from the cage and anesthetize the animals using $CO_2$ in a sealed chamber. Wait until the mouse stops moving and fails to respond to the hind-paw pinch before beginning dissection.

Perform cervical dislocation of the mice and place the mouse on a tray for dissection. Open abdominal cavity, remove embryos and place them in dissection media on ice contained in a 10mL petri dish.

Embryo micro-dissection:

Transfer embryos to laminar flow cell culture hood having a dissecting microscope with illumination.

Extract embryos from sac and place in a new petri dish with chilled dissection NB/B27 media.

Remove heads from embryos using scissors and place them in a new petri dish with dissection media.

Remove the skin first by carefully peeling it off with fine forceps under the macroscope.

Insert the pointed edge of the fine forceps and break the exoskeleton.

Peal the exoskeleton carefully and apply pressure on the sides to push the brain out of the cavity.

Place the whole brain in a new petri dish with dissection media.

Use a syringe and needle (26G) to perform micro-dissection of embryo brain.

Separate the cerebellum from the whole brain. Later, separate the two hemispheres and remove the meninges. Extract cerebral cortex and place it in a 15 ml centrifuge tube on ice.

Dissociate cells by pipetting up and down multiple times (5-7X), first using a 1mL pipette tip, followed by a 200µL pipette tip. Place suspension on ice. Please note there is no need to use enzymes for these steps as mechanical digestion is gentler to neurons and better for neuronal survival.

**Cell counting and plating:**

Place 10µL of cell suspension in a microcentrifuge tube and add 40µL Trypan Blue (0.4%).

Add 10µL of this solution to the hemocytometer. Allow the liquid to disperse through capillary action.

Count cells from multiple grids (4) and calculate cell concentration making sure to exclude cells that are Trypan Blue positive from the overall count:

cells/mL= (#cells counted/#grids counted) *(dilution factor) *(10,000 cells/mL)

Determine the volume of the cell suspension to be plated: C1*V1= C2*V2 for cells/well

Add the determined volume of the cell suspension to plating media (pre-warmed in 37°C water bath).

Add plating media (0.5mL for 24-well) containing cells to poly-L-lysine coated Seahorse XF$^e$ 24well plate (make sure to leave wells A1, B3, C4, & D6 empty as background, sensor correction wells) and transfer the plate to a 37°C incubator with 5% $CO_2$ /95% humidity.

**Media change (Day-3)**

Check the neurons to see if they are attached, spreading out and sending out neurites.

Change 2/3$^{rd}$ of the media with maintenance media that does not contain FBS to reduce the possibility of glial overgrowth.

**Assessing Bioenergetics in dissociated primary cortical neurons.**

**Seahorse Extracellular Flux Assay Kit preparation (Hydrate sensor cartridge)**

The Seahorse Extracellular Flux Assay Kit comprises a green-colored Seahorse XFe24 sensor cartridge, a transparent 24 well calibration plate, and a pink insert. Take off the sensor cartridge, green lid, and pink insert from the extracellular flux pack kit. Add 0.5ml of Seahorse XF$^e$24 calibrant per well and reassemble the flux kit. Incubate the flux kit overnight at 37°C non-$CO_2$ incubator.

**Seahorse XF$^e$24 cell culture plate preparation**

Warm the Seahorse XF$^e$24 base media to 37 °C.

In the meantime, turn on the Seahorse XF$^e$24 Bioanalyzer and the interface (monitor screen attached to the instrument). Open the Seahorse Wave (version 6 or higher) software and load the protocol.

Create protocol: Set temperature at 37$^0$C

1) basal 3 cycles: mix 3 mins, wait 2 mins, measure 3 mins

2) Port D drug addition: measurement 15 cycles, mix 3 mins, wait 2 mins, measure 3 mins,

3) Oligomycin 3 cycles (Port A): mix 3 mins wait 2 mins measure 3 mins,

4) FCCP 3 cycles (Port B): mix 3 mins, wait 2 mins, measure 3 mins,

5) Rotenone/antimycin (Port C) 3 cycles: mix 3 mins, wait 2 mins, measure 3 mins,

6) Assay complete eject plate, view results, save.

Warm up the $XF^e24$ Seahorse Bioanalyzer to 37°C (5 hours minimum).

Take the Seahorse $XF^e24$ plate from the 37°C incubator with 5% $CO_2$ /95% humidity and place it in the laminar flow cell culture hood.

Using an aspirator pipette, remove approximately 150 µL of the maintenance media and wash the wells (including correction wells) with 1 mL of Seahorse $XF^e24$ run media. Remove all but 150 µL of media from the wells making sure to aspirate from the side of the wells and not directly into the cells.

Add 525 µL of Seahorse $XF^e24$ run media (including correction wells) and keep the plate at 37°C in a non-$CO_2$ incubator for 1 hour.

**Drug preparation**

While the primary cortical neurons cultured on the 24 well Seahorse culture plate are incubating in the 37°C in a non-$CO_2$ incubator for 1 hour, prepare the drugs for injection heat to $37^O$ C.

Oligomycin 10X solution (25 µM): Add 50 µL of 1mM stock solution of oligomycin to 2 mL of Seahorse $XF^e24$ run media to make a sub-stock of oligomycin (25 µM). Add 56 µL of this sub-stock solution to port A of the calibrated sensor cartridge for a final concentration of 2.5 µM Oligomycin.

FCCP 10X solution (10 µM): Add 66.66 µL of 300 µM stock solution of FCCP to 2 ml of Seahorse XF$^e$24 run media to make a sub-stock of FCCP (10 µM). Add 62 µL of this sub-stock solution to port B of the calibrated sensor cartridge for a final concentration of 1 µM FCCP.

Rotenone/Antimycin A 10X solution (5 µM): Add 100 µL of 100 µM stock solution of rotenone plus 100uL of 100uM stock solution Antimycin A to 2 ml of Seahorse XF$^e$24 run media to make a sub-stock of rotenone /Antimycin A(5µM). Add 69 µL of this sub-stock solution to port C of the calibrated sensor cartridge for a final concentration of 0.5 µM Rotenone/Antimycin A.

BDNF (Experimental drug): Add 6 µL of BDNF (5 ng/µL) into seahorse media for a sum of 75 µL port D of the calibrated sensor cartridge for a final concentration of 30 ng/well

Ana12 (Experimental drug antagonist): Add 2 µL of 61 µM stock (200nM/well) with a sum of Ana12 and seahorse media 75µL for injections to port D.

Control all wells filled with 75 µL seahorse media port D.

**Bioenergetic measurement**

Login to the Seahorse Wave software on the interface and setup an experimental template by using the Assay Wizard option.

Group definitions, plate map, protocol, run assay: input the information regarding type of media used (NB/B27), type of cells, drugs employed for the assay (rotenone/antimycin A cocktail, FCCP, oligomycin, experimental drug), and their concentrations. Save the template and be sure that the "Save Directory" and "Save Name" fields contain the proper information.

Remove the Seahorse Extracellular Flux Assay Kit from the 37 °C non-$CO_2$ incubator. Add the drugs to the respective ports in the calibrated sensor cartridge using the concentrations indicated above.

Take the Seahorse Extracellular Flux Assay Kit containing the $XF^e$ calibrant in the calibrant plate wells and take it to the warmed-up (37°C) $XF^e24$ Seahorse Analyzer.

Remove the pink insert and the transparent lid of the Seahorse Extracellular Flux Assay Kit and place the sensor cartridge onto the calibrant plate containing the 0.5 mL of $XF^e$ calibrant solution per well.

Start the calibration step by clicking on the "Start" button. When the loading door opens, place the sensor cartridge with the calibration plate on the tray.

When the calibration/quality control process is complete, replace the calibration plate with the experimental cell plate and run assay.

**Immunocytochemistry and nuclear labeling**

At the end of the mitochondrial stress assay (approximately 3.5 to 4 hrs.,) remove the medium, follow with 1 wash of l X PBS making sure to aspirate the media on the side (not directly) of the wells to avoid lifting the delicate monolayer of primary neurons.

Fix sample in 4% paraformaldehyde for at least 15 minutes at room temperature.

Wash monolayer on each well 3 times in PBS (5 min./wash) to remove residual PFA.

Permeabilize cells with 0.3% Triton X-100 made in PBS solution for 15 min.

Wash monolayer on each well 1times with PBS.

Wash monolayer 5 times with PBB and block with 2% BSA for 45 minutes.

Wash monolayer 3 times with PBB.

Primary antibody: To stain for dendrites in primary neurons, dilute the desired concentration of rabbit anti-mouse MAP2B in PBB (vortex gently, spin down for 5 min. at 10-12K RPM to get rid of any aggregates)

Incubate overnight at 4°C with a gentle motion.

Remove primary antibody from the wells wash each well 5 times with PBB.

Add secondary antibody (647 anti-rabbit 1:500) into the wells and incubate for 60 minutes at room temperature.

Wash monolayer 5 times on each well with PBB.

Counterstain with DAPI (1:100,000) for 30 seconds in PBS.

Wash the monolayer 1 time on each well with PBS.

Store the cells in PBS with 0.05% sodium azide to avoid bacterial growth. Prepare for automated fluorescent imaging analyzed for neuronal morphology (analysis of neurite length/complexity and cell count) as described below.

**Imaging with ImageXpress Nano**

Switch on the ImageXpress Nano microscope, light source, and computer.

Open MetaXpress® software and click acquisition setup.

Place the Seahorse XF24 Cell Culture Microplate in the imaging chamber and close the lid.

Under the configure tab, select 40X objective. Adjust the correction collar if necessary.

Under the plate tab, click the drop-down list and select the Seahorse XFe24 plate. The dimension of the plate based on vendor specifications should be annotated and saved prior

to imaging cells for neurite analysis. Select the site to visit tab and select an appropriate number of sites.

Under the acquisition tab, select autofocus tab, and enable laser-based autofocusing. In well to well autofocus set focus to well bottom.

Under wavelength, select number, and choose FITC (mouse anti-human MAP2B) (488 anti-mouse) and DAPI filter. Select FITC wavelength and adjust settings.

In the plate map, select a well (right-click the well)

For adjusting image acquisition, select illumination setting and click focus. Make sure the image exposure is appropriate. Calculate offset to perform automatic focus determination.

Click focus again and check post-laser offset, and the image should be in focus.

Repeat for each subsequent wavelength.

Under the run tab, click experiment details and save protocol.

Click acquire plate to begin acquiring plate.

**Data analysis**

**OCR and ECAR determination**

Open the Wave software, select results and scan to the project of interest, and open.

With primary cortical neurons (post-mitotic), normalization using cell counts is appropriate. Select the normalization icon input DAPI numbers on the plate map with normalization unit: cell count and a scale factor: 1. This will update all the data and modify all the graphs, calculations, and analyses.

Once the data is normalized, export the data. Select export and export the seahorse $XF^e$ Cell Mito Stress Test Report Generator for results.

Results: summary printout >bar charts >measures sheet>assay parameters per well> sample calculations> and project information. Figure 2 shows an example of enhancement of oxidative phosphorylation (OCR line graph) and of glycolysis (ECAR line graph) in response to exposure of primary cortical neurons to BDNF but not in the presence of ANA12, an antagonist of the Trkβ receptor (Fig 2).

Export GraphPad Prism for statistics to run ordinary one-way ANOVA, column analyses, one-way ANOVA, multiple comparisons: compare the mean of each column with the mean of every other column, options: Tukey's test.

**Neurite length measurement**

The Neurite Outgrowth application module in MetaXpress software simultaneously identifies and measures cell bodies and neurites.

Select screening and click review plate data.

Select the type of plate from the database.

Select the appropriate wavelength (FITC for neurite outgrowth in MAP2B positive structures, and DAPI for nuclear count)

Under the analysis tab, select the neurite outgrowth module and configure module settings. Configuration of module settings includes measurement of length, breadth, and area of the cell body and neurites for automatic selection and analysis.

Run analysis and view result in the measurements tab. Figure 3 shows a representation of an analysis of neurite complexity in primary cortical neurons in response to BDNF, but not exposure to ANA12 (Fig. 3). The morphological data in Figure 3 shows a strong correlation of BDNF in enhancing dendrite length and bioenergetics (Fig. 2).

## Conclusion

This chapter has described a method to expand conventional bioenergetic experiments using Seahorse XF24$^{e}$ Bioanalyzer by adding ImageXpress Nano imaging platform to the experimental workflow. This enhances the information from a bioenergetic viewpoint to a neuronal functional endpoint. As an example of multiplexing both instruments to associate neuronal morphology with bioenergetics in response to the same treatments, our data shows that BDNF administration can simultaneously enhance mitochondrial oxidative phosphorylation and enhance dendrite outgrowth in a significant manner as measured as the mean neurite length per cell while ANA12, an inhibitor of BDNF, reduced dendrite outgrowth. The combination of multiplexing the Seahorse and ImageXpress Nano provided additional data to supplement the observations made in Chapter 2. BDNF treatment can rapidly increase both oxidative phosphorylation and glycolysis within hours of treatment, preceding the outgrowth and complexity of dendrites that is induced by BDNF after more than 24 hours of treatment in the same population of neurons. Furthermore, the data showed that a certain level of Trkβ activation is necessary to maintain dendrite length and development as ANA12 significantly reduces dendrite length.

## Notes

Make sure the cell culture plate doesn't have any contamination. The contaminating microbes could contribute to basal OCR and thereby skew the result.

Standardizing the cell density during plating is a crucial step and must be repeated with different cell types. Make sure the cells are evenly distributed on the plate surface as cell

clumps can alter the result. During pipetting steps, do not remove entire media and the tips should not touch the base of the well.

Temperature- Ensure the temperature of cells, drugs, media, and the machine are equilibrated to $37^0$C.

It is suggested to optimize FCCP does in the bioenergetic experiments as optimum concentration vary from cell line to cell line.

The cells after bioenergetics measurement are exposed to drugs with toxic effects. To preserve neuronal morphology for optimum immunocytochemistry results, fix the cells with 4% PFA as soon as possible after the Seahorse $XF^e$ Bioanalyzer run.

During analysis of mean dendrite connectivity, in addition to the wavelength of choice for labelling dendrites, supplementing DAPI input will enhance the cell labelling ability of the algorithm.

**7. Figure captions:**

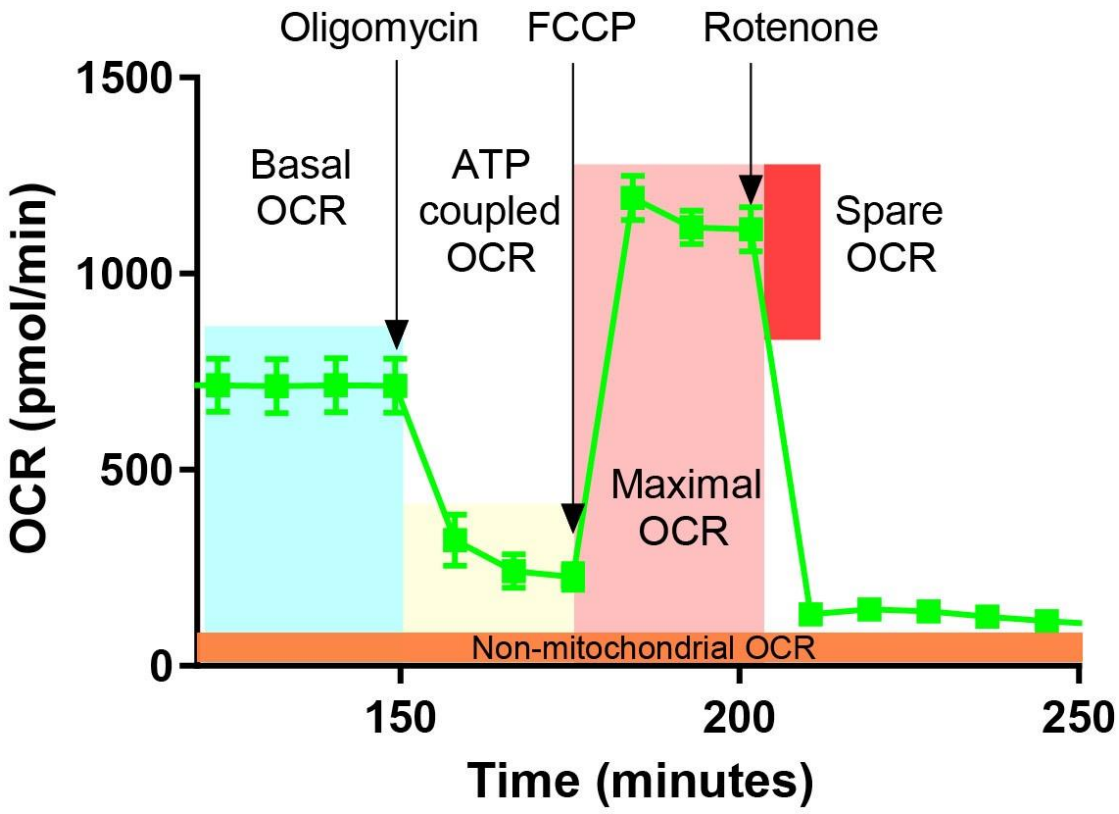


**Figure 1: Basal respiration:** OCR during basal respiration provides the measure of endogenous ATP demand driven by cellular function and dependent upon ATP utilization, substrate catabolism, and proton leak. Basal respiration rate is an ideal parameter to standardize cell density when performing initial experiments. **ATP linked respiration and proton leak:** Oligomycin injection blocks ATP synthase and reduces the OCR. The remaining rate of mitochondrial respiration, namely proton leak, is due to non-ATP-linked oxygen consumption. Enhanced ATP-linked OCR indicates increased ATP demand and diminished ATP linked OCR levels, indicating low ATP demand, substrate scarcity, or damage to oxidative phosphorylation machinery. Enhanced proton leak can be a sign of

mitochondrial dysfunction. **Maximal respiration:** An uncoupler such as FCCP is used to measure maximal respiration. A high FCCP-induced OCR compared with basal OCR indicates that the mitochondria are below the threshold of the maximal rate of electron transport, thereby increasing **spare capacity**. Oxidative stress induced mitochondrial dysfunction can reduce spare capacity. **Non-mitochondrial oxygen consumption:** non-mitochondrial respiration is due to cellular enzymes and is important to get an accurate measure of mitochondrial respiration.

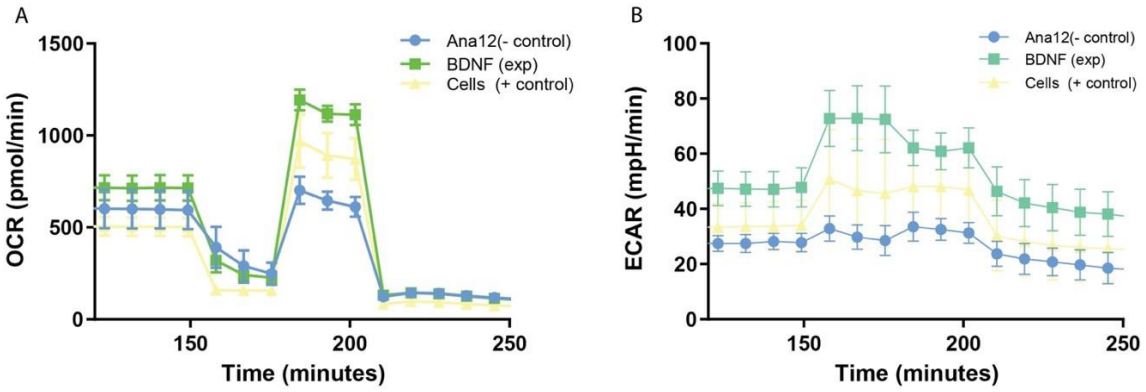


**Figure 2:** (A) shows treatment with BDNF (30 ngs, 2hrs.) significantly increases OCR in primary cortical neurons when compared to control, also, treatment with Trkβ (BDNF) receptor antagonist Ana12 (200nM, 2 hrs.) significantly decreases OCR in primary cortical neurons when compared to control. Statistics: Tukey's multiple comparisons test: Ana12(- control) vs. BDNF (exp) Significant Adjusted P Value **** <0.0001, Ana12(- control) vs. Cells (+ control) Significant Adjusted P Value ** 0.005, BDNF (exp) vs. Cells (+ control) Significant Adjusted P Value ** 0.0033. (B) shows treatment with BDNF (30 ng, 2hrs) significantly increases ECAR in primary cortical neurons when compared to control, also, treatment with Trkβ receptor antagonist Ana12 (200nM, 2 hrs.) decreases ECAR in primary cortical neurons when compared to control. Statistics: Tukey's multiple comparisons test: Ana12(- control) vs. BDNF (exp) Significant Adjusted P Value **** <0.0001, Ana12(- control) vs. Cells (+ control) Significant Adjusted P Value *** 0.0002, BDNF (exp) vs. Cells (+ control) Significant Adjusted P Value *** 0.0001.

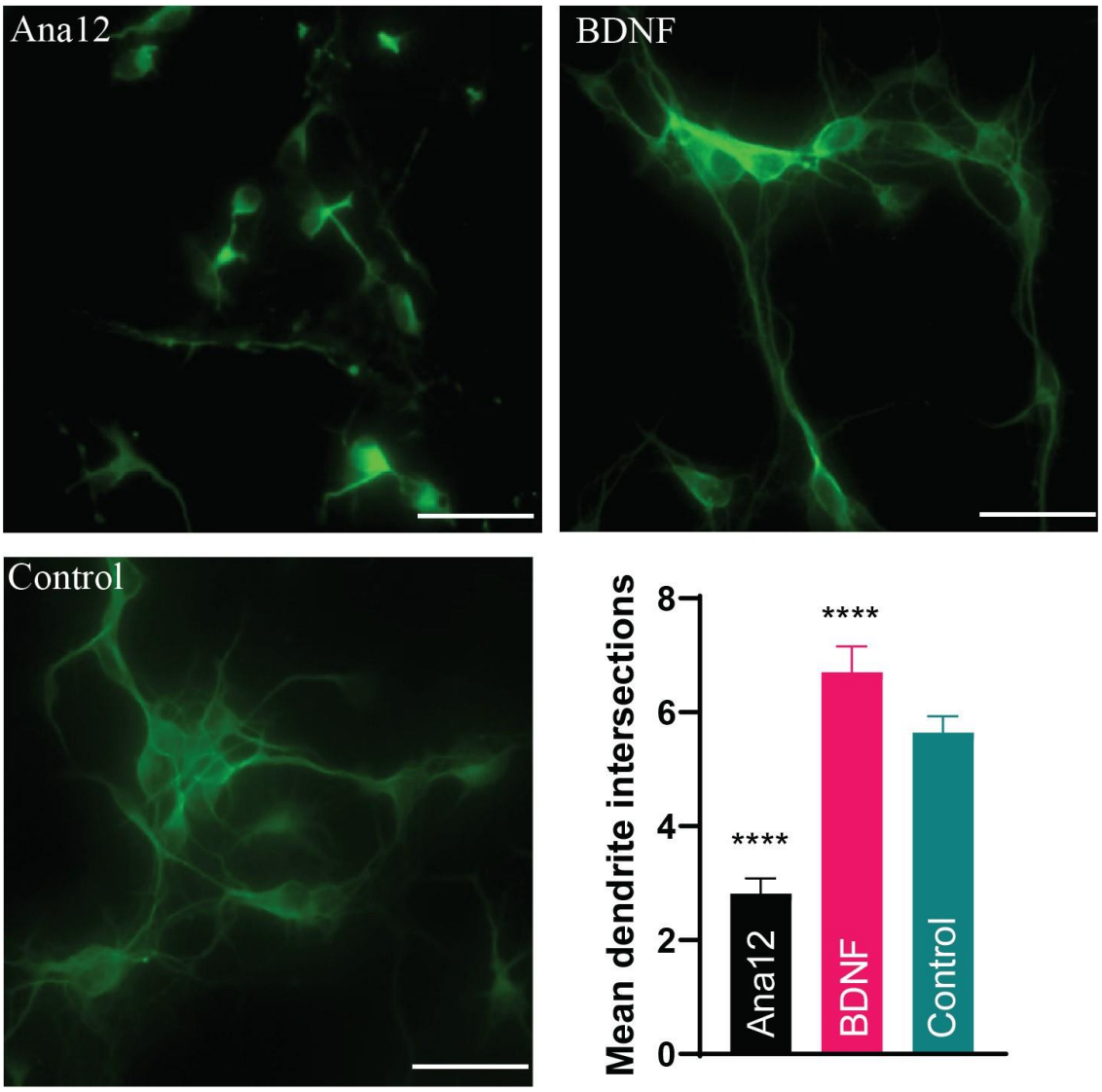


**Figure 3:** BDNF increases dendrite length whereas blocking the BDNF receptor abolishes neurite complexity. Treatment of primary cortical neurons with human recombinant BDNF (30 ngs, 2 hrs.) enhances dendrite outgrowth as measured by the number of intersections per cell whereas treatment with the BDNF receptor inhibitor ANA12 reduces neurite outgrowth. Scale bar in white= 15µM. Statistics: One-way ANOVA: Control vs. BDNF (exp) Significant Adjusted P Value **** <0.0001, Ana12 (- control) vs. Control Significant Adjusted P Value **** <0.0001.

# Chapter V

## Discussion and future directions

In summary, my compiled data collected during my doctoral training demonstrates how BDNF and PKA interplay in the brain to modulate mitochondrial structure/function, and neuronal connectivity in healthy neurons and protect neurons from oxidative stress in an in vitro model of Alzheimer's disease. Specifically, my data show that BDNF, by binding to its cognate receptor (Trkβ) can exert an indirect effect in regulating mitochondrial morphology, oxidative phosphorylation, transmembrane potential, levels of ROS, as well as mitochondrial movement (trafficking) via downstream activation of PKA in the cytosol and mitochondrial compartments. In the brain, this new signaling pathway governed by BDNF enhances mitochondrial dynamics by facilitating both the fusion and bi-directional transport of mitochondria to and from dendrites where energy demand is high, ultimately leading to increased metabolism, increasing the endogenous levels of D-AKAP1, and increasing energy currency through mitochondrial oxidative phosphorylation and ATP production (Swain et al., 2023). Given that BDNF can exert an immediate increase in PKA activity in neurons (< 2 hrs.), the physiological significance of PKA-mediated mitochondrial fusion, trafficking and mitochondrial content in dendrites and increased endogenous levels of D-AKAP1 include neuroprotection against ROS (e.g., superoxide) induced by different toxic insults including rotenone, a complex I inhibitor, and amyloid β. Specifically, we have shown that redirecting the endogenous pool of PKA the amount of PKA attached to the mitochondria in neurons via transiently expressing D-AKAP1 or by treating with pharmacological activators of PKA can protect neurons in an *in vitro* cell culture model of AD. Importantly, like BDNF, increased PKA signaling in the mitochondria

mediated can also be mediated by the Estrogen receptor β as pharmacological activation of estrogen receptors can increase PKA activity, promote mitochondrial fusion and anterograde trafficking of mitochondria and protect dendrites from amyloid β-mediated toxicity (T. D. Banerjee et al., 2021). Therefore, my data shows that both Trkβ and Estrogen receptors can modulate mitochondrial structure/function via downstream activation of PKA and thereby employ converging and redundant cytoprotective mechanisms to maintain neuronal homeostasis. The findings indicate that these receptors act as important regulators of mitochondrial dynamics and bioenergetics, contributing to the preservation of neuronal viability and function. These results highlight the importance of understanding the molecular mechanisms underlying the cytoprotective effects of Trkβ and Estrogen receptors on neuronal mitochondria, and how these mechanisms can be targeted for therapeutic purposes in neurodegenerative diseases.

Mechanistically, my research has shown that exogenous BDNF stimulates mitochondrial fusion in dendrites through PKA-dependent phosphorylation of Drp1 at S637. Exogenous BDNF treatment increased PKA activity and significantly increased endogenous level of D-AKAP1 in neuroblastoma SH-SY5Y cells. Moreover, BDNF-mediated increase in mitochondrial length (fusion) in dendrites was inhibited by PKA inhibitors. BDNF treatment also increased mitochondrial fusion in the presence of wild-type Drp1 but not in the presence of a PKA phosphorylation site-resistant Drp1 (Drp1-S656A). The data suggests that BDNF promotes mitochondrial fusion by enhancing PKA-mediated phosphorylation of Drp1, which was further confirmed using biochemical approaches (Phos-Tag™-mediated identification of Drp1) (Swain et al., 2023).

BDNF enhances mitochondrial trafficking in dendrites via PKA-dependent activation, promoting both anterograde and retrograde movement. BDNF stimulates phosphorylation of Miro-2, which is necessary for BDNF-mediated mitochondrial trafficking in dendrites (Swain et al., 2023). However, the specific phosphorylation sites on Miro-2 and the role of PKA has in regulating Miro-1 and dynein motors require further investigation. There are more than 10 potential sites of phosphorylation on Miro2, most of which are believed to be located in the N-terminus and can be targeted by PKA (Das Banerjee et al., 2017).

Based on my data garnered during my doctoral training, exogenous BDNF activates the Trkβ receptor, which leads to enhanced bioenergetics in neurons, as evident by enhanced oxygen consumption rates and basal glycolysis, and elevating mitochondrial transmembrane potential as well. These physiological effects are blocked by ANA12 co-treatment, indicating the involvement of the Trkβ receptor (Swain et al., 2023). While the precise mechanism of increased oxidative phosphorylation requires further investigation, BDNF may regulate complex I and complex IV electron flow and activity through PKA-dependent phosphorylation of subunit (S58) of COX subunit IV-1 (COXIV-1) and subunit (NDUFS4) complex I (CI; NADH: ubiquinone oxidoreductase) (Markham et al., 2004; Valsecchi et al., 2013). Future studies could investigate whether BDNF-mediated activation of the Trkβ receptor leads to PKA-dependent phosphorylation of complex I and IV subunits and subsequent modulation of electron flow and activity.

Alzheimer's disease (AD) is a neurodegenerative disorder that is associated with the accumulation of amyloid beta peptide (Aβ) and neurofibrillary tangles, which leads to loss of both cortical and hippocampal neurons. Mitochondrial dysfunction, including impaired oxidative phosphorylation, mitochondrial fragmentation, and increased ROS production, has also been implicated in the etiology of AD. Dysregulated PKA signaling has been linked to AD pathogenesis, such as decreased PKA activity at the mitochondria contributes to overt Drp1-mediated mitochondrial fission, dendritic degeneration followed by apoptosis (T. D. Banerjee et al., 2021). PKA phosphorylates Miro2, increasing mitochondrial trafficking to dendrites (Das Banerjee et al., 2017), and phosphorylates Drp1, preventing it from constricting mitochondria into a fission state, thus exerting neuroprotection (T. D. Banerjee et al., 2021). My research revealed that BDNF potently increases PKA activity and endogenous levels of D-AKAP1, physiological events that are associated with PKA-mediated phosphorylation of the OMM-localized PKA substrates Miro2 and Drp1 (Swain et al., 2023). The role of the cAMP/PKA signaling pathway in neuronal health and in AD pathogenesis has been extensively studied in AD models (Hu et al., 2017; Merrill et al., 2011). PKA activity is decreased in the brains of individuals with AD, which leads to reduced phosphorylation of CREB and decreased nuclear translocation of phosphorylated CREB, resulting in decreased transcription of CREB-regulated genes. The impaired mitochondrial function observed in AD is due, in part, to decreased activity, which contributes to the pathogenesis of the disease by impairing the ability of neurons to maintain proper mitochondrial function and respond to stress (Pugazhenthi et al., 2011b). The PKA signaling pathway in the cytosol and in the mitochondrion, specifically

mitochondrial D-AKAP1/PKA, are reduced in the 5X-FAD mouse model of AD and in primary cortical neurons treated with amyloid β (1-32) (T. D. Banerjee et al., 2021).

Future studies should focus on determining the extent that reduction in endogenous BDNF and Trkβ, as observed in *in vitro* and *in vivo* models of AD and in post-mortem brain tissue of AD patients, contribute to mitochondrial dysfunction, reduced brain energy as observed in AD and contribute to neurodegeneration of cortical and hippocampal neurons in AD. In further support of the notion that Trkβ may play a role in regulating mitochondrial function and deregulation may drive AD pathogenesis, other researchers have observed a reduction in the levels of full-length Trkβ receptor in mitochondria in relation to aging and in AD (Tejeda & Díaz-Guerra, 2017). This reduction in Trkβ receptor levels may have implications for altered ATP production and oxidative phosphorylation in AD. It is possible that reduced Trkβ or decreased trafficking of Trkβ to mitochondria is also exhibited in PD models, and this could contribute to the reduction in oxidative phosphorylation in both AD and PD. Therefore, based on current research, it is plausible that the reduction of BDNF and Trkβ in AD and PD could lead to decreased mitochondrial function and altered bioenergetics. Further studies are needed to fully elucidate the mechanisms underlying these effects and their potential therapeutic implications.

Exogenous recombinant human BDNF protects dendrites and mitochondria from oxidative stress and can reverse dendrite and mitochondrial loss induced by exposure of primary neurons to rotenone. BDNF also reduces the level of superoxide induced by rotenone and may protect dendritic mitochondria by decreasing the level of mitochondrial ROS

including superoxide. Moreover, BDNF has been observed to be protective in an *in vitro* model of PD (rotenone), not only by preserving dendrite length and structure but also by protecting mitochondrial length and content in dendrites (Swain et al., 2023).

BDNF promotes Trkβ translocation to mitochondria in neurons, where Trkβ complexes are localized. Treatment with exogenous BDNF significantly increases the translocation of Trkβ to mitochondria in the dendrites and soma, whereas ANA12, a pharmacological inhibitor of Trkβ, blocks this effect. ANA12 is a selective small molecule non-competitive antagonist that binds to Trkβ and blocks this effect, indicating Trkβ activation is required for the effects of BDNF on endocytosis of its receptor. Endogenous Trkβ was predominantly found in mitochondria compared to the cytosolic compartment in isolated brain fractions (CH2 Fig. 1). These research findings suggest that BDNF regulates mitochondrial structure and function by promoting Trkβ translocation to mitochondria in neurons, once in the proximity of the mitochondria the signaling endosome can conduct the PKA activity of phosphorylating Miro-2 to increase mitochondrial trafficking and phosphorylating Drp1 to increase mitochondrial fusion. The co-localization of BDNF/ Trkβ in neurons confirms their direct impact on mitochondria. Trkβ has been detected in isolated mitochondria, and BDNF treatment has been shown to increase mitochondrial membrane potential, suggesting that Trkβ activation by BDNF positively affects mitochondrial function (Swain et al., 2023).

Beyond using traditional methods to collect end-point biological data, I had the privilege of utilizing cutting-edge technologies to be able to understand how BDNF regulates both

neuronal metabolism and connectivity over time in the same population of cells. In this study, I utilized the Seahorse extracellular flux technology to measure oxidative phosphorylation and glycolytic metabolism, and the ImageXpress Nano microscope to provide rigorous and accurate high-content imaging. Therefore, by multiplexing both the XF24$^{e}$ Bioanalyzers and the ImageXPress Nano, a semi-confocal system that performs automated acquisition and quantification of fluorescence images in fixed immuno-stained neurons and tissues, I was able to garner additional data that shed light into the mechanisms by which exogenous BDNF regulates neuronal connectivity and bioenergetics. Understanding the bioenergetic variations that contribute to various diseases requires assessing mitochondrial function in cells and tissues. To achieve a comprehensive profile of bioenergetics and neuronal function, it is essential to combine different technologies.

To test if exogenous BDNF enhances bioenergetics and provides neuroprotection by activating Trkβ receptor in primary cortical neurons, we used this innovative multiplexed protocol. Overall, my research demonstrated that BDNF can exert an early increase in mitochondrial respiration and glycolysis and this increase in the energetic landscape of neurons precedes the increase in dendrite complexity and connectivity (> 24 hrs. posttreatment with BDNF), as observed through ImageXpress Nano system. The increase in OXPHO preceded the increase in dendrite length and connectivity, and both physiological events occurred concurrently in the same population of neurons. We observed an increase in dendrite branching complexity by BDNF, and both events were dependent on PKA (K Soman et al., 2022).

Importantly, the combination of the Seahorse extracellular flux technology and the ImageXpress Nano microscope allowed us to increase the reproducibility and rigor of our research by analyzing dendrite morphology and correlating it with bioenergetics. This approach allowed us to obtain a comprehensive profile of bioenergetics and neuronal function, which is critical for understanding the underlying mechanisms of diseases with bioenergetic variations. The multiplexed protocol combines two different technologies it provides a powerful tool to investigate complex biological processes and to obtain a more comprehensive understanding of cellular function.

In order to deepen our understanding of the link between the Trkβ receptor and mitochondrial function, it is possible that Trkβ can be intrinsically and directly targeted to the mitochondrion via an unknown molecular mechanism. Hence future research should investigate whether Trkβ harbors a cryptic mitochondrial leader sequence within the Trkβ receptor that mediates the localization of the receptor to the mitochondria. By using an algorithm termed MitoProt that can predict the presence of mitochondrial targeting signals preliminary and unpublished data suggest that Trkβ may contain a 42 amino acid mitochondrial targeting sequence that is not present in other neurotrophin receptors including TrkA. Additional future experiments should determine the precise sub compartment that Trkβ can be localized including the outer mitochondrial membrane, inner mitochondrial membrane and/or matrix. Additionally, the molecular mechanism by which Trkβ increases mitochondrial oxidative phosphorylation should be explored, such as whether it involves a mitochondrial PKA function or a direct interaction and phosphorylation of electron transport proteins by the Trkβ receptor.

Further investigation is necessary to determine whether the full-length or truncated isoforms of the Trkβ receptor are involved in regulating mitochondrial fusion, mobility (trafficking) and OXPHOS and whether a separate pathway exists for the synthesis of Trkβ in the ER and its translocation to the mitochondria. It is also important to explore the potential existence of an intercellular pool of BDNF that interacts with mitochondrial Trkβ. For instance, it is conceivable that the presence of the truncated T1 isoform of Trkβ may downregulate the function of full-length Trkβ and influence its expression levels on the cell surface. Hence, the ratio of full-length Trkβ to truncated Trkβ can have physiological implications for mitochondria and mitochondrial function, and it is plausible that this ratio decreases with aging in the brain, contributing to age-related mitochondrial dysfunction. Studies have shown that Trkβ surface expression levels change in response to BDNF treatment and that specific isoforms of the receptor can affect surface expression levels (Haapasalo et al., 2002). Therefore, understanding the underlying mechanisms of the regulation of Trkβ surface expression levels is crucial for understanding their potential implications for mitochondrial function in active neurons.

TrkA is transported to the axon terminal where it binds to NGF and initiates survival and growth signaling activation of multiple signaling pathways. TrkA is sorted into different endosomal compartments upon ligand binding, and recent studies have shown that TrkA ubiquitination promotes degradation, while TrkA on signaling endosomes is transported down the axon to amplify the signal (Conroy & Coulson, 2022). TrkA signaling endosomes are recycled to sustain retrograde signaling for neuronal survival. It is not known if TrkA

endosomes are governed by PKA. However, it has been proposed that TrkA and TrkC act as dependence receptors, proteins that mediate programmed cell death by monitoring the absence of certain trophic factors, during development, whereas Trkβ does not. This mechanism helps control cell numbers in developing sensory and sympathetic neurons that require trophic factors for survival (Marlin & Li, 2015).

Aging is a complex process that is influenced by both genetic and environmental factors. Among the most significant changes that occur during aging are epigenetic modifications, reductions in BDNF levels, and the accumulation of damaged mitochondria. These alterations can lead to a decline in energy production, increased oxidative stress, and cognitive decline, which are often observed in neurodegenerative disorders such as Alzheimer's disease (AD) and Parkinson's disease (PD).

Mitochondrial dysfunction is a hallmark of neurodegenerative diseases, and it is believed to play a crucial role in the pathology of AD and PD. Impaired mitophagy and autophagy contribute to the accumulation of dysfunctional mitochondria, resulting in electron leakage, reduced ATP generation, and increased ROS levels. Studies suggest that the reduced mitochondrial motility observed during aging is linked to various neurodegenerative diseases, including AD and PD. As a result, therapeutic approaches that target mitochondrial function and trafficking may hold promise for the development of disease-modifying therapies.

Currently, there are no disease-modifying therapies available for AD and PD. Antioxidants, which have shown promise in preclinical studies, have failed to demonstrate efficacy in phase 3 clinical trials. This underscores the need for novel therapeutic strategies that target the underlying mechanisms of these diseases. One potential approach is to target BDNF which has been shown to be transported to mitochondria, where it can enhance mitochondrial function and reduce oxidative stress. For instance, one potential therapeutic strategy is to intentionally target BDNF to the mitochondria by using pharmacological approaches such as nanotechnology, lipids, or vesicles targeted to mitochondria by using Mito-targeting moieties (TPP+, triphenylphosphonium-based carriers). This could potentially enhance mitochondrial function and reverse the loss of ATP and OXPHOS observed in AD and PD. Another potential approach is to increase the trafficking of Trkβ to the mitochondria to reactivate mitochondria. This may be challenging as there is currently limited understanding of the mechanisms involved in Trkβ trafficking and localization to mitochondria. However, ongoing research in this area may lead to the development of novel therapeutics that target mitochondrial function and trafficking for the treatment of neurodegenerative diseases.

**References:**

Acin-Perez, R., Salazar, E., Kamenetsky, M., Buck, J., Levin, L. R., & Manfredi, G. (2009). Cyclic AMP produced inside mitochondria regulates oxidative phosphorylation. *Cell Metab*, *9*(3), 265-276. https://doi.org/10.1016/j.cmet.2009.01.012

Adachi, N., Kohara, K., & Tsumoto, T. (2005). Difference in trafficking of brain-derived neurotrophic factor between axons and dendrites of cortical neurons, revealed by live-cell imaging. *BMC Neurosci*, *6*, 42. https://doi.org/10.1186/1471-2202-6-42

Affaitati, A., Cardone, L., de Cristofaro, T., Carlucci, A., Ginsberg, M. D., Varrone, S., . . . Feliciello, A. (2003). Essential role of A-kinase anchor protein 121 for cAMP signaling to mitochondria. *J Biol Chem*, *278*(6), 4286-4294.

Ahmed, S. B. M., & Prigent, S. A. (2017). Insights into the Shc Family of Adaptor Proteins. *J Mol Signal*, *12*, 2. https://doi.org/10.5334/1750-2187-12-2

Aicardi, G., Argilli, E., Cappello, S., Santi, S., Riccio, M., Thoenen, H., & Canossa, M. (2004). Induction of long-term potentiation and depression is reflected by corresponding changes in secretion of endogenous brain-derived neurotrophic factor. *Proc Natl Acad Sci U S A*, *101*(44), 15788-15792. https://doi.org/10.1073/pnas.0406960101

Almeida, R. D., Manadas, B. J., Melo, C. V., Gomes, J. R., Mendes, C. S., Grãos, M. M., . . . Duarte, C. B. (2005). Neuroprotection by BDNF against glutamate-induced apoptotic cell death is mediated by ERK and PI3-kinase pathways. *Cell Death Differ*, *12*(10), 1329-1343. https://doi.org/10.1038/sj.cdd.4401662

Alston, C. L., Rocha, M. C., Lax, N. Z., Turnbull, D. M., & Taylor, R. W. (2017). The genetics and pathology of mitochondrial disease. *The Journal of Pathology*, *241*(2), 236-250. https://doi.org/https://doi.org/10.1002/path.4809

Archer, S. L. (2013). Mitochondrial dynamics--mitochondrial fission and fusion in human diseases. *N Engl J Med*, *369*(23), 2236-2251. https://doi.org/10.1056/NEJMra1215233

Arvanitis, D. N., Ducatenzeiler, A., Ou, J. N., Grodstein, E., Andrews, S. D., Tendulkar, S. R., . . . Cuello, A. C. (2007). High intracellular concentrations of amyloid-beta block nuclear translocation of phosphorylated CREB. *J Neurochem*, *103*(1), 216-228. https://doi.org/10.1111/j.1471-4159.2007.04704.x

Baek, S. H., Park, S. J., Jeong, J. I., Kim, S. H., Han, J., Kyung, J. W., . . . Jo, D. G. (2017). Inhibition of Drp1 Ameliorates Synaptic Depression, Aβ Deposition, and Cognitive Impairment in an Alzheimer's Disease Model. *J Neurosci*, *37*(20), 5099-5110. https://doi.org/10.1523/JNEUROSCI.2385-16.2017

Banerjee, T. D., Reihl, K., Swain, M., Torres, M., & Dagda, R. K. (2021). Mitochondrial PKA Is Neuroprotective in a Cell Culture Model of Alzheimer's Disease. *Mol Neurobiol*, *58*(7), 3071-3083. https://doi.org/10.1007/s12035-021-02333-w

Banerjee, T. D., Reihl, K., Swain, M., Torres, M., & Dagda, R. K. (2021). Mitochondrial PKA Is Neuroprotective in a Cell Culture Model of Alzheimer’s Disease. *Molecular Neurobiology*, *58*(7), 3071-3083. https://doi.org/10.1007/s12035-021-02333-w

Bartolák-Suki, E., Imsirovic, J., Nishibori, Y., Krishnan, R., & Suki, B. (2017). Regulation of Mitochondrial Structure and Dynamics by the Cytoskeleton and Mechanical Factors. *Int J Mol Sci*, *18*(8). https://doi.org/10.3390/ijms18081812

Bathina, S., & Das, U. N. (2015). Brain-derived neurotrophic factor and its clinical implications. *Arch Med Sci*, *11*(6), 1164-1178. https://doi.org/10.5114/aoms.2015.56342

Bifrare, Y.-D., Kummer, J., Joss, P., Täuber, M. G., & Leib, S. L. (2005). Brain-Derived Neurotrophic Factor Protects against Multiple Forms of Brain Injury in Bacterial Meningitis. *The Journal of Infectious Diseases*, *191*(1), 40-45. https://doi.org/10.1086/426399

Brandon, E. P., Idzerda, R. L., & McKnight, G. S. (1997). PKA isoforms, neural pathways, and behaviour: making the connection. *Curr Opin Neurobiol*, *7*(3), 397-403.

Calkins, M. J., & Reddy, P. H. (2011). Amyloid beta impairs mitochondrial anterograde transport and degenerates synapses in Alzheimer's disease neurons. *Biochim Biophys Acta*, *1812*(4), 507-513. https://doi.org/10.1016/j.bbadis.2011.01.007

Cao, W., Sohail, M., Liu, G., Koumbadinga, G. A., Lobo, V. G., & Xie, J. (2011). Differential effects of PKA-controlled CaMKK2 variants on neuronal differentiation. *RNA Biol*, *8*(6), 1061-1072. https://doi.org/10.4161/rna.8.6.16691

Cardone, L., Carlucci, A., Affaitati, A., Livigni, A., DeCristofaro, T., Garbi, C., . . . Feliciello, A. (2004). Mitochondrial AKAP121 binds and targets protein tyrosine phosphatase D1, a novel positive regulator of src signaling. *Mol Cell Biol*, *24*(11), 4613-4626. https://doi.org/10.1128/MCB.24.11.4613-4626.2004

Cardone, L., de Cristofaro, T., Affaitati, A., Garbi, C., Ginsberg, M. D., Saviano, M., . . . Feliciello, A. (2002). A-kinase anchor protein 84/121 are targeted to mitochondria and mitotic spindles by overlapping amino-terminal motifs. *J Mol Biol*, *320*(3), 663-675.

Carnegie, G. K., Means, C. K., & Scott, J. D. (2009). A-kinase anchoring proteins: from protein complexes to physiology and disease. *IUBMB Life*, *61*(4), 394-406. https://doi.org/10.1002/iub.168

Cha, M. Y., Han, S. H., Son, S. M., Hong, H. S., Choi, Y. J., Byun, J., & Mook-Jung, I. (2012). Mitochondria-specific accumulation of amyloid beta induces mitochondrial dysfunction leading to apoptotic cell death. *PLoS ONE*, *7*(4), e34929. https://doi.org/10.1371/journal.pone.0034929

Chacko, B. K., Kramer, P. A., Ravi, S., Benavides, G. A., Mitchell, T., Dranka, B. P., . . . Darley-Usmar, V. M. (2014). The Bioenergetic Health Index: a new concept in mitochondrial translational research. *Clinical science (London, England : 1979)*, *127*(6), 367-373. https://doi.org/10.1042/CS20140101

Chan, D. C. (2020). Mitochondrial Dynamics and Its Involvement in Disease. *Annu Rev Pathol*, *15*, 235-259. https://doi.org/10.1146/annurev-pathmechdis-012419-032711

Cheng, A., Hou, Y., & Mattson, M. P. (2010). Mitochondria and neuroplasticity. *ASN Neuro*, *2*(5), e00045. https://doi.org/10.1042/AN20100019

Cheng, A., Wan, R., Yang, J. L., Kamimura, N., Son, T. G., Ouyang, X., . . . Mattson, M. P. (2012). Involvement of PGC-1α in the formation and maintenance of neuronal dendritic spines. *Nat Commun*, *3*, 1250. https://doi.org/10.1038/ncomms2238

Colucci-D'Amato, L., Speranza, L., & Volpicelli, F. (2020). Neurotrophic Factor BDNF, Physiological Functions and Therapeutic Potential in Depression, Neurodegeneration and Brain Cancer. *Int J Mol Sci*, *21*(20). https://doi.org/10.3390/ijms21207777

Conroy, J. N., & Coulson, E. J. (2022). High-affinity TrkA and p75 neurotrophin receptor complexes: A twisted affair. *J Biol Chem*, *298*(3), 101568. https://doi.org/10.1016/j.jbc.2022.101568

Costa, R. O., Perestrelo, T., & Almeida, R. D. (2018). PROneurotrophins and CONSequences. *Mol Neurobiol*, *55*(4), 2934-2951. https://doi.org/10.1007/s12035-017-0505-7

Course, M. M., & Wang, X. (2016). Transporting mitochondria in neurons. *F1000Research*, *5*, 1735. https://doi.org/10.12688/f1000research.7864.1

Cribbs, J. T., & Strack, S. (2007). Reversible phosphorylation of Drp1 by cyclic AMP-dependent protein kinase and calcineurin regulates mitochondrial fission and cell death. *EMBO Rep*, *8*(10), 939-944.

Cribbs, J. T., & Strack, S. (2007). Reversible phosphorylation of Drp1 by cyclic AMP-dependent protein kinase and calcineurin regulates mitochondrial fission and cell death. *EMBO reports*, *8*(10), 939-944. https://doi.org/10.1038/sj.embor.7401062

Dagda, R. K., Cherra, S. J., 3rd, Kulich, S. M., Tandon, A., Park, D., & Chu, C. T. (2009). Loss of PINK1 function promotes mitophagy through effects on oxidative stress and mitochondrial fission. *J Biol Chem*, *284*(20), 13843-13855.

Dagda, R. K., Cherra, S. J., Kulich, S. M., Tandon, A., Park, D., & Chu, C. T. (2009). Loss of PINK1 function promotes mitophagy through effects on oxidative stress and mitochondrial fission. *Journal of Biological Chemistry*, *284*(20), 13843-13855.

Dagda, R. K., & Chu, C. T. (2009). Mitochondrial quality control: insights on how Parkinson's disease related genes PINK1, parkin, and Omi/HtrA2 interact to

maintain mitochondrial homeostasis. *J Bioenerg Biomembr*, *41*(6), 473-479. https://doi.org/10.1007/s10863-009-9255-1

Dagda, R. K., & Das Banerjee, T. (2015). Role of protein kinase A in regulating mitochondrial function and neuronal development: implications to neurodegenerative diseases. *Rev Neurosci*, *26*(3), 359-370. https://doi.org/10.1515/revneuro-2014-0085

Dagda, R. K., Gusdon, A. M., Pien, I., Strack, S., Green, S., Li, C., . . . Chu, C. T. (2011). Mitochondrially localized PKA reverses mitochondrial pathology and dysfunction in a cellular model of Parkinson's disease. *Cell Death Differ*, *18*(12), 1914-1923.

Dagda, R. K., Pien, I., Wang, R., Zhu, J., Wang, K. Z., Callio, J., . . . Chu, C. T. (2014). Beyond the mitochondrion: cytosolic PINK1 remodels dendrites through protein kinase A. *J Neurochem*, *128*(6), 864-877. https://doi.org/10.1111/jnc.12494

Dagda, R. K., Zhu, J., Kulich, S. M., & Chu, C. T. (2008). Mitochondrially localized ERK2 regulates mitophagy and autophagic cell stress: implications for Parkinson's disease. *Autophagy*, *4*(6), 770-782. https://doi.org/10.4161/auto.6458

Das Banerjee, T., Dagda, R. Y., Dagda, M., Chu, C. T., Rice, M., Vazquez-Mayorga, E., & Dagda, R. K. (2017). PINK1 regulates mitochondrial trafficking in dendrites of cortical neurons through mitochondrial PKA. *J Neurochem*, *142*(4), 545-559. https://doi.org/10.1111/jnc.14083

Delezie, J., Weihrauch, M., Maier, G., Tejero, R., Ham, D. J., Gill, J. F., . . . Handschin, C. (2019). BDNF is a mediator of glycolytic fiber-type specification in mouse skeletal muscle. *Proc Natl Acad Sci U S A*, *116*(32), 16111-16120. https://doi.org/10.1073/pnas.1900544116

Devi, L., & Anandatheerthavarada, H. K. (2010). Mitochondrial trafficking of APP and alpha synuclein: Relevance to mitochondrial dysfunction in Alzheimer's and Parkinson's diseases. *Biochim Biophys Acta*, *1802*(1), 11-19. https://doi.org/10.1016/j.bbadis.2009.07.007

Dickey, A. S., & Strack, S. (2011). PKA/AKAP1 and PP2A/Bbeta2 regulate neuronal morphogenesis via Drp1 phosphorylation and mitochondrial bioenergetics. *J Neurosci*, *31*(44), 15716-15726.

Dykens, J. A., Simpkins, J. W., Wang, J., & Gordon, K. (2003). Polycyclic phenols, estrogens and neuroprotection: a proposed mitochondrial mechanism. *Exp Gerontol*, *38*(1-2), 101-107.

Eggert, S., Kins, S., Endres, K., & Brigadski, T. (2022). Brothers in arms: proBDNF/BDNF and sAPPα/Aβ-signaling and their common interplay with ADAM10, TrkB, p75NTR, sortilin, and sorLA in the progression of Alzheimer's disease. *Biol Chem*, *403*(1), 43-71. https://doi.org/10.1515/hsz-2021-0330

Eimer, W. A., & Vassar, R. (2013). Neuron loss in the 5XFAD mouse model of Alzheimer's disease correlates with intraneuronal Abeta42 accumulation and Caspase-3 activation. *Mol Neurodegener*, *8*, 2. https://doi.org/10.1186/1750-1326-8-2

Esvald, E. E., Tuvikene, J., Sirp, A., Patil, S., Bramham, C. R., & Timmusk, T. (2020). CREB Family Transcription Factors Are Major Mediators of BDNF Transcriptional Autoregulation in Cortical Neurons. *J Neurosci*, *40*(7), 1405-1426. https://doi.org/10.1523/JNEUROSCI.0367-19.2019

Faria-Pereira, A., & Morais, V. A. (2022). Synapses: The Brain's Energy-Demanding Sites. *Int J Mol Sci*, *23*(7). https://doi.org/10.3390/ijms23073627

Fassbender, K., Masters, C., & Beyreuther, K. (2001). Alzheimer's disease: molecular concepts and therapeutic targets. *Naturwissenschaften*, *88*(6), 261-267.

Feliciello, A., Gottesman, M. E., & Avvedimento, E. V. (2001). The biological functions of A-kinase anchor proteins. *J Mol Biol*, *308*(2), 99-114.

Fernandez-Marcos, P. J., & Auwerx, J. (2011). Regulation of PGC-1α, a nodal regulator of mitochondrial biogenesis. *Am J Clin Nutr*, *93*(4), 884S-890. https://doi.org/10.3945/ajcn.110.001917

Ferrer, I. (2009). Altered mitochondria, energy metabolism, voltage-dependent anion channel, and lipid rafts converge to exhaust neurons in Alzheimer's disease. *J Bioenerg Biomembr*, *41*(5), 425-431. https://doi.org/10.1007/s10863-009-9243-5

Forero, D. A., Casadesus, G., Perry, G., & Arboleda, H. (2006). Synaptic dysfunction and oxidative stress in Alzheimer's disease: emerging mechanisms. *J Cell Mol Med*, *10*(3), 796-805. https://doi.org/10.1111/j.1582-4934.2006.tb00439.x

Giménez-Palomo, A., Dodd, S., Anmella, G., Carvalho, A. F., Scaini, G., Quevedo, J., . . . Berk, M. (2021). The Role of Mitochondria in Mood Disorders: From Physiology to Pathophysiology and to Treatment. *Front Psychiatry*, *12*, 546801. https://doi.org/10.3389/fpsyt.2021.546801

Ginsberg, M. D., Feliciello, A., Jones, J. K., Avvedimento, E. V., & Gottesman, M. E. (2003). PKA-dependent binding of mRNA to the mitochondrial AKAP121 protein. *J Mol Biol*, *327*(4), 885-897.

Giorgi, C., Marchi, S., Simoes, I. C. M., Ren, Z., Morciano, G., Perrone, M., . . . Wieckowski, M. R. (2018). Mitochondria and Reactive Oxygen Species in Aging

and Age-Related Diseases. *Int Rev Cell Mol Biol, 340*, 209-344. https://doi.org/10.1016/bs.ircmb.2018.05.006

Girard, S. D., Jacquet, M., Baranger, K., Migliorati, M., Escoffier, G., Bernard, A., . . . Marchetti, E. (2014). Onset of hippocampus-dependent memory impairments in 5XFAD transgenic mouse model of Alzheimer's disease. *Hippocampus, 24*(7), 762-772. https://doi.org/10.1002/hipo.22267

Gomes, L. C., Di Benedetto, G., & Scorrano, L. (2011). During autophagy mitochondria elongate, are spared from degradation and sustain cell viability. *Nat Cell Biol, 13*(5), 589-598. https://doi.org/10.1038/ncb2220

González-Gutiérrez, A., Lazo, O. M., & Bronfman, F. C. (2020). The Rab5-Rab11 Endosomal Pathway is Required for BDNF-Induced CREB Transcriptional Regulation in Hippocampal Neurons. *J Neurosci, 40*(42), 8042-8054. https://doi.org/10.1523/JNEUROSCI.2063-19.2020

Gorman, G. S., Chinnery, P. F., DiMauro, S., Hirano, M., Koga, Y., McFarland, R., . . . Turnbull, D. M. (2016). Mitochondrial diseases. *Nature Reviews Disease Primers, 2*(1), 16080. https://doi.org/10.1038/nrdp.2016.80

Grigoruţă, M., Dagda, R. K., Díaz-Sánchez, Á. G., & Martínez-Martínez, A. (2020). Psychological distress and lack of PINK1 promote bioenergetics alterations in peripheral blood mononuclear cells. *Scientific Reports, 10*(1), 9820. https://doi.org/10.1038/s41598-020-66745-9

Guan, R., Lv, J., Xiao, F., Tu, Y., Xie, Y., & Li, L. (2019). Potential role of the cAMP/PKA/CREB signalling pathway in hypoxic preconditioning and effect on

propofol-induced neurotoxicity in the hippocampus of neonatal rats. *Mol Med Rep*, *20*(2), 1837-1845. https://doi.org/10.3892/mmr.2019.10397

Gupta, V. K., You, Y., Gupta, V. B., Klistorner, A., & Graham, S. L. (2013). TrkB receptor signalling: implications in neurodegenerative, psychiatric and proliferative disorders. *Int J Mol Sci*, *14*(5), 10122-10142. https://doi.org/10.3390/ijms140510122

Haapasalo, A., Sipola, I., Larsson, K., Akerman, K. E., Stoilov, P., Stamm, S., . . . Castren, E. (2002). Regulation of TRKB surface expression by brain-derived neurotrophic factor and truncated TRKB isoforms. *J Biol Chem*, *277*(45), 43160-43167. https://doi.org/10.1074/jbc.M205202200

Houten, S. M., Violante, S., Ventura, F. V., & Wanders, R. J. (2016). The Biochemistry and Physiology of Mitochondrial Fatty Acid β-Oxidation and Its Genetic Disorders. *Annu Rev Physiol*, *78*, 23-44. https://doi.org/10.1146/annurev-physiol-021115-105045

Hu, C., Huang, Y., & Li, L. (2017). Drp1-Dependent Mitochondrial Fission Plays Critical Roles in Physiological and Pathological Progresses in Mammals. *Int J Mol Sci*, *18*(1). https://doi.org/10.3390/ijms18010144

Huang, L. J., Durick, K., Weiner, J. A., Chun, J., & Taylor, S. S. (1997). Identification of a novel protein kinase A anchoring protein that binds both type I and type II regulatory subunits. *J Biol Chem*, *272*(12), 8057-8064.

Iijima-Ando, K., Hearn, S. A., Shenton, C., Gatt, A., Zhao, L., & Iijima, K. (2009). Mitochondrial mislocalization underlies Abeta42-induced neuronal dysfunction in

a Drosophila model of Alzheimer's disease. *PLoS ONE*, *4*(12), e8310. https://doi.org/10.1371/journal.pone.0008310

Ilouz, R., Lev-Ram, V., Bushong, E. A., Stiles, T. L., Friedmann-Morvinski, D., Douglas, C., . . . Taylor, S. S. (2017). Isoform-specific subcellular localization and function of protein kinase A identified by mosaic imaging of mouse brain. *Elife*, *6*. https://doi.org/10.7554/eLife.17681

Ishii, T., Warabi, E., & Mann, G. E. (2018). Circadian control of p75 neurotrophin receptor leads to alternate activation of Nrf2 and c-Rel to reset energy metabolism in astrocytes via brain-derived neurotrophic factor. *Free Radic Biol Med*, *119*, 34-44. https://doi.org/10.1016/j.freeradbiomed.2018.01.026

Ishii, T., Warabi, E., & Mann, G. E. (2019). Circadian control of BDNF-mediated Nrf2 activation in astrocytes protects dopaminergic neurons from ferroptosis. *Free Radic Biol Med*, *133*, 169-178. https://doi.org/10.1016/j.freeradbiomed.2018.09.002

Jiao, S. S., Shen, L. L., Zhu, C., Bu, X. L., Liu, Y. H., Liu, C. H., . . . Wang, Y. J. (2016). Brain-derived neurotrophic factor protects against tau-related neurodegeneration of Alzheimer's disease. *Transl Psychiatry*, *6*(10), e907. https://doi.org/10.1038/tp.2016.186

Jin, H., Zhu, Y., Li, Y., Ding, X., Ma, W., Han, X., & Wang, B. (2019). BDNF-mediated mitophagy alleviates high-glucose-induced brain microvascular endothelial cell injury. *Apoptosis*, *24*(5-6), 511-528. https://doi.org/10.1007/s10495-019-01535-x

K Soman, S., Swain, M., & Dagda, R. K. (2022). Multiplexing Seahorse XF. *Methods Mol Biol*, *2497*, 349-362. https://doi.org/10.1007/978-1-0716-2309-1_26

Kashatus, J. A., Nascimento, A., Myers, L. J., Sher, A., Byrne, F. L., Hoehn, K. L., . . . Kashatus, D. F. (2015). Erk2 phosphorylation of Drp1 promotes mitochondrial fission and MAPK-driven tumor growth. *Mol Cell*, *57*(3), 537-551. https://doi.org/10.1016/j.molcel.2015.01.002

Kim, D. I., Lee, K. H., Gabr, A. A., Choi, G. E., Kim, J. S., Ko, S. H., & Han, H. J. (2016). Abeta-Induced Drp1 phosphorylation through Akt activation promotes excessive mitochondrial fission leading to neuronal apoptosis. *Biochim Biophys Acta*, *1863*(11), 2820-2834. https://doi.org/10.1016/j.bbamcr.2016.09.003

Kim, J. E., Choi, H. C., Song, H. K., & Kang, T. C. (2019). Blockade of AMPA Receptor Regulates Mitochondrial Dynamics by Modulating ERK1/2 and PP1/PP2A-Mediated DRP1-S616 Phosphorylations in the Normal Rat Hippocampus. *Front Cell Neurosci*, *13*, 179. https://doi.org/10.3389/fncel.2019.00179

Klener, P., Andera, L., Necas, E., & Zivný, J. (2006). Cell death signalling pathways in the pathogenesis and therapy of haematologic malignancies: overview of apoptotic pathways. *Folia Biol (Praha)*, *52*(1-2), 34-44.

Kryl, D., Yacoubian, T., Haapasalo, A., Castren, E., Lo, D., & Barker, P. A. (1999). Subcellular localization of full-length and truncated Trk receptor isoforms in polarized neurons and epithelial cells. *J Neurosci*, *19*(14), 5823-5833. https://doi.org/10.1523/JNEUROSCI.19-14-05823.1999

Kumar, S., Kostin, S., Flacke, J. P., Reusch, H. P., & Ladilov, Y. (2009). Soluble adenylyl cyclase controls mitochondria-dependent apoptosis in coronary endothelial cells. *J Biol Chem*, *284*(22), 14760-14768. https://doi.org/10.1074/jbc.M900925200

Lai, H. C., Chang, Q. Y., & Hsieh, C. L. (2019). Signal Transduction Pathways of Acupuncture for Treating Some Nervous System Diseases. *Evid Based Complement Alternat Med*, *2019*, 2909632. https://doi.org/10.1155/2019/2909632

Langston, J. W. (2017). The MPTP Story. *J Parkinsons Dis*, *7*(s1), S11-s19. https://doi.org/10.3233/jpd-179006

Lazo, O. M., & Schiavo, G. (2023). Rab10 regulates the sorting of internalised TrkB for retrograde axonal transport. *Elife*, *12*. https://doi.org/10.7554/eLife.81532

Leal, G., Comprido, D., & Duarte, C. B. (2014). BDNF-induced local protein synthesis and synaptic plasticity. *Neuropharmacology*, *76 Pt C*, 639-656. https://doi.org/10.1016/j.neuropharm.2013.04.005

Lessmann, V., & Brigadski, T. (2009). Mechanisms, locations, and kinetics of synaptic BDNF secretion: an update. *Neurosci Res*, *65*(1), 11-22. https://doi.org/10.1016/j.neures.2009.06.004

Leung, A., Ohadi, D., Pekkurnaz, G., & Rangamani, P. (2021). Systems modeling predicts that mitochondria ER contact sites regulate the postsynaptic energy landscape. *NPJ Syst Biol Appl*, *7*(1), 26. https://doi.org/10.1038/s41540-021-00185-7

Lewin, G. R., & Carter, B. D. (2014). *Neurotrophic Factors* (Vol. 220). Springer.

Lima Giacobbo, B., Doorduin, J., Klein, H. C., Dierckx, R. A. J. O., Bromberg, E., & de Vries, E. F. J. (2019). Brain-Derived Neurotrophic Factor in Brain Disorders: Focus on Neuroinflammation. *Mol Neurobiol*, *56*(5), 3295-3312. https://doi.org/10.1007/s12035-018-1283-6

Lipsky, R. H., & Marini, A. M. (2007). Brain-derived neurotrophic factor in neuronal survival and behavior-related plasticity. *Ann N Y Acad Sci, 1122*, 130-143. https://doi.org/10.1196/annals.1403.009

Liu, F., Day, M., Muniz, L. C., Bitran, D., Arias, R., Revilla-Sanchez, R., . . . Brandon, N. J. (2008). Activation of estrogen receptor-beta regulates hippocampal synaptic plasticity and improves memory. *Nat Neurosci, 11*(3), 334-343. https://doi.org/10.1038/nn2057

Liu, Y., Encinas, M., Comella, J. X., Aldea, M., & Gallego, C. (2004). Basic helix-loop-helix proteins bind to TrkB and p21(Cip1) promoters linking differentiation and cell cycle arrest in neuroblastoma cells. *Mol Cell Biol, 24*(7), 2662-2672. https://doi.org/10.1128/MCB.24.7.2662-2672.2004

Lu, Y., Christian, K., & Lu, B. (2008). BDNF: a key regulator for protein synthesis-dependent LTP and long-term memory? *Neurobiology of learning and memory, 89*(3), 312-323. https://doi.org/10.1016/j.nlm.2007.08.018

Lujan, B., Kushmerick, C., Banerjee, T. D., Dagda, R. K., & Renden, R. (2016). Glycolysis selectively shapes the presynaptic action potential waveform. *J Neurophysiol, 116*(6), 2523-2540. https://doi.org/10.1152/jn.00629.2016

Manczak, M., Calkins, M. J., & Reddy, P. H. (2011). Impaired mitochondrial dynamics and abnormal interaction of amyloid beta with mitochondrial protein Drp1 in neurons from patients with Alzheimer's disease: implications for neuronal damage. *Hum Mol Genet, 20*(13), 2495-2509. https://doi.org/10.1093/hmg/ddr139

Manczak, M., Kandimalla, R., Yin, X., & Reddy, P. H. (2018). Hippocampal mutant APP and amyloid beta-induced cognitive decline, dendritic spine loss, defective

autophagy, mitophagy and mitochondrial abnormalities in a mouse model of Alzheimer's disease. *Hum Mol Genet*, *27*(8), 1332-1342. https://doi.org/10.1093/hmg/ddy042

Manczak, M., & Reddy, P. H. (2012). Abnormal interaction between the mitochondrial fission protein Drp1 and hyperphosphorylated tau in Alzheimer's disease neurons: implications for mitochondrial dysfunction and neuronal damage. *Hum Mol Genet*, *21*(11), 2538-2547. https://doi.org/10.1093/hmg/dds072

Markham, A., Bains, R., Franklin, P., & Spedding, M. (2014). Changes in mitochondrial function are pivotal in neurodegenerative and psychiatric disorders: how important is BDNF? *Br J Pharmacol*, *171*(8), 2206-2229. https://doi.org/10.1111/bph.12531

Markham, A., Cameron, I., Franklin, P., & Spedding, M. (2004). BDNF increases rat brain mitochondrial respiratory coupling at complex I, but not complex II. *Eur J Neurosci*, *20*(5), 1189-1196. https://doi.org/10.1111/j.1460-9568.2004.03578.x

Marlin, M. C., & Li, G. (2015). Biogenesis and function of the NGF/TrkA signaling endosome. *Int Rev Cell Mol Biol*, *314*, 239-257. https://doi.org/10.1016/bs.ircmb.2014.10.002

Marosi, K., & Mattson, M. P. (2014). BDNF mediates adaptive brain and body responses to energetic challenges. *Trends Endocrinol Metab*, *25*(2), 89-98. https://doi.org/10.1016/j.tem.2013.10.006

Martens, L. K., Kirschner, K. M., Warnecke, C., & Scholz, H. (2007). Hypoxia-inducible factor-1 (HIF-1) is a transcriptional activator of the TrkB neurotrophin receptor gene. *J Biol Chem*, *282*(19), 14379-14388. https://doi.org/10.1074/jbc.M609857200

Maryann, S., Soman, S., Kylea, T., Raul, D., & Ruben, D. (2023). BDNF Regulates Mitochondrial Physiology and function in Neurons through PKA Dependent Mechanisms. In: Journal of Neurochemistry.

Merrill, R. A., Dagda, R. K., Dickey, A. S., Cribbs, J. T., Green, S. H., Usachev, Y. M., & Strack, S. (2011). Mechanism of neuroprotective mitochondrial remodeling by PKA/AKAP1. *PLoS Biol*, *9*(4), e1000612. https://doi.org/10.1371/journal.pbio.1000612

Merrill, R. A., & Strack, S. (2014). Mitochondria: a kinase anchoring protein 1, a signaling platform for mitochondrial form and function. *Int J Biochem Cell Biol*, *48*, 92-96. https://doi.org/10.1016/j.biocel.2013.12.012

Meyer, J. N., Leuthner, T. C., & Luz, A. L. (2017). Mitochondrial fusion, fission, and mitochondrial toxicity. *Toxicology*, *391*, 42-53. https://doi.org/10.1016/j.tox.2017.07.019

Middlemas, D. S., Meisenhelder, J., & Hunter, T. (1994). Identification of TrkB autophosphorylation sites and evidence that phospholipase C-gamma 1 is a substrate of the TrkB receptor. *J Biol Chem*, *269*(7), 5458-5466.

Moya-Alvarado, G., Guerra, M. V., Tiburcio, R., Bravo, E., & Bronfman, F. C. (2022). The Rab11-regulated endocytic pathway and BDNF/TrkB signaling: Roles in plasticity changes and neurodegenerative diseases. *Neurobiol Dis*, *171*, 105796. https://doi.org/10.1016/j.nbd.2022.105796

Nguyen, D., Bharat, V., Conradson, D. M., Nandakishore, P., & Wang, X. (2021). Miro1 Impairment in a Parkinson's At-Risk Cohort. *Front Mol Neurosci*, *14*, 734273. https://doi.org/10.3389/fnmol.2021.734273

Nikoletopoulou, V., Markaki, M., Palikaras, K., & Tavernarakis, N. (2013). Crosstalk between apoptosis, necrosis and autophagy. *Biochim Biophys Acta*, *1833*(12), 3448-3459. https://doi.org/10.1016/j.bbamcr.2013.06.001

Nilsen, J., Chen, S., Irwin, R. W., Iwamoto, S., & Brinton, R. D. (2006). Estrogen protects neuronal cells from amyloid beta-induced apoptosis via regulation of mitochondrial proteins and function. *BMC Neurosci*, *7*, 74. https://doi.org/10.1186/1471-2202-7-74

Notaras, M., & van den Buuse, M. (2019). Brain-Derived Neurotrophic Factor (BDNF): Novel Insights into Regulation and Genetic Variation. *Neuroscientist*, *25*(5), 434-454. https://doi.org/10.1177/1073858418810142

Ould Amer, Y., & Hebert-Chatelain, E. (2018). Mitochondrial cAMP-PKA signaling: What do we really know? *Biochim Biophys Acta Bioenerg*, *1859*(9), 868-877. https://doi.org/10.1016/j.bbabio.2018.04.005

Palasz, E., Wysocka, A., Gasiorowska, A., Chalimoniuk, M., Niewiadomski, W., & Niewiadomska, G. (2020). BDNF as a Promising Therapeutic Agent in Parkinson's Disease. *Int J Mol Sci*, *21*(3). https://doi.org/10.3390/ijms21031170

Pallafacchina, G., Zanin, S., & Rizzuto, R. (2018). Recent advances in the molecular mechanism of mitochondrial calcium uptake. *F1000Res*, *7*. https://doi.org/10.12688/f1000research.15723.1

Pang, P. T., Teng, H. K., Zaitsev, E., Woo, N. T., Sakata, K., Zhen, S., . . . Lu, B. (2004). Cleavage of proBDNF by tPA/plasmin is essential for long-term hippocampal plasticity. *Science*, *306*(5695), 487-491. https://doi.org/10.1126/science.1100135

Papa, S., Martino, P. L., Capitanio, G., Gaballo, A., De Rasmo, D., Signorile, A., & Petruzzella, V. (2012). The oxidative phosphorylation system in mammalian mitochondria. *Adv Exp Med Biol*, *942*, 3-37. https://doi.org/10.1007/978-94-007-2869-1_1

Peng, S., Wuu, J., Mufson, E. J., & Fahnestock, M. (2005). Precursor form of brain-derived neurotrophic factor and mature brain-derived neurotrophic factor are decreased in the pre-clinical stages of Alzheimer's disease. *J Neurochem*, *93*(6), 1412-1421. https://doi.org/10.1111/j.1471-4159.2005.03135.x

Phuyal, S., & Farhan, H. (2019). Multifaceted Rho GTPase Signaling at the Endomembranes. *Front Cell Dev Biol*, *7*, 127. https://doi.org/10.3389/fcell.2019.00127

Piccini, A., Perlini, L. E., Cancedda, L., Benfenati, F., & Giovedì, S. (2015). Phosphorylation by PKA and Cdk5 Mediates the Early Effects of Synapsin III in Neuronal Morphological Maturation. *J Neurosci*, *35*(38), 13148-13159. https://doi.org/10.1523/jneurosci.1379-15.2015

Pugazhenthi, S., Wang, M., Pham, S., Sze, C. I., & Eckman, C. B. (2011a). Downregulation of CREB expression in Alzheimer's brain and in Abeta-treated rat hippocampal neurons. *Mol Neurodegener*, *6*, 60. https://doi.org/10.1186/1750-1326-6-60

Pugazhenthi, S., Wang, M., Pham, S., Sze, C. I., & Eckman, C. B. (2011b). Downregulation of CREB expression in Alzheimer's brain and in Aβ-treated rat hippocampal neurons. *Mol Neurodegener*, *6*, 60. https://doi.org/10.1186/1750-1326-6-60

Quinn, P. G. (2002). Mechanisms of basal and kinase-inducible transcription activation by CREB. *Prog Nucleic Acid Res Mol Biol*, *72*, 269-305. https://doi.org/10.1016/s0079-6603(02)72072-2

Rasmo, D., & Technikova-Dobrova, Z. P., Damiano Signorile, Anna Scacco, Salvatore Petruzzella, Vittoria Papa, Francesco Palmisano, Giuseppe Gnoni, Antonio Micelli, Loris Sardanelli, Anna Maria. (2012). Respiratory chain complex I, a main regulatory target of the cAMP/PKA pathway is defective in different human diseases. *FEBS Letters*, 568-577.

Reddy, P. H., Manczak, M., & Yin, X. (2017). Mitochondria-Division Inhibitor 1 Protects Against Amyloid-beta induced Mitochondrial Fragmentation and Synaptic Damage in Alzheimer's Disease. *J Alzheimers Dis*, *58*(1), 147-162. https://doi.org/10.3233/JAD-170051

Reddy, P. H., Manczak, M., Yin, X., & Reddy, A. P. (2018). Synergistic Protective Effects of Mitochondrial Division Inhibitor 1 and Mitochondria-Targeted Small Peptide SS31 in Alzheimer's Disease. *J Alzheimers Dis*, *62*(4), 1549-1565. https://doi.org/10.3233/JAD-170988

Reddy, P. H., Yin, X., Manczak, M., Kumar, S., Pradeepkiran, J. A., Vijayan, M., & Reddy, A. P. (2018). Mutant APP and amyloid beta-induced defective autophagy, mitophagy, mitochondrial structural and functional changes and synaptic damage in hippocampal neurons from Alzheimer's disease. *Hum Mol Genet*, *27*(14), 2502-2516. https://doi.org/10.1093/hmg/ddy154

Reichardt, L. F. (2006). Neurotrophin-regulated signalling pathways. *Philos Trans R Soc Lond B Biol Sci*, *361*(1473), 1545-1564. https://doi.org/10.1098/rstb.2006.1894

Righi, M., Tongiorgi, E., & Cattaneo, A. (2000). Brain-derived neurotrophic factor (BDNF) induces dendritic targeting of BDNF and tyrosine kinase B mRNAs in hippocampal neurons through a phosphatidylinositol-3 kinase-dependent pathway. *J Neurosci*, *20*(9), 3165-3174. https://doi.org/10.1523/jneurosci.20-09-03165.2000

Rocío, F., & Silvina, D. (2016). BDNF isoforms: a round trip ticket between neurogenesis and serotonin? *Journal of Neurochemistry*, *138*, 204-221.

Rogne, M., Landsverk, H. B., Van Eynde, A., Beullens, M., Bollen, M., Collas, P., & Kuntziger, T. (2006). The KH-Tudor domain of a-kinase anchoring protein 149 mediates RNA-dependent self-association. *Biochemistry*, *45*(50), 14980-14989. https://doi.org/10.1021/bi061418y

Rowe, G. C., Jiang, A., & Arany, Z. (2010). PGC-1 coactivators in cardiac development and disease. *Circ Res*, *107*(7), 825-838. https://doi.org/10.1161/circresaha.110.223818

Saragovi, H. U., Galan, A., & Levin, L. A. (2019). Neuroprotection: Pro-survival and Anti-neurotoxic Mechanisms as Therapeutic Strategies in Neurodegeneration. *Front Cell Neurosci*, *13*, 231. https://doi.org/10.3389/fncel.2019.00231

Saraiva, A. A., Borges, M. M., Madeira, M. D., Tavares, M. A., & Paula-Barbosa, M. M. (1985). Mitochondrial abnormalities in cortical dendrites from patients with Alzheimer's disease. *J Submicrosc Cytol*, *17*(3), 459-464.

Sarkar, S., Jun, S., & Simpkins, J. W. (2015). Estrogen amelioration of Abeta-induced defects in mitochondria is mediated by mitochondrial signaling pathway involving ERbeta, AKAP and Drp1. *Brain Res*, *1616*, 101-111. https://doi.org/10.1016/j.brainres.2015.04.059

Schapira, A. H., Cooper, J. M., Dexter, D., Clark, J. B., Jenner, P., & Marsden, C. D. (1990). Mitochondrial complex I deficiency in Parkinson's disease. *J Neurochem*, *54*(3), 823-827. https://doi.org/10.1111/j.1471-4159.1990.tb02325.x

Schuettauf, F., Vorwerk, C., Naskar, R., Orlin, A., Quinto, K., Zurakowski, D., . . . Bennett, J. (2004). Adeno-associated viruses containing bFGF or BDNF are neuroprotective against excitotoxicity. *Curr Eye Res*, *29*(6), 379-386. https://doi.org/10.1080/02713680490517872

Shen, T., You, Y., Joseph, C., Mirzaei, M., Klistorner, A., Graham, S. L., & Gupta, V. (2018). BDNF Polymorphism: A Review of Its Diagnostic and Clinical Relevance in Neurodegenerative Disorders. *Aging Dis*, *9*(3), 523-536. https://doi.org/10.14336/ad.2017.0717

Sheng, B., Wang, X., Su, B., Lee, H. G., Casadesus, G., Perry, G., & Zhu, X. (2012). Impaired mitochondrial biogenesis contributes to mitochondrial dysfunction in Alzheimer's disease. *J Neurochem*, *120*(3), 419-429. https://doi.org/10.1111/j.1471-4159.2011.07581.x

Sheng, Z. H. (2017). The Interplay of Axonal Energy Homeostasis and Mitochondrial Trafficking and Anchoring. *Trends Cell Biol*, *27*(6), 403-416. https://doi.org/10.1016/j.tcb.2017.01.005

Singh, S., Fereshetyan, K., Shorter, S., Paliokha, R., Dremencov, E., Yenkoyan, K., & Ovsepian, S. V. (2023). Brain-derived neurotrophic factor (BDNF) in perinatal depression: Side show or pivotal factor? *Drug Discov Today*, *28*(2), 103467. https://doi.org/10.1016/j.drudis.2022.103467

Smith, H. L., Bourne, J. N., Cao, G., Chirillo, M. A., Ostroff, L. E., Watson, D. J., & Harris, K. M. (2016). Mitochondrial support of persistent presynaptic vesicle mobilization with age-dependent synaptic growth after LTP. *Elife*, *5*. https://doi.org/10.7554/eLife.15275

Soman, S., Keatinge, M., Moein, M., Da Costa, M., Mortiboys, H., Skupin, A., . . . Bandmann, O. (2017). Inhibition of the mitochondrial calcium uniporter rescues dopaminergic neurons in pink1(-/-) zebrafish. *The European journal of neuroscience*, *45*(4), 528-535. https://doi.org/10.1111/ejn.13473

Soman, S. K., & Dagda, R. K. (2021). Role of Cleaved PINK1 in Neuronal Development, Synaptogenesis, and Plasticity: Implications for Parkinson's Disease. *Front Neurosci, 15*, 769331. https://doi.org/10.3389/fnins.2021.769331

Soman, S. K., Swain, M., & Dagda, R. K. (2022). Multiplexing Seahorse XF(e)24 and ImageXpress(®) Nano Platforms for Comprehensive Evaluation of Mitochondrial Bioenergetic Profile and Neuronal Morphology. *Methods Mol Biol, 2497*, 349-362. https://doi.org/10.1007/978-1-0716-2309-1_26

Soman, S. K., Tingle, D., Dagda, R. Y., Torres, M., Dagda, M., & Dagda, R. K. (2021). Cleaved PINK1 induces neuronal plasticity through PKA-mediated BDNF functional regulation. *J Neurosci Res*. https://doi.org/10.1002/jnr.24854

Swain, M., Smijin, S., Tapia, K., Dagda, R., & Dagda, R. (2023). BDNF Regulates Mitochondrial Physiology and function in Neurons through PKA Dependent Mechanisms.

Tebano, M. T., Martire, A., Chiodi, V., Ferrante, A., & Popoli, P. (2010). Role of adenosine A(2A) receptors in modulating synaptic functions and brain levels of BDNF: a

possible key mechanism in the pathophysiology of Huntington's disease. *ScientificWorldJournal, 10,* 1768-1782. https://doi.org/10.1100/tsw.2010.164

Tejeda, G. S., & Díaz-Guerra, M. (2017). Integral Characterization of Defective BDNF/TrkB Signalling in Neurological and Psychiatric Disorders Leads the Way to New Therapies. *Int J Mol Sci, 18*(2). https://doi.org/10.3390/ijms18020268

Theurey, P., Connolly, N. M. C., Fortunati, I., Basso, E., Lauwen, S., Ferrante, C., . . . Prehn, J. H. M. (2019). Systems biology identifies preserved integrity but impaired metabolism of mitochondria due to a glycolytic defect in Alzheimer's disease neurons. *Aging Cell, 18*(3), e12924. https://doi.org/10.1111/acel.12924

Thies, W. (2011). Stopping a thief and killer: Alzheimer's disease crisis demands greater commitment to research. *Alzheimers Dement, 7*(2), 175-176. https://doi.org/10.1016/j.jalz.2011.02.002

Trigo, D., Avelar, C., Fernandes, M., Sá, J., & da Cruz E Silva, O. (2022). Mitochondria, energy, and metabolism in neuronal health and disease. *FEBS Lett, 596*(9), 1095-1110. https://doi.org/10.1002/1873-3468.14298

Uittenbogaard, M., & Chiaramello, A. (2014). Mitochondrial biogenesis: a therapeutic target for neurodevelopmental disorders and neurodegenerative diseases. *Curr Pharm Des, 20*(35), 5574-5593. https://doi.org/10.2174/1381612820666140305224906

Valsecchi, F., Ramos-Espiritu, L. S., Buck, J., Levin, L. R., & Manfredi, G. (2013). cAMP and mitochondria. *Physiology (Bethesda), 28*(3), 199-209. https://doi.org/10.1152/physiol.00004.2013

Vaz, S. H., Lérias, S. R., Parreira, S., Diógenes, M. J., & Sebastião, A. M. (2015). Adenosine A2A receptor activation is determinant for BDNF actions upon GABA and glutamate release from rat hippocampal synaptosomes. *Purinergic Signal*, *11*(4), 607-612. https://doi.org/10.1007/s11302-015-9476-1

Vidaurre, O. G., Gascón, S., Deogracias, R., Sobrado, M., Cuadrado, E., Montaner, J., . . . Díaz-Guerra, M. (2012). Imbalance of neurotrophin receptor isoforms TrkB-FL/TrkB-T1 induces neuronal death in excitotoxicity. *Cell Death Dis*, *3*(1), e256. https://doi.org/10.1038/cddis.2011.143

Vitolo, O. V., Sant'Angelo, A., Costanzo, V., Battaglia, F., Arancio, O., & Shelanski, M. (2002). Amyloid beta -peptide inhibition of the PKA/CREB pathway and long-term potentiation: reversibility by drugs that enhance cAMP signaling. *Proc Natl Acad Sci U S A*, *99*(20), 13217-13221. https://doi.org/10.1073/pnas.172504199

Wang, D., Yuen, E. Y., Zhou, Y., Yan, Z., & Xiang, Y. K. (2011). Amyloid beta peptide-(1-42) induces internalization and degradation of beta2 adrenergic receptors in prefrontal cortical neurons. *J Biol Chem*, *286*(36), 31852-31863. https://doi.org/10.1074/jbc.M111.244335

Wood, J., Tse, M. C. L., Yang, X., Brobst, D., Liu, Z., Pang, B. P. S., . . . Chan, C. B. (2018). BDNF mimetic alleviates body weight gain in obese mice by enhancing mitochondrial biogenesis in skeletal muscle. *Metabolism*, *87*, 113-122. https://doi.org/10.1016/j.metabol.2018.06.007

Wrann, C. D., White, J. P., Salogiannnis, J., Laznik-Bogoslavski, D., Wu, J., Ma, D., . . . Spiegelman, B. M. (2013). Exercise induces hippocampal BDNF through a PGC-

1α/FNDC5 pathway. *Cell Metab*, *18*(5), 649-659. https://doi.org/10.1016/j.cmet.2013.09.008

You, Y., Li, W., Gong, Y., Yin, B., Qiang, B., Yuan, J., & Peng, X. (2010). ShcD interacts with TrkB via its PTB and SH2 domains and regulates BDNF-induced MAPK activation. *BMB Rep*, *43*(7), 485-490. https://doi.org/10.5483/bmbrep.2010.43.7.485

Youle, R. J., & van der Bliek, A. M. (2012). Mitochondrial fission, fusion, and stress. *Science*, *337*(6098), 1062-1065. https://doi.org/10.1126/science.1219855

Youmans, K. L., Tai, L. M., Kanekiyo, T., Stine, W. B., Jr., Michon, S. C., Nwabuisi-Heath, E., . . . LaDu, M. J. (2012). Intraneuronal Abeta detection in 5xFAD mice by a new Abeta-specific antibody. *Mol Neurodegener*, *7*, 8. https://doi.org/10.1186/1750-1326-7-8

Yu, F., Liu, Y., & Xu, J. (2018). Pro-BDNF Contributes to Hypoxia/Reoxygenation Injury in Myocardial Microvascular Endothelial Cells: Roles of Receptors p75. *Oxid Med Cell Longev*, *2018*, 3091424. https://doi.org/10.1155/2018/3091424

Yu, R., Liu, T., Ning, C., Tan, F., Jin, S. B., Lendahl, U., . . . Nistér, M. (2019). The phosphorylation status of Ser-637 in dynamin-related protein 1 (Drp1) does not determine Drp1 recruitment to mitochondria. *J Biol Chem*, *294*(46), 17262-17277. https://doi.org/10.1074/jbc.RA119.008202

Zhang, J., Feng, J., Ma, D., Wang, F., Wang, Y., Li, C., . . . Zhang, Y. (2019). Neuroprotective Mitochondrial Remodeling by AKAP121/PKA Protects HT22 Cell from Glutamate-Induced Oxidative Stress. *Mol Neurobiol*, *56*(8), 5586-5607. https://doi.org/10.1007/s12035-018-1464-3

Zhang, P., Smith-Nguyen, E. V., Keshwani, M. M., Deal, M. S., Kornev, A. P., & Taylor, S. S. (2012). Structure and allostery of the PKA RIIβ tetrameric holoenzyme. *Science*, *335*(6069), 712-716. https://doi.org/10.1126/science.1213979

Zheng, C. X., Lu, M., Guo, Y. B., Zhang, F. X., Liu, H., Guo, F., . . . Han, X. H. (2016). Electroacupuncture Ameliorates Learning and Memory and Improves Synaptic Plasticity via Activation of the PKA/CREB Signaling Pathway in Cerebral Hypoperfusion. *Evid Based Complement Alternat Med*, *2016*, 7893710. https://doi.org/10.1155/2016/7893710

Zheng, F., Luo, Y., & Wang, H. (2009). Regulation of brain-derived neurotrophic factor-mediated transcription of the immediate early gene Arc by intracellular calcium and calmodulin. *J Neurosci Res*, *87*(2), 380-392. https://doi.org/10.1002/jnr.21863

Zheng, X., Boyer, L., Jin, M., Mertens, J., Kim, Y., Ma, L., . . . Hunter, T. (2016). Metabolic reprogramming during neuronal differentiation from aerobic glycolysis to neuronal oxidative phosphorylation. *Elife*, *5*. https://doi.org/10.7554/eLife.13374

Zorzano, A., Liesa, M., Sebastián, D., Segalés, J., & Palacín, M. (2010). Mitochondrial fusion proteins: dual regulators of morphology and metabolism. *Semin Cell Dev Biol*, *21*(6), 566-574. https://doi.org/10.1016/j.semcdb.2010.01.002